REPUBLIC OF TÜRKİYE
YILDIZ TECHNICAL UNIVERSITY
GRADUATE SCHOOL OF SCIENCE AND ENGINEERING

RECOMBINANT PRODUCTION AND BIOCHEMICAL ANALYSIS OF 1-DEOXY-D-XYLULOSE 5-PHOSPHATE REDUCTOISOMERASE FOR DRUG DEVELOPMENT STUDIES

Maria ORLENCO

MASTER OF SCIENCE THESIS
Department of Bioengineering
Program of Bioengineering

Supervisor
Prof. Dr. Dilek BALIK

Co-supervisor
Prof. Dr. Björn WINDSHÜGEL

January, 2024

REPUBLIC OF TÜRKİYE
YILDIZ TECHNICAL UNIVERSITY
GRADUATE SCHOOL OF SCIENCE AND ENGINEERING

RECOMBINANT PRODUCTION AND BIOCHEMICAL ANALYSIS OF 1-DEOXY-D-XYLULOSE 5-PHOSPHATE REDUCTOISOMERASE FOR DRUG DEVELOPMENT STUDIES

A thesis submitted by Maria ORLENCO in partial fulfillment of the requirements for the degree of **MASTER OF SCIENCE** is approved by the committee on 15.01.2024 in Department of Bioengineering, Program of Bioengineering.

Prof. Dr. Dilek BALIK
Yildiz Technical University
Supervisor

Prof. Dr. Björn WINDSHÜGEL
Fraunhofer Institute for Translational Medicine and Pharmacology
Co-supervisor

Approved By the Examining Committee

Prof. Dr. Dilek BALIK, Supervisor
Yildiz Technical University _____

Assoc. Prof. Emrah Şefik ABAMOR, Member
Yildiz Technical University _____

Assoc. Prof. Sezen CANIM ATEŞ, Member
Istanbul Yeni Yuzyil University _____

I hereby declare that I have obtained the required legal permissions during data collection and exploitation procedures, that I have made the in-text citations and cited the references properly, that I haven't falsified and/or fabricated research data and results of the study and that I have abided by the principles of the scientific research and ethics during my Thesis Study under the title of RECOMBINANT PRODUCTION AND BIOCHEMICAL ANALYSIS OF 1-DEOXY-D-XYLULOSE 5-PHOSPHATE REDUCTOISOMERASE FOR DRUG DEVELOPMENT STUDIES supervised by my supervisor, Prof. Dr. Dilek BALIK. In the case of a discovery of false statement, I am to acknowledge any legal consequence.

Maria ORLENCO

Signature

This work was supported by the the project no “121N818 of THE SCIENTIFIC AND TECHNOLOGICAL RESEARCH COUNCIL OF TÜRKİYE (TÜBİTAK)”

Dedicated to my grandmother...

ACKNOWLEDGEMENTS

I would like to express my profound appreciation to my thesis supervisor, Prof. Dr. Dilek BALIK. She consistently provided me during my thesis, encouraging me to overcome obstacles and endless support during moments of need. The opportunity to work with Prof. Dr. Dilek BALIK and benefit from her profound scientific knowledge and exceptional human qualities was a great privilege and honour.

I sincerely thank my co-supervisor, Prof. Dr. Björn WINDSHÜGEL, for his support, guidance and constructive feedbacks during my thesis study.

I am grateful to Yildiz Technical University for providing opportunities to do my master's thesis.

I want to acknowledge the Scientific and Technological Research Council of Türkiye for the financial support within the scientific research project (Number: 121N818) and for supporting me with the BIDEB/2224-A Grant Program for Participation in Scientific Meetings Abroad scholarship, which allowed me to present my work to the international academic community.

My sincere thanks are addressed to our international partners Assoc. Prof. Ratana LAWUNG and Prof. Dr. Wanchai DEEKNAMKUL, and national project researchers for sharing their valuable insights, experience, and time.

I would like to thank Assoc. Prof. Tulin ARASOĞLU, Prof. Dr. Ergun PINARBAŞI, Assoc. Prof. Emel ORDU and Assist. Prof. Evren Doruk ENGİN for providing vectors and cell lines required for the experiments.

My special gratitude goes to Dr. Erennur UĞUREL for her patience, encouragement and assistance in every step of my thesis study and her endless support in academics and every subject in daily life.

I express deep appreciation to all the other members of the Recombinant DNA Technology Laboratory; Dr. Osman Mutluhan UĞUREL, Tuğba Gul İNCİ, Abdullah Enes DOĞRUSOY, Mustafa Necati HAŞİMOĞLU, Buse TAŞPULAT, Recepcan ATLI, and Emre Can YİLDİZ, for their invaluable support, contributions,

and enjoyable working environment.

I am deeply thankful to my delightful companion, Selcan AKAR; without her help and friendship, accomplishing this work would have been significantly more challenging.

I thank my beloved friends Yana CASAP, Zeynep ALKAN, Svetlana NEDEALCO, Burge KÖSE,Beyza KARACAOĞLU, Hilal ÇALIK, Gulcan Ayşin KARACA and Ayşe Seda ERGÜN for always being by my side.

My special thanks go to my family for consistently maintaining faith in my abilities and their endless support during my lifespan.

I express my eternal appreciation to my beloved and deeply missed grandfather and grandmother for their love, moral support and, most importantly, my happy childhood.

Lastly, I sincerely thank Dr. Ali Can ÖZARSLAN for his support, motivation and belief in me.

Maria ORLENCO

TABLE OF CONTENTS

LIST OF SYMBOLS

A	Absorbance
bp	Base pair
°C	Degree Celsius
g	Gram
IC_{50}	Half-Maximal Inhibitory Concentration
h	Hour(s)
L	Liter
V_{max}	Maximum rate of reaction
K_m	Michaelis-Menten constant
μg	Microgram
μL	Microliter
μmol	Micromol
μM	Micromolar
mg	Milligram
mM	Millimolar
min	Minute(s)
ϵ	Molar absorption coefficient
M	Molar
mA	Milliampere
mol	Mole
ng	Nanogram
nm	Nanometer
nM	Nanomolar

OD	Optical Density
rpm	Revolutions per minute
sec	Second(s)
u	Enzyme unit
V_T	Total reaction volume
V	Volt

LIST OF ABBREVIATIONS

AMR	Antimicrobial resistance
ATP	Adenosine triphosphate
Asn	Asparagine
Asp	Aspartic acid
ATCC	American Type Culture Collection
BSA	Bovine Serum Albumin
CDP-ME	4-diphosphocytidyl-2C-methyl-D-erythritol
CDP-MEP	4-diphosphocytidyl-2C-methyl-D-erythritol 2-phosphate
CMP	Cytidine monophosphate
CTP	Cytidine triphosphate
DAB	3,3′-diaminobenzidine tetrahydrochloride
DGI	Disseminated Gonococcal Infection
DHFR	Dihydrofolate reductase
DMAPP	Dimethylallyl diphosphate
DMSO	Dimethyl sulfoxide
DNA	Deoxyribonucleic acid
DTT	Dithiothreitol
DXP	1-deoxy-D-xylulose 5-phosphate
DXR	1-deoxy-D-xylulose 5-phosphate reductoisomerase
DXS	1-deoxy-D-xylulose 5-phosphate synthase
E. coli	*Escherichia coli*
Ecdxr	*Escherichia coli* (ATCC 25922) *dxr* gene
*Ec*DXR	*Escherichia coli* DXR enzyme

EDTA	Ethylenediaminetetraacetic acid
EMBL-EBI	European Molecular Biology Laboratory-European Bioinformatics Institute
FSM	Fosmidomycin
Glu	Glutamic acid
gor	Glutathione reductase
GST	Glutathione S-transferase
HIV	Human Immunodeficiency Virus
His	Histidine
HMBPP	1-hydroxy-2-methyl-2-(E)-butenyl 4-diphosphate
I	Non-recombinant IPTG-induced
IPP	Isopentenyl diphosphate
IPTG	Isopropyl β-D-1-thiogalactopyranoside
IspD	4-diphosphocytidyl-2C-methyl-D-erythritol synthase
IspE	4-Di-phosphocytidyl-2C-methyl-D-erythritol kinase
IspF	2C-methyl-D-erythritol 2,4-cyclodiphosphate synthase
IspG	1-hydroxy-2- methyl-2(E)-butenyl-4-diphosphate synthase
IspH	1-hydroxy-2-methyl-2(E)-butenyl-4-diphosphate reductase
LB	Luria-Bertani
LIC	Lingation Independent Cloning
LOS	Lipooligosaccharides
Lys	Lysine
MBP	Maltose Binding Protein
MEcPP	2C-methyl-D-erythritol-2,4-cyclo-diphosphate
MEP	Methylerythritol 4-phosphate pathway
MEP	2-C-methyl-D-erythritol 4-phosphat
MUSCLE	Multiple Sequence Comparison by Log-Expectation
MVA	Mevalonate pathway
N.gonorrhoeae	*Neisseria gonorrhoeae*

NCBI	National Center for Biotechnology Information
*Ng*DXR	*Neisseria gonorrhoeae* DXR enzyme
NI	Non-recombinant, uninduced
Opt*Ngdxr*	*Neisseria gonorrhoeae* (ATCC 49226) *dxr* codon optimized and harmonized gene
PBS	Phosphate Buffered Saline
PCR	Polymerase Chain Reaction
PDB	Protein Data Bank
PMSF	Phenyl-methylsulfonyl fluoride
R I	Recombinant IPTG-induced
R NI	Recombinant uninduced
SAB	Sample Application Buffer
SDS-PAGE	Sodium Dodecyl Sulfate Polyacrylamide Gel Electrophoresis
Ser	Serine
SOC	Super Optimal broth with Catabolite
STI	Sexually Transmitted Infection
SUMO	Small ubiquitin-like modifier
TAE	Tris-Acetate-EDTA
*Ta*ENO	*Theileria annulata* enolase
TB	Terrific Broth
TEMED	Tetramethylethylenediamine
TetM	Tetracycline resistance protein
Trp	Tryptophan
Trx	Thioredoxin
trxB	Thioredoxin reductase
Tween-20	Polyoxyethylene (20) sorbitan monolaurate
WB	Western Blot
WHO	World Health Organization
WT*Ngdxr*	*Neisseria gonorrhoeae* (ATCC 49226) *dxr* gene

LIST OF FIGURES

LIST OF TABLES

ABSTRACT

RECOMBINANT PRODUCTION AND BIOCHEMICAL ANALYSIS OF 1-DEOXY-D-XYLULOSE 5-PHOSPHATE REDUCTOISOMERASE FOR DRUG DEVELOPMENT STUDIES

Maria ORLENCO

Department of Bioengineering
Master of Science Thesis

Supervisor: Prof. Dr. Dilek BALIK
Co-supervisor: Prof. Dr. Björn WINDSHÜGEL

Antimicrobial resistance, has the potential to become a primary leading cause of death, with an estimated 10 million deaths per year by 2050. To increase awareness and emphasize the urgency of the problem, the WHO published a list of pathogens that urgently need the development of new antimicrobials and the causative agent of gonorrhea, *Neisseria gonorrhoeae*, was categorized as a high-priority pathogen. Distinct pathways are involved in the synthesis of vital cellular isoprenoid precursors in higher eukaryotes and bacteria, enabling biosynthetic pathways to be used as drug targets. Most bacteria, including *N. gonorrhoeae*, utilize the methylerythritol 4-phosphate pathway (MEP). The second step in the pathway involves the conversion of 1-deoxy-D-xylulose 5-phosphate to 2-C-methyl-D-erythritol 4-phosphate by 1-deoxy-D-xylulose 5-phosphate reductoisomerase (DXR). This study aims recombinant production and biochemical analysis of *N. gonorrhoeae* DXR with the ultimate purpose of being used in high-throughput screening. C-terminal His-tagged *Ng*DXR was expressed in *Escherichia coli* BL21(DE3) using the pLATE31 expression vector system. Although the protein produced was obtained in low amounts in soluble form, it was mainly observed in the pellet fraction. Numerous strategies were applied to improve the expression yield of the soluble protein; nevertheless, the expressed protein was

still insufficient for biochemical analysis. Based on the literature review and multiple sequence alignment analysis of DXR amino acids sequences, the active site functional residues of *E. coli* DXR were observed to be conserved in *Ng*DXR. Consequently, the recombinant production of *Ec*DXR was aimed, and protein expression using the pLATE31 vector system in *E. coli* BL21(DE3) host strain was performed with 0.5 mM IPTG induction at 30°C, for 3 hours. The *Ec*DXR with purity over 95% was subjected to biochemical analysis, the K_m and V_{max} values were determined as 103.4±17.05 μM and 0.5985±0.03497 μmol/min.mg, respectively. As a result of the inhibition study with fosmidomycin (FSM), the IC_{50} value of FSM against *Ec*DXR was determined as 160 nM.

Within the scope of the thesis, it was concluded that recombinantly produced *Ec*DXR, which has no equivalent in humans and can be obtained at high concentrations, may be used in drug development studies.

Keywords: Antimicrobial resistance, Sexually transmitted infection, *Neisseria gonorrhoeae*, Methylerythritol 4-phosphate pathway, 1-deoxy-D-xylulose 5-phosphate reductoisomerase

ÖZET

İLAÇ GELİŞTİRME ÇALIŞMALARI İÇİN 1-DEOKSİ-D-SELÜLOZ 5-FOSFAT REDÜKTOİZOMERAZIN REKOMBİNANT ÜRETİMİ VE BİYOKİMYASAL ANALİZİ

Maria ORLENCO

Biyomühendislik Anabilim Dalı
Yüksek Lisans Tezi

Danışman: Prof. Dr. Dilek BALIK
Eş-Danışman: Prof. Dr. Björn WINDSHÜGEL

Antimikrobiyal direnç, 2050 yılına kadar yılda tahmini 10 milyon ölümle, önde gelen ölüm nedenlerinden biri olma potansiyeline sahiptir. Farkındalığı artırmak ve sorunun aciliyetini vurgulamak amacıyla DSÖ, acilen yeni antimikrobiyallerin geliştirilmesine ihtiyaç duyan patojenlerin bir listesini yayınlamış ve belsoğukluğu etkeni *Neisseria gonorrhoeae*, yüksek öncelikli patojen olarak kategorize edilmiştir. Yüksek ökaryotlarda ve bakterilerde hayati önem taşıyan hücresel izoprenoid öncüllerinin sentezinde farklı yolaklar yer alır ve bu da biyosentetik yolakların ilaç hedefi olarak kullanılmasını sağlar. *N. gonorrhoeae* dahil olmak üzere çoğu bakteri metil eritritol 4-fosfat yolağını (MEP) kullanır. Yolaktaki ikinci adım, 1-deoksi-D-ksilüloz 5-fosfatın 1-deoksi-D-ksilüloz 5-fosfat redüktoizomeraz (DXR) tarafından 2-C-metil-D-eritritol 4-fosfata dönüştürülmesini içerir. Bu çalışma, yüksek verimli taramada kullanılmak üzere *N. gonorrhoeae* DXR'nin rekombinant üretimini ve biyokimyasal analizini amaçlamaktadır. C-terminal His etiketli *Ng*DXR, pLATE31 ifade vektör sistemi kullanılarak *Escherichia coli* BL21(DE3)'te ifade edilmiştir. Üretilen protein, çözünür formda düşük miktarlarda elde edilmesine rağmen, esas olarak pelet fraksiyonunda gözlenmiştir. Çözünür proteinin ekspresyon verimini artırmak için çok sayıda strateji uygulanmasına rağmen, eksprese edilen proteinin biyokimyasal analiz için yeterli olmadığı belirlenmiştir. Literatür taramasına ve DXR amino asit dizilerinin çoklu

dizi hizalama analizine dayanarak, *E. coli* DXR'nin aktif bölge fonksiyonel kalıntılarının *Ng*DXR'de korunduğu gözlenmiştir. Sonuç olarak, *Ec*DXR'nin rekombinant üretimi amaçlanmış ve *E. coli* BL21(DE3) konak suşunda pLATE31 vektör sistemi kullanılarak protein ekspresyonu 30°C'de 3 saat boyunca 0,5 mM IPTG indüksiyonu ile gerçekleştirilmiştir. % 95'in üzeri saflıkta elde edilen *Ec*DXR, biyokimyasal analize tabi tutulmuş, K_m ve V_{max} değerleri sırasıyla 103,4±17,05 μM ve 0,5985±0,03497 μmol/dk.mg olarak belirlenmiştir. Fosmidomisin (FSM) ile yapılan inhibisyon çalışması sonucunda, FSM'nin *Ec*DXR'ye karşı IC_{50} değeri 160 nM olarak belirlenmiştir.

Tez kapsamında, insanlarda eşdeğeri bulunmayan ve yüksek konsantrasyonlarda elde edilebilen rekombinant olarak üretilmiş *Ec*DXR'nin ilaç geliştirme çalışmalarında kullanılabileceği sonucuna varılmıştır.

Anahtar Kelimeler: Antimikrobiyal direnç, Cinsel yolla bulaşan enfeksiyon, *Neisseria gonorrhoeae*, Metil eritritol 4-fosfat yolağı, 1-deoksi-D-ksilüloz 5-fosfat redüktoizomeraz

1
INTRODUCTION

1.1 Literature Review

Antimicrobial resistance, poses a significant public health risk, with a predicted 10 million deaths per year by 2050 [1, 2]. The importance of bacterial antimicrobial resistance is of particular concern, emphasized by the the World Health Organization's list of priority pathogens that urgently need the development of new antibiotics [3, 4]. The sexually transmitted infections are the growing public concern facing humanity. More than 1 million new cases of sexually transmitted infections emerges worldwide daily, arising from any of the four curable infections [5]. Gonorrhea is the second most common bacterial sexually transmitted infection caused by the bacterium *Neisseria gonorrhoeae*, which is categorized by the WHO as a high-priority pathogen based on the developed multidrug resistance [4, 6]. *N. gonorrhoeae* penetrates the mucosa of different vulnerable anatomical locations, such as the urogenital tract, rectum, pharynx, and conjunctivae [7]. The delayed identification or inadequate treatment of infection leads to complications such as epididymitis in males and cervical inflammation, endometriosis, and pelvic inflammatory disease in women [8, 9]. Besides being transmitted by sexual contact, the infection can be transmitted from the infected mother to the newborn, potentially leading to neonatal blindness [10].

Sulfonamide, penicillin, tetracycline, spectinomycin, macrolides, fluoroquinolones, and cephalosporins were implemented as monotherapy for gonorrhea treatment. However, *N. gonorrhoeae* developed resistance against all applied therapies over the years [9, 11, 12]. Due to the emergence of resistance to all antibiotics used as a monotherapy treatment, dual therapy has been suggested as a solution [13]. However, the reported ineffectiveness of dual therapy highlights the severity of infection [6, 13]. The rapid evolution of antimicrobial resistance has driven scientists to search for specific targets within the vital metabolic pathways found in causative agents of infections [14].

Isoprenoids are a diverse group of compounds that play a vital role in sustaining essential biological activities such as cell wall formation, electron transportation, intracellular signaling, defence, and photosynthesis. Irrespective of their variations in structure and function, all isoprenoids are synthesized from the isopentenyl diphosphate (IPP) and dimethylallyl diphosphate (DMAPP) precursors [15–17]. Two distinct biosynthetic pathways with identical end products are utilized by organisms for isoprenoid precursor biosynthesis [18]. Higher eukaryotes employ the six-step mevalonate (MVA) pathway, whereas most bacteria use the seven-step methylerythritol 4-phosphate (MEP) pathway [19]. Enzymes of the MEP pathway are considered as potential therapeutic targets due to absence in humans and their vital role in the survival of pathogens [14]. The second rate-limiting step of the MEP pathway comprises the reductive isomerization of 1-deoxy-D-xylulose 5-phosphate (DXP) substrate to 2-C-methyl-D-erythritol 4-phosphat (MEP) product by 1-deoxy-D-xylulose 5-phosphate reductoisomerase (DXR) enzyme in the presence of a divalent cation and NADPH cofactor [20]. DXR exhibits a homodimeric structure. Each V-like monomer of the enzyme consists of three domains: an N-terminal domain, a central catalytic domain, and a C-terminal domain [21, 22]. The isomerization of DXP into intermediate aldehyde occurs in a divalent metal ion-dependent reaction, and the NADPH cofactor mediates subsequent reduction to MEP [20, 23]. The antibiotic fosmidomycin (FSM) has an inhibitory effect against the DXR of many bacteria (*Escherichia coli* [24], *Yersinia pestis* [25], *Mycobacterium tuberculosis* [26], and *Francisella tularensis* [27]) and apicomplexan parasites (*Babesia microti* [15], *Plasmodium falciparum* [28]). However, there are no reported drug discovery studies targeting DXR of *N. gonorrhoeae*.

1.2 Objective of the Thesis

Multi-drug resistant *Neisseria gonorrhoeae*, the causative agent of sexually transmitted gonorrhea infection, is classified as a high-priority pathogen by the WHO for research and development of new antimicrobials. The ability of *N. gonorrhoeae* to develop resistance to all treatments implemented to date raises concerns about incurable gonorrhea.

In this study, the methylerythritol 4-phosphate pathway (MEP), which is absent in the human host and is used by *N. gonorrhoeae* in biosynthesis of vital bacterial isoprenoid precursors, was selected for potential drug targeting to overcome the problem. The study aims recombinant production and biochemical analysis of second rate-limiting 1-deoxy-D-xylulose 5-phosphate-reductoisomerase in the

MEP pathway to be used in high-throughput screening with the ultimate aim of small molecules and natural products identification as initial structures for drug development against *N. gonorrhoeae*.

2
GENERAL INFORMATION

2.1 Antimicrobial Drug Resistance

Antimicrobials are the therapeutic agents used in the management of infections driven by bacteria, viruses, fungi, and parasites [29]. The ability of microorganisms to overcome the effect of therapeutic agents by different mechanisms [30] is known as antimicrobial resistance (AMR) [31]. Although AMR can be considered as natural phenomenon that arises over time, factors such as overuse and misuse of antimicrobials may speed up its development [32, 33]. AMR poses a significant threat to human health, emerging as a silent pandemic that renders antibiotics and other antimicrobials ineffective in tackling diseases [1]. AMR is defined as one of the top 10 public health threats [34] and is estimated to cause 10 million deaths annually by 2050 [2]. The problem of AMR poses a particular importance related to antibiotic resistance in bacteria [3]. Based on the data analysis study in 2019, 4.95 million deaths were associated with bacterial AMR, with 1.27 million directly accounting for bacterial AMR [35]. In 2017, the World Health Organization (WHO) published a list of priority pathogens that need new antibiotics, indicating the urgency of the situation [4].

2.2 Sexually Transmitted Infections

Sexually transmitted infections (STIs) are bacterial, viral, and parasitic causative conditions that are transmitted through sexual behavior [36]. In addition, there are nonsexual routes of STI transmission by blood or from mother to child [37]. Young age, multiple sexual partners, and uncontrolled sexual conduct are the main risk factors associated with the case increase in STIs [38–40]. A substantial impact on STI incidences is maintained by four incurable (hepatitis B, herpes simplex virus, human immunodeficiency virus (HIV), human papillomavirus) and four curable (syphilis, gonorrhea, chlamydia, trichomoniasis) STIs [5, 37].

In 2020, the WHO predicted 374.3 million new cases of four curable STIs across

adults, with the highest number of incidences attributed to protozoan-caused trichomoniasis (156.3 million), followed by bacterial-caused infections: chlamydia (128.5 million), gonorrhea (82.4 million) and syphilis (7.1 million) [5]. STIs are generally asymptomatic and can lead to serious health implications as a result of remaining undiagnosed [36, 41]. Even though both men and women are prone to developing STIs, female anatomy facilitates greater susceptibility to infections [38, 42].

2.3 Gonorrhea

Gonorrhea is the second most prevalent bacterial sexually transmitted infection caused by *Neisseria gonorrhoeae*. The term "gonorrhea" denoting "uncontrolled seminal discharge" was initially employed by the Greek physician Galen in the second century to describe a condition observed in males [6, 43]. Despite being classified as a treatable STI, gonorrhea can cause serious health complications [41].

2.3.1 Epidemiology of Gonorrhea

Based on the incidence estimates provided by the WHO in 2020, out of the reported incidences of curable sexually transmitted infections, 82.4 million cases were attributed to gonorrhea among individuals aged 15-49 [44]. Regarding the WHO regional data, the Western Pacific Region exhibited the highest recorded number of 23.2 million gonorrhea cases in 2020 [5]. The latest report [44] indicates a significant incidence increase over eight years compared to the estimated 78 million cases in 2012 [30]. According to information on gonorrhea provided by the Centre for Disease Control and Prevention, an estimated 1.6 million cases occurred in the United States in 2018, leading to a significant economic impact of approximately 270 million United States dollars [41]. *N. gonorrhoeae* has been included in the list of prioritized targets in the global strategy effort to eliminate STIs, and goals have been established to accomplish a 90% reduction in the number of gonorrhea cases by the year 2030 [45]. The progress line toward the targets by 2030 is given in Figure 2.1.

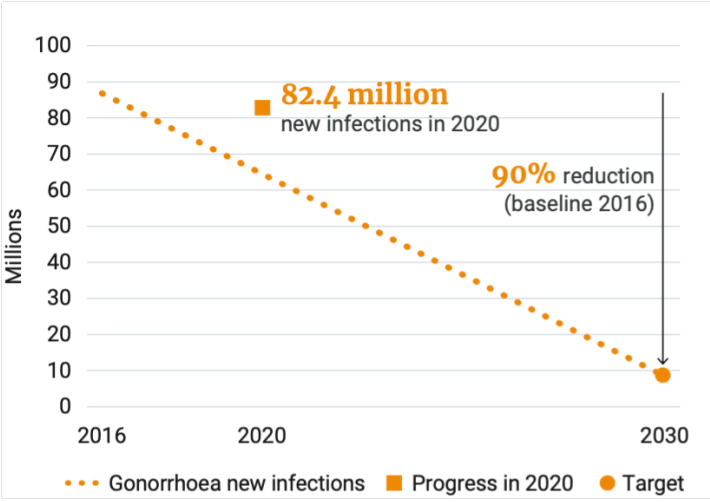

Figure 2.1 Progress towards 2030 targets to reduce the number of gonorrhea cases [5]

2.3.2 Route of Transmission and Gonorrhea Outcomes

The epithelia of the urogenital tract is the primary colonization site of the etiological agent of the infection [8]. The ability of *N. gonorrhoeae* to attach to sperm allows it to be transmitted from men to women during sexual contact [46]. The predicted risk of transfer from a male genital organ to a female genital organ is about 50% per sexual contact, whereas the contrary transmission chance is approximately 20% [7]. Transmission of the infection between individuals occurs through the transfer of infected mucosal secretions to uninfected mucosa [47]. The risk of transmission as a result of a single sexual contact with an infected individual is thought to be between 30% and 70% [48]. In women, the epithelial cells of the endocervix are the primary target invaded by *N. gonorrhoeae* after the transmission from the carrier. The potential of *N. gonorrhoeae* to invade vaginal cells has not been observed [49, 50]. From a clinical perspective, as a result of infection, men may experience distinct and characteristic symptoms such as purulent exudate from the penis and resultant painful urination; in contrast, unnoticed symptoms may be encountered in women [46]. Late detection or insufficient infection treatment causes the spread of the etiological agent to the upper regions of the urogenital tract. The bacterial dissemination can give rise to severe outcomes such as epididymitis in men and cervical inflammation, endometriosis and pelvic inflammatory disease in women [8, 9]. At least 90% of men exhibit symptoms within 2-5 days after infection [51, 52]. In addition to urogenital invasion, *N. gonorrhoeae* can also be detected in extra-genital sites as a result of unprotected oral and anal sexual activity [53]. Although the dissemination of *N. gonorrhoeae* via the bloodstream from the primary site of infection is uncommon, the developed spread leads to life-threatening disseminated gonococcal infection (DGI) [8, 54]. DGI,

seen in 0.5-3% of infected individuals, causes clinical symptoms such as arthritis, endocarditis and meningitis [54, 55]. Infections observed in pregnant women can impact the progression of pregnancy and lead to consequences such as spontaneous abortion, early birth and intraamniotic infection [10]. Neonatal blindness is another consequence of gonorrhea caused by transmission from infected mother to child during birth [10, 46]. Furthermore, gonorrhea may contribute to the development and spread of several sexually transmitted infections, such as HIV [56, 57].

2.3.3 Prevention and Treatment Options for Gonorrhea

In the Medieval era, many natural compounds such as honey mixed with water or milk, goat or breast milk, an extract derived from the Spanish fly, and mercury were utilized to combat gonorrhea [11]. The antibiotic era in gonorrhea started with the introduction of sulfonamide as the treatment agent, with cure rates of 80%-90% [58]. Based on the emergence of bacterial resistance to sulfonamide, penicillin was employed to treat the infection [12]. In response to the decreasing efficacy of penicillin against gonorrhea, several classes of antibiotics, including tetracycline, spectinomycin, macrolides, fluoroquinolones, and cephalosporins, have been used as monotherapy at different times to deal with the infection [9, 11, 12]. However, resistance was observed to all antibiotics applied [57, 59]. According to the failure of monotherapies, dual therapy against gonococcal infections was introduced to overcome the increasing antibiotic resistance developed by *N. gonorrhoeae* [10, 56]. Dual therapy, recommended by the WHO and other health organizations around the world comprises the use of a broad spectrum of cephalosporins along with azithromycin for the management of gonorrhea [60–62]. Timeline of recommended treatments and AMR developments is given in Figure 2.2.

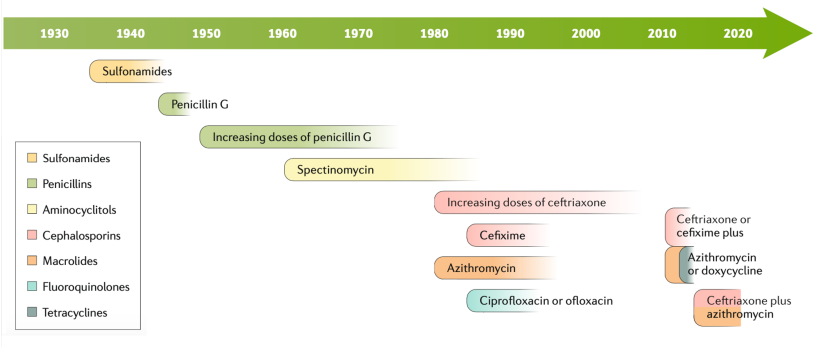

Figure 2.2 Chronological order of recommended therapies and AMR developments (adapted from [9])

2.4 The Bacterium *Neisseria gonorrhoeae*

N. gonorrhoeae, the causative agent of gonorrhea, was identified by Albert L. S. Neisser in 1879 [54]. *N. gonorrhoeae* is the human-specific pathogenic species of the genus *Neisseria* belonging to the family *Neisseriaceae* of the betaproteobacteria phylogenetic group [50, 63]. The Gram-negative aerobic bacterium with the morphology of diplococcus (Figure 2.3) invades mucosal surfaces and exhibits structural similarities with other Gram-negative bacteria [64, 65]. The *N. gonorrhoeae* genome has an approximate size of 2 megabases. Nevertheless, *N. gonorrhoeae* can obtain DNA material, such as penicillinase-encoding plasmids, by horizontal genetic transfer from other *Neisseria* species. The cell envelope comprises an inner cytoplasmic membrane and an outer membrane separated by a peptidoglycan cell wall [9]. Along with the lipooligosaccharides (LOS) and phospholipids, the outer membrane has other proteins that participate in cell adhesion, invasion, and defense against the immune response of the host [66]. Five target-specific efflux pumps at the surface of *N. gonorrhoeae*, MtrC-MtrD-MtrE, MacA-MacB-MtrE, NorM, FarA-FarB-MtrE and MtrF provide the ability to remove toxic compounds from bacteria and excreting antimicrobial agents from the cell [9].

Figure 2.3 3D image of *N. gonorrhoeae* (James Archer, Centers for Disease Control and Prevention, USA) [67]

2.4.1 Pathogenesis of *Neisseria gonorrhoeae*

As the bacteria has been transmitted, the attachment to the epithelium is maintained primarily by type IV pili, opacity and LOS proteins in the outer membrane [9, 46, 66]. The initial interaction is established by type IV pili with CD46 and CR3 receptors of the host cell, followed by the interaction of opacity proteins with carcinoembryonic antigen-related cell adhesion molecule receptors and other cell surface molecules, such as heparin sulfate [41, 46]. In addition to the

abovementioned interactions, bacterial binding is also mediated by LOS attachment to the asialoglycoprotein receptor of the host [41]. Once binding to the epithelium is achieved, bacteria undergo replication and invade the cell through transcytosis. During the invasion process, the bacteria release peptidoglycan fragments, outer membrane vesicles and LOS that stimulate the immunological response of the host cell [9, 10, 41, 46].

2.4.2 Antimicrobial Resistance of *Neisseria gonorrhoeae*

The emergence of antimicrobial resistance in *N. gonorrhoeae* was first observed in the mid-1930s with the introduction of sulfonamides as therapeutic agents and subsequently, *N. gonorrhoeae* continued to develop resistance to all antimicrobial classes applied [9, 56, 59]. *N. gonorrhoeae* exhibited all known processes associated with AMR, including elimination of the antimicrobial agent, modification of the antimicrobial target, and enhanced or reduced antimicrobial efflux [46, 59]. Although AMR in *N. gonorrhoeae* is caused predominantly by mutated chromosomal genes, plasmid-mediated resistance is observed against penicillin and tetracyclines [68].

The effect of sulfonamides targeting bacterial dihydropteroate synthase on *N. gonorrhoeae* has been overcome by mutation in the encoding *folP* gene or by excessive expression of *p*-aminobenzoic acid, which has a diluting potential on the antimicrobial [69].

Cephalosporins and penicillins are β-lactam antibiotics that mainly target penicillin-binding proteins to ensure the destabilization of the cell wall. Chromosomal mutation-induced changes in the target protein provide resistance to cephalosporins, while resistance to penicillins is mediated by chromosomal mutations and β-lactamase (plasmid-mediated resistance) [70]. β-lactamase directly breaks down penicillin, however resistance through gene mutations affects processes such as binding to the target, influx or efflux of the antibiotic [56].

Resistance to fluoroquinolones, which have an inhibitory effect on the topoisomerase II (gyrase) and topoisomerase IV enzymes, is developed by bacteria through alteration of the amino acid sequence of the enzymes [70]. Bacteria develop both chromosomal and plasmid-mediated resistance to tetracycline in order to prevent ribosomal 30S subunit targeting from tetracycline. The plasmid-encoded TetM protein binds to the 30S subunit of the ribosome, hence inhibiting the association of tetracycline with the target. However, chromosomal mutations lead to increased efflux of tetracycline from the cell, decreased entry into the cell and sequence changes in the ribosomal S10 protein [69, 70].

Resistance to spectinomycin targeting 16S rRNA is related to the single nucleotide

polymorphism in the binding site of the antimicrobial agent [56, 69]. The development of resistance to macrolides, used to prevent protein synthesis, is achieved by structural changes in the target or by overexpression of the efflux pump responsible for the excretion of inhibitors out of the cell [69]. The tendency of *N. gonorrhoeae* to develop resistance to all antibiotics utilized for treatment, poses a threat to the emergence of untreatable gonorrhea [6, 46].

2.5 Biosynthetic Pathways as Drug Targets

Isoprenoids are the most diverse group of natural compounds, containing more than 80,000 identified molecules with a broad range of functionalities [71, 72]. Synthesized by all organisms, isoprenoids play a role in maintaining vital biological processes such as cell wall synthesis, electron transport, intracellular signalling, defence, and photosynthesis [16, 17, 73]. Regardless of their structural and functional differences, all isoprenoids are formed from the isopentenyl diphosphate (IPP) and dimethylallyl diphosphate (DMAPP) building blocks [74, 75]. The synthesis of 5-carbon isoprenoid precursors is committed by two distinct biosynthetic pathways: mevalonate pathway (MVA) and methylerythritol 4-phosphate (MEP) [18, 76]. Although their end products are identical, MVA or MEP utilization is organism-dependent [18, 72]. The MVA pathway is predominantly used by archaea and eukaryotes, including humans, however, the presence of the pathway in some Gram-positive bacteria, such as *Staphylococcus aureus* and *Streptococcus pneumoniae*, has also been reported [19, 72, 74]. Most bacteria and photosynthetic eukaryotes harbour the MEP pathway, nevertheless, plants possess both pathways in different cellular compartments [19, 77].

2.5.1 The Mevalonate Pathway

For a long time, isoprenoid precursors were thought to be synthesized in all organisms by the six enzymatic-stepped MVA pathways [20]. IPP and DMAPP synthesis through the MEP pathway initiates with acetyl-CoA conversion to acetoacetyl-CoA via acetyl CoA acetyltransferase carried reaction. The obtained product is then transformed into 3-hydroxy-3-methylglutaryl-CoA (HMG-CoA), which is subsequently reduced to mevalonate. Mevalonate is subjected to phosphorylation, and the generated mevalonic-5-monophosphate (MVA-P). In the next step, the obtained product is converted by phosphorylation into mevalonic-5-diphosphate (MVA-PP). At the last step of the reaction, IPP and DMAPP are produced as a result of decarboxylation of MVA-PP using an adenosine triphosphate (ATP) [74, 78].

2.5.2 The Methylerythritol 4-Phosphate Pathway

MEP pathway with different starter compounds, intermediate molecules and enzymes was identified in 1993 by Rohmer et al. [79, 80]. The biosynthesis of IPP and DMAPP precursors by the MEP pathway is carried out in seven enzymatic steps (Figure 2.4), initiated by the conversion of pyruvate and glyceraldehyde-3-phosphate to 1-deoxy-D-xylulose 5-phosphate (DXP) maintained by DXP synthase (DXS) and a molecule of carbon dioxide releases along with DXP [81]. Following DXP generation, 1-deoxy-D-xylulose 5-phosphate reductoisomerase (DXR) enables single-stepped reductive isomerization of DXP to 2-C-methyl-D-erythritol 4-phosphate (MEP) in the presence of NADPH and divalent cations (Mg^{2+}, Mn^{2+}, or Co^{2+}) [82]. Then, 4-diphosphocytidyl-2C-methyl-D-erythritol synthase (IspD) catalyzed, cytidine triphosphate (CTP)-dependent reaction step converts MEP to 4-diphosphocytidyl-2C-methyl-D-erythritol (CDP-ME), which is subsequently phosphorylated using ATP to generate 4-diphosphocytidyl-2C-methyl-D-erythritol 2-phosphate (CDP-MEP) by 4-Di-phosphocytidyl-2C-methyl-D-erythritol kinase (IspE) catalyzed reaction [81]. In the 2C-methyl-D-erythritol 2,4-cyclodiphosphate synthase (IspF) performed reaction, CDP-MEP is transformed to the cyclic product 2C-methyl-D-erythritol-2,4-cyclo-diphosphate (MEcPP) and accompanied with the release of cytidine monophosphate (CMP). Consequently, the reductive deoxygenation of MEcPP by 1-hydroxy-2- methyl-2(E)-butenyl-4-diphosphate synthase (IspG) leads to 1-hydroxy-2-methyl-2-(E)-butenyl 4-diphosphate (HMBPP) production. At the final step of the reaction, the generation of IPP and DMAPP from HMBPP is mediated by 1-hydroxy-2-methyl-2(E)-butenyl-4-diphosphate reductase (IspH) [20, 83].

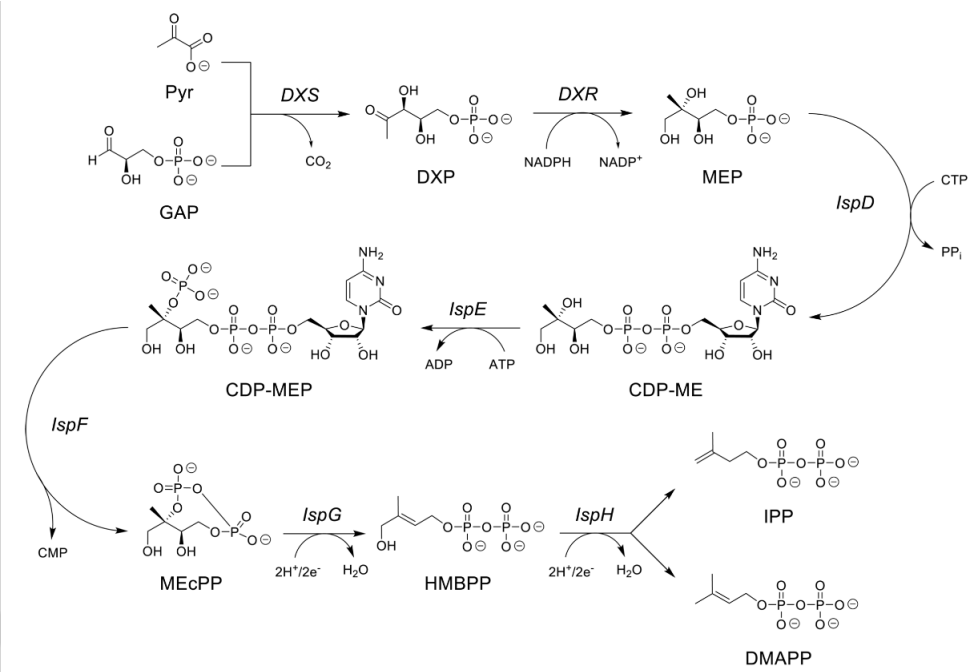

Figure 2.4 The methylerythritol 4-phosphate pathway [20]

The fact that the MEP pathway, vital for pathogens, is not found in humans makes it essential for drug targeting [19, 84].

2.6 1-Deoxy-D-Xylulose 5-Phosphate Reductoisomerase as a Drug Target

2.6.1 Structure and Function

DXR possesses an overall homodimer structure, with V-shaped monomers composed of an N-terminal, a central catalytic, and a C-terminal domains [21, 22]. The N-terminal domain is involved in the binding of NADPH cofactor [85]. The central catalytic domain, along with active site functional residues for binding catalytically essential divalent metal ion (Mg^{2+}, Mn^{2+}, or Co^{2+}) and substrate or inhibitor, contains a flexible loop region that covers the active site by the substrate/inhibitor binding [86, 87]. The α-helical C-terminal domain provides structural support to the catalytic domain [85, 88].

The second step of the MEP pathway, mediated by DXR, comprises the transformation of DXP to MEP. The conversion reaction consists of divalent metal ion-dependent intramolecular isomerization followed by an NADPH cofactor-assisted reduction (Figure 2.5) [81, 89].

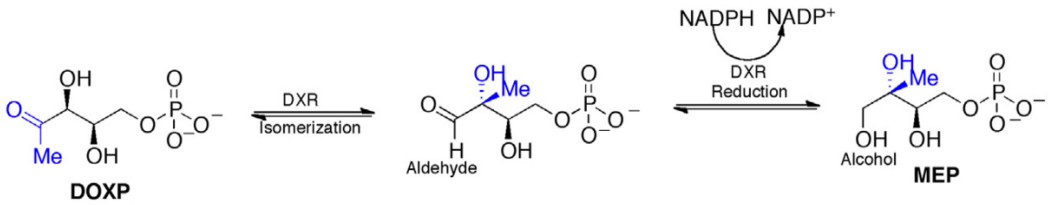

Figure 2.5 DXR-catalyzed reaction steps [23]

Conformational changes induced by NADPH binding facilitate the substrate and inhibitor binding to the enzyme [86, 90]. The catalysis reaction occurs within the enclosed catalytic pocket of the enzyme, created by a flexible loop folding over the active site as a result of substrate or inhibitor binding [21, 91, 92]. Substrate binding to DXR triggers the isomerization step of the reaction, which occurs through either proposed α-ketol-rearrangement or retro-aldol/aldol mechanisms, resulting in intermediate aldehyde generation [23, 92, 93]. The subsequent reduction step involves transfer of pro-S hydride ion from NADPH to *re* face of the formed intermediate [23, 78], and according to the exhibited stereochemical features related to NADPH-mediated reduction, DXR has been categorized as a class B dehydrogenase [78, 94].

2.6.2 Fosmidomycin an Inhibitor of 1-Deoxy-D-Xylulose 5-Phosphate Reductoisomerase

Fosmidomycin is a natural compound isolated from *Streptomyces lavendulae* [81]. Although its mechanism of action has not been identified, fosmidomycin was tested up to early phase II research as a potential treatment for urinary tract infections in the early 1980s [95]. The better antimicrobial activity against Gram-negative bacteria compared to Gram-positive bacteria elucidated the potential inhibitory effect of fosmidomycin on the MEP pathway [81]. According to the structural similarities observed between DXP and fosmidomycin, it has been proposed that fosmidomycin specifically targets the DXR in the MEP pathway [96, 97]. Initially, mixed and competitive mechanisms of fosmidomycin inhibition against DXR were reported [98]. Further study revealed that fosmidomycin inhibits DXR in a competitive mode with DXP but also demonstrates a non-competitive mode with respect to NADPH cofactor. This work conducted by Koppisch et al. describes fosmidomycin as a non-classical competitive inhibitor for DXP based on its observed slow, tight binding action [99].

3
MATERIALS AND METHODS

3.1 Materials

3.1.1 Enzymes, Kits and Chemicals

Taq DNA Polymerase (A.B.T Laboratory Industry, Türkiye, #cat. no. E01-01-50), Phusion High-Fidelity DNA Polymerase (Thermo Fisher Scientific, Lithuania, #cat. no. F-530L), their buffer solutions and $MgCl_2$ solution were used in polymerase chain reaction (PCR) for DNA amplification.

Primers designed for PCR were commercially synthesized by Triogen Biotechnology. PCR product purification was performed by Wizard SV Gel and PCR Clean-up System (Promega, USA, #cat. no. A9281). Plasmid isolation was executed by Wizard Plus SV Miniprep DNA Purification System (Promega, USA, #cat. no. A1330).

The presence of DNA and the length of PCR products were determined in agarose gel electrophoresis by GeneRuler DNA Ladder Mix (Thermo Scientific, USA, #cat. no. SM0333). DNA product concentration was determined in agarose gel by Lambda DNA *Hind*III Digest which was purchased from Amersham Pharmacia Biotech (USA, #cat. no. 27-4048-01). PageRuler Prestained Protein Ladder (Thermo Scientific, USA, #cat. no. 26616) and Spectra Multicolor Broad Range Protein Ladder (Thermo Scientific, USA, #cat. no. 26634) were used to assess the molecular weight of the proteins in SDS-PAGE gel electrophoresis.

*Nde*I and *Hind*III restriction endonucleases and corresponding buffers (Promega) were used in digestion reactions during the thesis. T4 DNA Ligase and Buffer solution of T4 DNA Ligase for ligation reaction were supplied from Promega (#cat. no. M1801). Immobilon-P Polyvinylidene Difluoride Membranes (Sigma-Aldrich, Germany, #cat. no. P2938-1ROL) and Extra Thick Blot Paper (Bio-Rad, USA, #cat. no. 1703967) were used in Western Blot analysis.

All other chemicals used in the experimental studies were supplied by Aldrich, BDH, Bio-Rad, BioFroxx, Sigma, Sigma-Aldrich, Roche, Merck, Eschelon Biosciences, and Invitrogen.

3.1.2 Cloning and Expression Vector Systems

In this thesis study, aLICator Ligation Independent Cloning and Expression Kit 3, Kit 1, Kit 2 (Thermo Scientific, USA); TAGZyme pQE-2; pQE-9, pQE-30, pQE-40 (QIAGEN, Germany); pET101/D-TOPO (Invitrogen, USA); pET-40b(+), pET-41a(+) (Novagen, USA) expression vector systems were used.

3.1.2.1 aLICator Ligation Independent Cloning and Expression Vector Systems

aLICator Ligation Independent Cloning and Expression Systems ensure rapid and effective directional ligation-independent cloning of the target gene and the high-yield expression of encoded protein under the control of the bacteriophage T7 promoter. Protein expression is stimulated by isopropyl β-D-1-thiogalactopyranoside (IPTG) [100]. Each aLICator Ligation Independent Cloning and Expression System Kit provides unique features for bacterial protein expression. The main features of the Kits used in this thesis were described below.

aLICator Ligation Independent Cloning and Expression Kit 3 pLATE31 vector system encodes a C-terminal 6xHis tag, Kit 1 pLATE11 ensures untagged protein expression, Kit 2 pLATE51 encodes an N-terminal 6xHis tag and enterokinase cleavage site. The structures of ampicillin-resistant vectors are given in Figure 3.1.

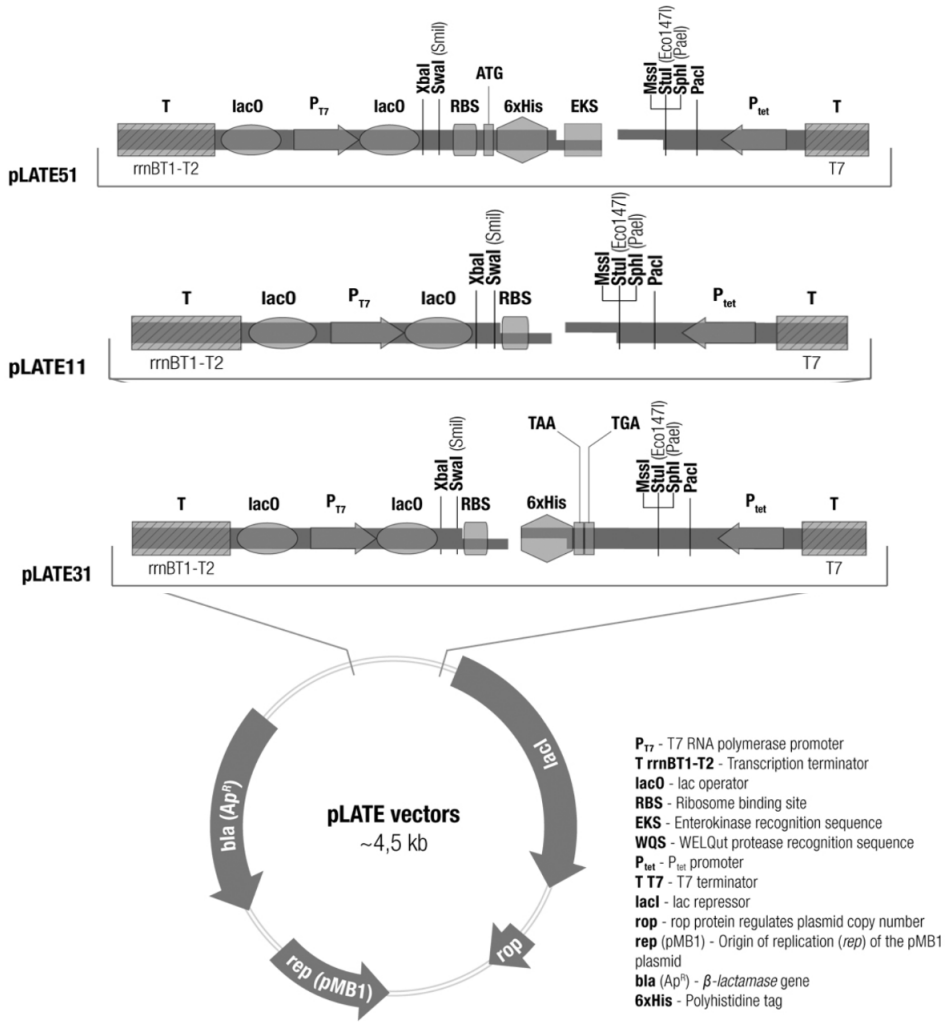

Figure 3.1 aLICator Ligation Independent Cloning and Expression Kit 3, Kit 1, Kit 2 vector constructs [100]

3.1.2.2 pET Expression Vector System

pET expression vector systems provide recombinant protein expression in *E. coli* under the control of the IPTG-inducible T7 promoter. A wide variety of pET vector systems offer distinct properties for protein production. The main features of the pET-40b(+) and pET-41a(+) vector systems used in this thesis were mentioned below.

The pET-40b(+) expression vector system encodes an N-terminal DsbC sequence. Target protein fusion with DsbC enables periplasmic translocation of the protein and the isomerization of disulfide bonds in the periplasmic space. The pET-41a(+) expression vector system encodes an N-terminal Glutathione S-transferase (GST) protein sequence, which is known to enhance the solubility of the fusion protein. Both vector systems encode C-terminal His tags [101]. The kanamycin-resistant

pET-40b(+) and pET-41a(+) vector maps are given in Figure 3.2.

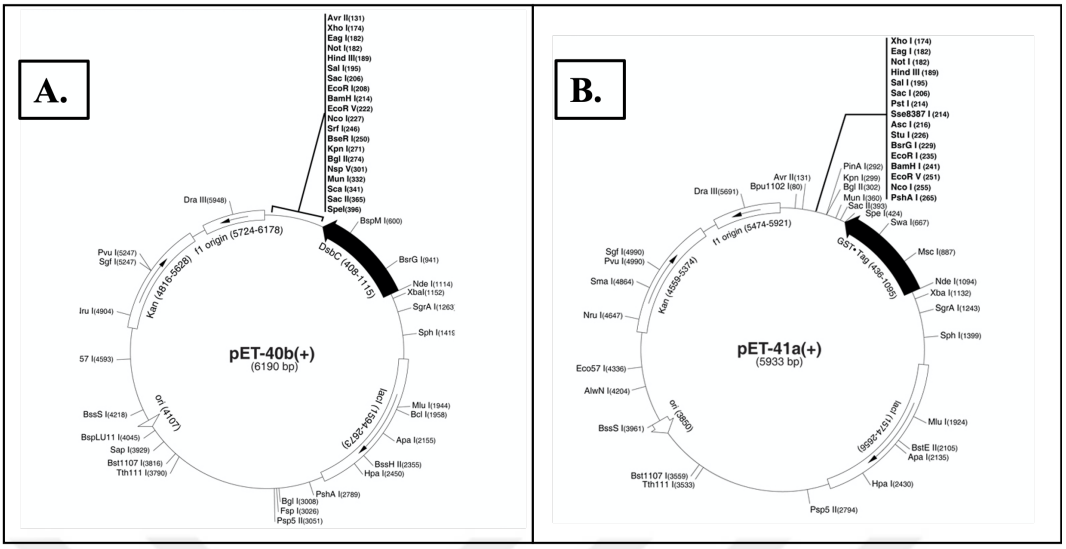

Figure 3.2 pET expression vector maps; A. pET-40b(+) expression vector [102], B. pET-41a(+) expression vector [103]

3.1.2.3 TAGZyme and pQE Expression Vector Systems

The high-yield production of 6xHis-tagged proteins with pQE vector systems in *E. coli* is controlled by the T5 promoter. T5 promoter suppression in pQE vector systems is coordinated by two *lac* operator sequences [104]. The general representation of the pQE vector systems is given in Figure 3.3.

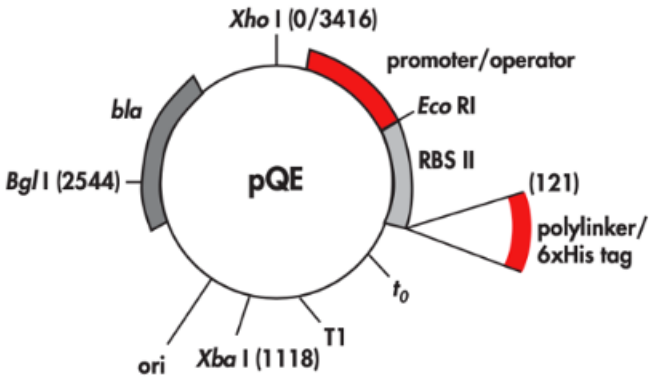

Figure 3.3 pQE expression vector map [104]

Qiagen offers a range of pQE vector sets with different features. pQE vectors used in this thesis study were detailed below. The TAGZyme pQE-2 expression vector derived from pQE-80 vectors ensures high-level N-terminal 6xHis-tagged protein expression and permits exopeptidase tag removal [104, 105]. pQE-9, pQE-30, and pQE-40 expression vector systems encode 6xHis tag on their N-terminal. pQE-40 expression vector also contains a sequence encoding dihydrofolate reductase

(DHFR) fusion protein (6xHis-DHFR tag) for efficient protein translation, correct folding, and stability of peptides. The elements of ampicillin-resistant vectors are given in Figure 3.4.

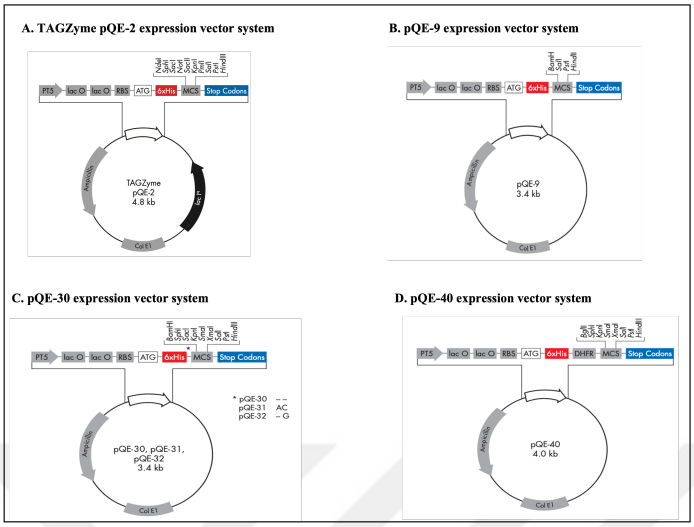

Figure 3.4 TAGZyme pQE-2 (A); pQE-9 (B), pQE-30 (C), pQE-40 (D) vector constructs [104, 105]

3.1.2.4 pET101/D-TOPO Expression Vector System

pET101/D-TOPO expression vector system permits directional cloning of the target gene. The IPTG-inducible T7 promoter enables high-level target protein expression by the pET101/D-TOPO vector system. The expression vector system encodes a C-terminal 6xHis tag for protein purification and detection. In addition, a C-terminal V5 epitope sequence ensures protein detection by the Anti-V5 antibodies [106]. The vector construct is given in Figure 3.5.

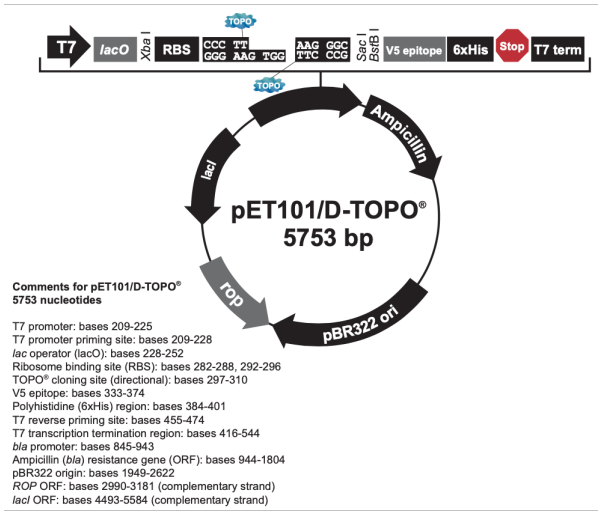

Figure 3.5 pET101/D-TOPO vector elements [106]

3.1.3 Chaperone Plasmids

Chaperone expression in TAKARA chaperone plasmids is controlled by the L-arabinose-inducible *araB* and tetracycline-inducible *Pzt-1* promoters. The chaperone plasmids used in this study, the encoded chaperones, and their promoters are mentioned in Table 3.1.

Table 3.1 TAKARA chaperone plasmids [107]

Plasmid	Chaperone	Promoter
pG-KJE8	*dnaK-dnaJ-grpE-groES-groEL*	*araB* *Pzt-1*
pGro7	*groES-groEL*	*araB*
pG-Tf2	*groES-groEL-tig*	*Pzt-1*

These chaperone plasmids comprise an origin of replication derived from pACYC and a chloramphenicol resistance gene as a marker. The specified features of the chaperone plasmids enable their utilization in combination with *E. coli* expression systems that employ ColE1-type plasmids and possess the ampicillin resistance gene [107].

3.1.4 Primers

Specially designed and commercially synthesized primers for gene cloning studies were listed in Table 3.2.

Table 3.2 Primers used in cloning studies

Organism	Vector System	Gene	Primer	Primer Sequence
N. gonorrhoeae	pLATE31	WT*Ngdxr*	NgdxrF	5'AGAAGGAGATATAACTATGACACCACAAGTCC3'
			NgdxrR	5'GTGGTGGTGATGGTGATGGCCGCGCAGTGTGC3'
		WT*Ngdxr*	17aaNgDxrF	5'AGAAGGAGATATAACTATGCCGTCTGAAAACGC3'
			NgdxrR	5'GTGGTGGTGATGGTGATGGCCGCGCAGTGTGC3'
		WT*Ngdxr*	TPNgdxrF	5'AGAAGGAGATATAACTATGCAAGTCCTGACC3'
			NgdxrR	5'GTGGTGGTGATGGTGATGGCCGCGCAGTGTGC3'
		Opt*Ngdxr*	NgDxrF(H)	5'AGAAGGAGATATAACTATGACCCCGCAGGTTC3'
			NgDxrR(H)	5'GTGGTGGTGATGGTGATGGCCACGGAGGGTACC3'
	pLATE11	WT*Ngdxr*	11FNgdxr	5'AGAAGGAGATATAACTATGACACCACAAGTCCTGACC3'
			11RNgdxr	5'GGAGATGGGAAGTCATTAGCGCAGTGTGCCG3'
	pLATE51	WT*Ngdxr*	51FNgdxr	5'GGTGATGATGATGACAAGACACCACAAGTCCTGACC3'
			51RNgdxr	5'GGAGATGGGAAGTCATTAGCGCAGTGTGCCG3'
	TAGZyme pQE-2	Opt*Ngdxr*	pQE2NgdxrF	5'CGTCATATGATGACCCCGCAGGTTC3'
			pQE2NgdxrR	5'ACCGAAGCTTTAAACGGAGGGTACCG3'
	pQE-9, -30, -40 pET-40b(+) pET-41a(+)	Opt*Ngdxr*	pQENgdxrF	5'AAGCTTACCCCGCAGGTTCTGACC3'
			pQE2NgdxrR	5'ACCGAAGCTTTAAACGGAGGGTACCG3'
	pET101/D-TOPO	Opt*Ngdxr*	101TOPONgdxr(H)F	5'CACCATGACCCCGCAGG3'
			101TOPONgdxr(H)R	5'AACGGAGGGTACCGATGAACGC3'
E. coli	pLATE31	*Ecdxr*	pLATE31Ec(25922)dxrF	5'AGAAGGAGATATAACTATGAAGCAACTCACC3'
			pLATE31Ec(25922)dxrR	5'GTGGTGGTGATGGTGATGGCCGCTTGCGAGACGC3'

3.1.5 *Escherichia coli* Host Strains

BL21(DE3), BL21(DE3) Codon Plus, SHuffle T7 (25 μg/mL streptomycin), XL1-Blue (1 μg/mL tetracycline), JM105 (1 μg/mL tetracycline).

3.1.6 Bacterial Culture Media

Luria-Bertani Medium 100 mL

Table 3.3 Components of Luria-Bertani medium

Ingredient	Amount (g)
Yeast Extract	0.5
Sodium chloride	1
Tryptone	1

All ingredients were dissolved in dH_20 and sterilized by autoclave at 121°C.

Luria-Bertani Agar 100 mL

Table 3.4 Components of Luria-Bertani agar

Ingredient	Amount (g)
Yeast Extract	0.5
Sodium chloride	1
Tryptone	1
Agar	1.5

All ingredients were dissolved in dH_20 and sterilized by autoclave at 121°C.

Super Optimal broth with Catabolite repression Media 100 mL

Table 3.5 Composition of SOC media

Ingredient	Stock Concentration	Amount
Yeast Extract*		2 g
Tryptone*		0.5 g
Sodium chloride*	1 M	1 mL
KCl*	1 M	0.25 mL
Mg^{+2} (filtered)**	2 M	1 mL
Glucose (filtered)**	2 M	1 mL

Step 1: * Ingredients were dissolved in 97 mL of sterile water, then autoclaved and cooled to ambient temperature.
Step 2: ** Ingredients were added to the prepared sterile solution, in step 1, before use.

Terrific Broth 1 L

Table 3.6 Components of Terrific Broth

Ingredient	Working Concentration	Amount
Yeast Extract*	24 g/L	24 g
Tryptone*	20 g/L	20 g
Glycerol*	4 mL/L	4 mL
KH_2PO_4**	0.017 M	2.3 g
K_2HPO_4**	0.094 M	16.4 g

Step 1: * Ingredients at the mentioned amount in Table 3.6 were dissolved in 896 mL of dH_20 and autoclaved.
Step 2: ** Ingredients at the mentioned amount in Table 3.6 were dissolved in 100 mL of dH_20 and autoclaved.
Step 3: Prepared solutions (*, **) were combined.

3.1.7 Stock Solutions and Buffers

Ampicillin (100 mg/mL), Streptomycin (50 mg/mL), Tetracycline (1 mg/mL), Kanamycin (50 mg/mL), Carbenicillin (100 mg/mL), L-arabinose (100 mg/mL), Isopropyl β-D-1-thiogalactopyranoside (20 mg/mL) were dissolved in sterile water and Chloramphenicol (50 mg/mL) was dissolved in 95% ethanol, all prepared stock solutions were sterilized by filtering, and stored at -20°C.

$CaCl_2$ Solution 100 ml

Table 3.7 Components of $CaCl_2$ solution

Ingredient	Amount
100 mM $CaCl_2.2H_2O$	1.47 g
5 mM $MgCl_2.6H_2O$	0.1017 g
5 mM Tris HCl (pH: 7.6)	500 μL

All ingredients were dissolved in dH_20 and sterilized by autoclave at 121°C.

1% Agarose Gel 100 mL

Table 3.8 Components of 1% agarose gel

Ingredient	Amount
Agarose	1 g
1x TAE	100 mL
Ethidium bromide	3.5 μL

30% Acrylamide/Bis-acrylamide 10 mL

Table 3.9 Components of 30% acrylamide/bis-acrylamide

Ingredient	Amount (g)
Acrylamide	2.9
N,N'-Methylene-bis-acrylamide	0.1

Ingredients were dissolved in dH_20.

SDS-PAGE Separating Gel (12%) 20 mL

Table 3.10 Components of SDS-PAGE separating gel

Ingredient	Stock Concentration	Amount
dH_2O		6.7 mL
Tris-HCl (pH: 8.8)	1.5 M	5 mL
SDS	10%	200 μL
Acrylamide/Bis	30%	8 mL
Ammonium Persulfate	10%	150 μL
TEMED		30 μL

SDS-PAGE Stacking Gel (4%) 10 mL

Table 3.11 Components of SDS-PAGE Stacking Gel

Ingredient	Stock Concentration	Amount
dH_2O		6.1 mL
Tris-HCl (pH: 6.8)	0.5 M	2.5 mL
SDS	10%	100 μL
Acrylamide/Bis	30%	1.3 mL
Ammonium Persulfate	10%	60 μL
TEMED		12 μL

Sample Application Buffer for SDS-PAGE 20 mL

Table 3.12 Components of sample application buffer for SDS-PAGE

Ingredient	Working Concentration	Amount
SDS	10%	2 g
Tris-HCl (pH: 6.8)	0.5 M	17.5 mL
Glycerol	5%	1 mL
2-Mercaptoethanol	2.5%	500 μL
Bromphenol blue	0.05%	0.01 g

5x SDS-PAGE Tank Buffer 500 mL

Table 3.13 Components of 5x SDS-PAGE tank buffer

Ingredient	Working Concentration	Amount (g)
Trizma Base	0.025 M	7.5
Glycine	0.192 M	36
SDS	0.1%	2.5

Ingredients were dissolved in dH_20.

Protein Staining Solution 50 mL

Table 3.14 Components of protein staining solution

Ingredient	Working Concentration	Amount
Coomassie Brilliant Blue	0.1%	0.05 g
Methanol	40%	20 mL
Glacial Acetic Acid	10%	5 mL

Final volume was adjusted with dH_2O.

Protein Destaining Solution 500 mL

Table 3.15 Composition of protein destaining solution

Ingredient	Working Concentration	Amount
Methanol	5%	25 mL
Glacial Acetic Acid	7%	35 mL

Final volume was adjusted with dH_2O.

3.1.7.1 Lysis Buffers

Lysis buffer A (pH: 8.0) 1 L

Table 3.16 Composition and preparation instruction of lysis buffer A

Ingredient	Working Concentration	Amount	Application
NaH_2PO_4	50 mM	5.998 g	pH is adjusted with NaOH
Sodium chloride	300 mM	17.54 g	
Imidazole	10 mM	0.68 g	

Final volume was adjusted with dH_2O.

Lysis buffer B (pH: 8.0) 50 mL

Table 3.17 Composition and preparation instruction of lysis buffer B

Ingredient	Working Concentration	Amount	Application
Sodium chloride	100 mM	0.292 g	pH is adjusted with HCl
Tris-HCl (pH: 8.0)	10 mM	500 μL	
2-mercaptoethanol	2 mM	7 μL	

3.1.7.2 Purification Buffers

Equilibration Buffer (pH: 8.0) 500 mL

Table 3.18 Composition and preparation instruction of equilibration buffer

Ingredient	Working Concentration	Amount (g)	Application
NaH_2PO_4	50 mM	2.999	pH is adjusted with NaOH
Sodium chloride	300 mM	8.77	
Imidazole	10 mM	0.34	

Wash buffer (pH: 8.0) 500 mL

Table 3.19 Composition and preparation instruction of wash buffer

Ingredient	Working Concentration	Amount (g)	Application
NaH_2PO_4	50 mM	2.999	pH is adjusted with NaOH
Sodium chloride	300 mM	8.77	
Imidazole	20 mM	0.68	

Elution buffer (pH: 8.0) 500 mL

Table 3.20 Composition and preparation instruction of elution buffer

Ingredient	Working Concentration	Amount (g)	Application
NaH_2PO_4	50 mM	2.999	pH is adjusted with NaOH
Sodium chloride	300 mM	8.77	
Imidazole	150 mM	5.1	

3.1.7.3 Western-Blot Buffers

Phosphate Buffered Saline 1 L

Table 3.21 Composition of phosphate buffered saline

Ingredient	Working Concentration	Amount
Sodium chloride	0.15 M	900 mL
Na_2HPO_4 (pH: 7.4)*	0.1 M	100 mL

* pH adjustment of Na_2HPO_4 was carried out with KH_2PO_4.

Phosphate Buffered Saline-Tween-20

Table 3.22 Composition of phosphate buffered saline-Tween-20

Ingredient	Amount
PBS	1000 mL
Tween-20	2 mL

Ingredients were mixed.

Transfer Buffer 1 L

Table 3.23 Composition of transfer buffer

Ingredient	Working Concentration	Amount
Glycine*	39 mM	2.93 g
Trisma-Base*	48 mM	5.81 g
SDS*	1.3 mM	0.375 g
Methanol	20%	200 mL

Step 1: * Ingredients were dissolved in 800 mL of dH_20.
Step 2: Methanol was added to the solution just before application.

Blocking Buffer (5%)

Table 3.24 Composition of 5% blocking buffer

Ingredient	Amount
Non-fat milk powder	5 g
PBS-Tween 20	100 mL

3.1.7.4 Buffer Solutions for Enzyme Activity and Inhibition Studies

Tris-HCl Buffer (pH: 8.0)

The reaction stock solution of 108 mM Tris-HCl (pH: 8.0) was prepared by diluting the 0.5 M Tris-HCl. HCl was used for pH adjustment.

Substrate Stock Solution (DXP)
50 mM stock DXP solution, prepared using sterile dH_2O.

Cofactor Stock Solution (NADPH)
50 mM stock NADPH solution, prepared using sterile dH_2O.

$MgCl_2$ Stock Solution
833.33 mM stock $MgCl_2$ solution, prepared using sterile dH_2O.

Inhibitor Stock Solution (Fosmidomycin)
200 mM stock FSM solution, prepared using sterile dH_2O.

3.1.7.5 Laboratory Equipments Used in Experiments

Table 3.25 List of laboratory equipment used in the study

Equipment	Purpose of use
Thermal cycler - Eppendorf	Amplification of target DNA sequences
Horizontal electrophoresis system - Bio-Rad	Analyzing and size-based separation of DNA
Vertical electrophoresis system - Bio-Rad	Size-based separation and analyzing of proteins
UV-Visible spectrophotometer - Shimadzu	OD measurement
Autoclave - Systec	Material and equipment sterilization
Incubator - Binder	Microbial culture development
Microcentrifuge - Sigma	Substance precipitation and separation
Vortex - Heidolph	Substance mixing
pH meter - Cyberscan	pH measurement
Water bath - Kerman	Heat shock transformation
Magnetic stirrer - Heidolph	Substance mixing
Refrigerated centrifuge - Sigma	Temperature-depended separation
Sonicator - Bandelin	Cell disruption
Shaking incubator - GFL	Microbial culture development, protein expression
Refrigerator (-80°C) - Heto	Storage of culture stocks
Refrigerator (-20°C) - Beko	Storage
Refrigerator (+4°C) - Arçelik	Storage
Microplate reader - Epoch	Activity, Kinetic, Inhibition studies
Transfer Cell - Bio-Rad	Western Blot
Ice maker machine - Optic ivymen system	Transformation
Shaker - Labnet	Western Blot

3.2 Methods

Unless otherwise stated, all experimental procedures were applied according to Sambrook et al [108].

3.2.1 Target Gene Identification

The *dxr* gene was the target for cloning and expression studies in this thesis. In the first stage of the thesis, the DXR-encoding gene sequence of *Neisseria gonorrhoeae*

(ATCC 49226) was downloaded from the NCBI database [109] and synthesized commercially. In the next stage, the DXR-encoding gene sequence of *Neisseria gonorrhoeae* (ATCC 49226) was synthesized as a codon-optimized and harmonized gene sequence. Then, cloning and expression studies were carried out for the *dxr* gene encoded by *E. coli* ATCC 25922 [110]. DNA of *E. coli* ATCC 25922 from the laboratory infrastructure was used as a template for *E. coli*-encoded *dxr* gene cloning. The genes were named for traceability throughout the thesis and mentioned in Table 3.26.

Table 3.26 Gene sequence accession numbers and nomenclatures

Gene	NCBI ID	ATCC Bank	Nomenclature
Neisseria gonorrhoeae (ATCC 49226) *dxr*	CP045728.1	-	WT*Ngdxr*
Neisseria gonorrhoeae (ATCC 49226) *dxr* – codon optimized and harmonized	-	-	Opt*Ngdxr*
Escherichia coli (ATCC 25922) *dxr*	-	ATCC 25922	*Ecdxr*

3.2.2 Cloning of Target Gene into the Expression Vector Systems

3.2.2.1 Design of Oligonucleotide Primers

Specific primers were designed according to the target gene sequence and the vector manufacturer's instructions [100, 101, 104–106]. All designed primers are given in Table 3.2.

3.2.2.2 Polymerase Chain Reaction

Polymerase chain reaction (PCR) for a gene to be cloned was performed with the Phusion High-Fidelity DNA Polymerase. Phusion High-Fidelity DNA Polymerase performed reaction components were mentioned based on the WT*Ngdxr* amplification reaction with forward (NgdxrF) and reverse (NgdxrR) primers and were given in Table 3.27. First, the components listed in Table 3.27, except the enzyme, were added to the tube.

Table 3.27 PCR components

Reagent	Amount/Concentration
dH_2O	29.5 μL
5XPhusion HF buffer	10 μL
2 mM dNTP mix	0.2 mM
20 μM Forward Primer	0.5 μM
20 μM Reverse Primer	0.5 μM
Template DNA (1 ng/μL)	1 ng
DMSO	1.5 μL
Phusion High-Fidelity DNA Polymerase (stok 2u/μL)	1 u

The reaction was subjected to pre-denaturation at 95°C for 5 min. After enzyme addition, the reaction was carried out for 30 cycles: denaturation at 94°C for 90 seconds, annealing at 55°C for 120 seconds, and elongation at 72°C for 120 seconds. Finally, the reaction was terminated by a final elongation step at 72°C for 10 minutes.

3.2.2.3 Agarose Gel Electrophoresis

DNA sequence analyses were carried out using agarose gel electrophoresis. 1% agarose gel preparation and analysis procedure are described below. 1 g agarose was mixed with 100 mL 1x TAE and dissolved by heating for 5 minutes in the microwave. Then, 3.5 μL of ethidium bromide was added to the solution. The solution was poured into the gel mold after comb insertion. The process of gelation was conducted for 30 minutes. After gel solidification, enough buffer was added to cover the gel surface, and the combs were removed. Samples were treated with SAB and loaded onto the gel. In addition, GeneRuler DNA Ladder Mix and Lambda DNA *Hind*III Digest were also loaded onto the gel. Samples were exposed to a constant electric field of 45 mA for 1 hour. The gel was visualized under UV light at the end of the electrophoresis.

3.2.2.4 Preparation of Competent Host Cells Using $CaCl_2$

The cells from -80°C stock were streaked on LB agar by streak plate technique. Plates were incubated overnight at 37°C. A single bacterial colony was collected from agar with a sterile toothpick and inoculated into 5 mL LB broth for overnight incubation at 37°C, 180 rpm. 500 μL of an overnight culture was transferred into 50 mL LB broth. The culture was incubated at 37°C, 180 rpm until an optical density at a wavelength of 600 nanometers (OD_{600nm}) range of 0.3-0.4. 50 mL of culture was divided into two sterile tubes and centrifuged at 4°C, 5000 rpm for 5 minutes. The supernatant fraction was discarded from the tubes the pellets were resuspended in 25 mL of $CaCl_2$ and kept on ice for 30 minutes. Cells were subjected to the second centrifugation for 5 minutes at 4°C, 5000 rpm. Finally, supernatants were discarded; pellets were resuspended in 1 mL of $CaCl_2$ solution and placed on ice for 2 hours [108].

3.2.2.5 Target Gene Cloning into the aLICator Ligation Independent Cloning and Expression Vector System

The PCR products were purified with Promega Wizard SV Gel and PCR Cleaning System according to the manufacturer's instructions [111]. The concentration

of purified PCR product before gene cloning into pLATE31, pLATE11, and pLATE51 aLICator Ligation Independent Cloning and Expression Vector Systems was determined by agarose gel electrophoresis. The optimal amount of PCR product for Ligation Independent Cloning (LIC) reaction was calculated according to the vector system handbook. Based on the LIC reaction similarities, only the LIC reaction of the WT*Ngdxr* gene to the pLATE31 system will be detailed in this section to avoid repetition. The components of the LIC reaction for WT*Ngdxr* cloning into pLATE31 were presented in Table 3.28.

Table 3.28 LIC reaction components for WT*Ngdxr* gene cloning into pLATE31

Component	Amount
5X LIC Buffer	2 μL
Purified PCR product (100 ng/μL)	77 ng
Water, nuclease-free	6.23 μL
T4 DNA Polymerase (1u/μL)	1 u

The prepared mixture was incubated at room temperature for 5 minutes. 0.5 M EDTA at a volume of 6 μL was added to the mixture for reaction termination. Adding 1 μL (60 ng) of the pLATE vector to the reaction provides the target gene annealing into the vector system. The final mixture was mixed well and incubated at room temperature for 5 minutes [100].

3.2.2.6 Opt*Ngdxr* Cloning into the pQE and pET Expression Vector Systems

Cloning the target gene into the pQE and pET expression vector systems was performed by restriction digestion of the insert and vector and subsequent ligation with T4 ligase (Promega, #cat. no. M180B) [108]. Appropriate restriction endonucleases were selected according to the gene sequence and vector multiple cloning site analysis. Due to the more than one pQE/pET vector system usage in this thesis, to avoid confusion, digestion ligation reactions only for TAGZyme pQE-2 and the target Opt*Ngdxr* gene were presented in this section. The target gene cloning into the pQE and pET vector systems was performed similarly. The TAGZyme pQE-2 vector and target Opt*Ngdxr* gene digestion reaction components were given in Table 3.29.

Table 3.29 Digestion reaction components

Reagent	Working Amount	
	Vector Digestion	Gene Digestion
Sterile, deionized water	-	6.8 μL
MULTI-CORE Buffer	2 μL	2 μL
Acetylated BSA (10 μg/μL)	0.1 μg	0.1 μg
TAGZyme pQE-2 miniprep (0.05 μg/μL)	0.048 μg	-
Opt*Ngdxr* clean-up (0.1 μg/μL)	-	0.05 μg
*Nde*I (10 u/μL)	0.25 u	0.25 u
*Hind*III (10 u/μL)	0.25 u	0.25 u
Nuclease-free water was added to a final volume of 20 μl		

The prepared reaction mixtures were incubated at 37°C for 1 hour. Clean-up was executed for digestion products, and the product concentration before ligation was determined by agarose gel electrophoresis. Ligation reactions at different molar ratios (insert:vector) were prepared according to the T4 DNA ligase manufacturer's instructions [112], and reaction components were provided in Table 3.30.

Table 3.30 Ligation reaction components

Reagent	Working Amount		
	1:1	**1:3**	**3:1**
Vector DNA (55 ng/μL)	5.5 ng	5.5 ng	5.5 ng
Insert DNA (55 ng/μL)	13.7 ng	4.57 ng	41.09 ng
Ligase 10X Buffer	1 μl	1 μl	1 μl
T4 DNA Ligase	1 μl	1 μl	1 μl
Nuclease-free water was added to a final volume of 10 μl			

The ligation reaction was carried out for 3 hours at room temperature.

3.2.2.7 Target Gene Cloning into the pET101/D-TOPO Expression Vector Systems

The target gene cloning into the pET101/D-TOPO vector system was conducted according to the manufacturer's instructions [106]. The cloning reaction was prepared in two ratios (Table 3.31) according to the protocol indicated for subsequent *E. coli* Chemically Competent Cell transformation.

Table 3.31 pET101/D-TOPO cloning reaction components

Reagent	Working Amount	
	1:2	**2:1**
Clean-up (45 ng/μl)	20.43 ng	81.72 ng
Salt Solution	1 μl	1 μl
Sterile water	3.546 μl	2.14 μl
TOPO vector	1 μl	1 μl
Sterile water was added to a final volume of 6 μl		

3.2.2.8 Transformation of the Recombinant Plasmid into the *E. coli* Cells

200 μL of competent *E. coli* cells were mixed with samples from LIC/ligation reactions. The recombinant plasmid and competent cell mixture was incubated on ice for 30 minutes. After being incubated on ice, the sample was exposed to heat shock at 42°C for 90 seconds in a water bath. Then, the sample was gently placed on ice and held for 2 minutes. 800 μL SOC medium was added to the sample and incubated at 37°C for 30 minutes. Transformed cells were spread onto LB agar plates supplemented with appropriate antibiotics and incubated overnight at 37°C. Recombinant pET101/D-TOPO vector system transformation into the BL21 Star(DE3) One Shot Chemically Competent *E. coli* host strain was performed according to the manufacturer's instructions [106].

3.2.2.9 Transformation of the Recombinant Plasmid into the Chaperone-competent *E. coli* Cells

The transformation of recombinant pLATE31 (WT*Ngdxr* in pLATE31) into the chaperone-competent *E. coli* BL21(DE3) host strain was performed according to the TAKARA Chaperone Plasmid System manual [107]. Briefly, the isolated recombinant pLATE31 vector at a volume of 2 μL was added to 50 μL of chaperone-competent *E. coli* BL21(DE3) cells. The recombinant vector and chaperone-competent *E. coli* BL21(DE3) cell mixture was incubated for 30 minutes on ice and then subjected to heat shock at 42°C for 90 seconds. The samples were incubated on ice for 2 minutes. 350 μL SOC medium was introduced to the sample, and the sample was incubated for 30 minutes at 37°C, 180 rpm. Transformed cells were spread onto 20 μg/mL chloramphenicol and 100 μg/mL ampicillin-supplemented LB agar and incubated overnight at 37°C.

3.2.2.10 Genomic DNA isolation

100 μL of overnight culture was centrifuged for 7 minutes at 13000 rpm under ambient conditions (all centrifugation steps were performed under ambient conditions). The obtained pellet was dissolved in 100 μL of sterile dH_2O and then boiled for 10 minutes. The sample was centrifugated for 15 minutes at 13000 rpm, and the collected supernatant was used as the DNA template.

3.2.2.11 Recombinant Plasmid DNA Isolation

The Wizard Plus SV Minipreps DNA Purification System was used to isolate the recombinant plasmid from the host cell. All steps were performed according to the

manufacturer's instructions [113]. The pure recombinant vector was eluted with 40 μL of nuclease-free water.

3.2.2.12 Colony PCR for the Analysis of Recombinant Clones

Colony PCR was carried out with *Taq* DNA Polymerase. First, the components listed in Table 3.32, except the enzyme, were introduced into the tube.

Table 3.32 Colony PCR components

Reagent	Amount/Concentration
dH_2O	13.5 μL
10x PCR Buffer	2.5 μL
2 mM dNTP mix	0.2 mM
20 μM Forward Primer	0.5 μM
20 μM Reverse Primer	0.5 μM
Template DNA (Miniprep DNA)	5 μL
Taq DNA Polymerase (2.5 u/μL)	0.625 u

The reaction was subjected to pre-denaturation at 95°C for 5 min. Then, the reaction was carried out in 30 cycles by enzyme addition, each comprising denaturation at 95°C for 30 seconds, binding at 55°C for 30 seconds, and elongation at 72°C for 60 seconds. The final elongation step was performed at 72°C for 5 minutes.
T7 Promoter primer (TAATACGACTCACTATAGGG) was used to control the availability of the target gene in pET vector systems. In addition to the T7 Promoter primer, the T7 Terminal primer (GCTAGTTATTGCTCAGCGG) was used in cloned gene confirmation in pQE expression vector systems. However, colony PCR for other clones was carried out using gene-specific primers.

3.2.2.13 Gene Sequencing for the Analysis of Recombinant Clones

The WT*Ngdxr* cloned pLATE31 vector system was isolated from the host cell [113], and bidirectionally sequenced for target gene confirmation. Bidirectional sequencing was performed by the Sanger sequencing method using the universal T7 promoter (Forward) (5'TAATACGACTCACTATAGGG3') and M13/pUC (Reverse) (5'AGCGGATAACAATTTCACAGG3') primers. Gene sequencing was performed only for WT*Ngdxr* in pLATE31; all other clones were confirmed by colony PCR.

3.2.3 Expression Studies of 1-Deoxy-D-Xylulose 5-Phosphate Reductoisomerase

Recombinant *E. coli* BL21(DE3) cells were incubated overnight in 5 mL LB broth supplemented with appropriate antibiotic at 37°C, 180 rpm. 500 μL of the overnight culture was introduced into 50 mL of LB broth supplemented with the same antibiotic. The recombinant cells were incubated at 37°C, 180 rpm, until the OD_{600nm} reached a range of 0.5–0.6. The gene expression was induced by the addition of 0.5 mM IPTG. Sample collection at a volume of 3 mL was carried out at the 3rd hour, 5th hour, and overnight. Samples were centrifuged for 20 minutes at 4°C, 500 rpm. The obtained cell pellets were resuspended in 500 μL of lysis buffer. The cells were lysed by sonication for 2 minutes (10 sec on, 10 sec off) at 20% amplitude and then harvested by centrifugation at 14000 rpm for 20 minutes at 4°C. Supernatants were gently separated from pellets, and pellets were resuspended in 200 μL of sterile dH_2O. The standard protocol for protein expression is detailed above. Any changes/optimizations will be specified in the Results and Discussion chapter.

3.2.3.1 Co-expression with Chaperone Plasmids

Co-expression of WT*Ngdxr* in pLATE31 with the chaperone plasmids in the *E. coli* BL21(DE3) host strain was performed according to the TAKARA Chaperone Plasmid System manual [107]. Briefly, chaperone-competent *E. coli* BL21(DE3) cells containing recombinant pLATE31 were overnight incubated in 5 mL LB Broth supplemented with 20 μg/mL chloramphenicol and 100 μg/mL ampicillin at 37°C, 180 rpm. 500 μL from the overnight culture was inoculated into the 50 mL of LB broth supplemented with the relevant antibiotics, as well as 0.5 mg/mL L-arabinose and 1 ng/ml tetracycline for induction of chaperone expression. The culture was incubated at 37°C, 180 rpm, until the OD_{600nm} reached about 0.5-0.6. At this stage, recombinant protein induction was performed with IPTG at a final concentration of 0.5 mM. All subsequent steps applied after IPTG induction were the same as those mentioned in subsection 3.2.3.

3.2.4 Molecular Weight Calculation

The estimated molecular weight of the target protein was calculated by the Expasy ProtParam tool [114] and the AAT Bioquest Peptide and Protein Molecular Weight Calculator[115].

3.2.5 Recombinant Protein Purification

The recombinant 6xHis-tagged proteins were purified by the HisTALON Gravity Column (Clontech, #cat. no. 635655) [116]. The column was initially equilibrated with 10 mL of equilibration buffer. The cell lysate was loaded into the column. Upon the flow of the cell lysate through the column, the column was equilibrated with 8 mL equilibration buffer and washed with 7 mL wash buffer. His-tagged protein was eluted from the column with the 5 mL of elution buffer. For each purification step, the flow through, wash (W1-W3), and elution (E1-E8) samples were collected. At the end of purification, column regeneration was performed with a 20 mL equilibration buffer.

3.2.6 Sodium Dodecyl Sulphate Polyacrylamide Gel Electrophoresis

Expressed and purified proteins were confirmed by SDS-PAGE analysis. 12% separating and 4% stacking gels were prepared using the components indicated in Table 3.10 and Table 3.11. The collected supernatants and resuspended pellets were prepared by mixing with the SDS sample application buffer at a 1:1 ratio. Then, samples were kept in boiled water for 5 minutes before loading onto the gel. The SDS-PAGE tank was filled with 1x SDS-PAGE Tank Buffer and an electric field at 85 V was applied for sample migration. After running, the gel was stained in protein staining solution at 60°C, 70 rpm for 15 minutes. Treatment with the destaining solution was performed twice for 10 minutes at 60°C, 70 rpm, and 37°C, 70 rpm, respectively. Protein bands were visualized as a consequence of the applied steps [117].

3.2.7 Western Blot Analysis

The prepared samples were separated on SDS-PAGE and were blotted from the gel onto the nitrocellulose extra blotting membranes with transfer buffer at 15 V for 15 min. After 10 minutes of washing in PBS-Tween 20, the membrane was blocked overnight at 4°C in a 5% blocking solution. The blocking step was followed with membrane washing within PBS-Tween 20 for 10 minutes. The membrane was incubated for 1 hour with primary Anti-6-His antibody produced in rabbit (#cat. no. SAB4301134) diluted in blocking solution at a ratio of 1:250. The primary antibody-treated membrane was washed 3 times with PBS-Tween 20. Subsequently, the membrane was incubated for 1 hour with a Goat Anti-Rabbit IgG (H+L) (Human IgG Adsorbed) Horseradish Peroxidase Conjugate (#cat. no. 170-6515) secondary antibody diluted in blocking solution at 1:5000. The membrane was washed twice with PBS-Tween 20, once with PBS and once with dH_2O, respectively. In the

last step, the membrane was immersed in the 3,3′-Diaminobenzidine (DAB) colour development solution to visualize the protein band, and finally reaction was stopped with dH_2O.

3.2.8 Bradford Assay

The protein concentration in the collected elution samples was determined with the Bradford Assay. BSA samples were used as standards, and the reaction mixture at the final volume of 200 μL (194 μL 1x dye reagent was gently mixed with 4 μL BSA standards) was prepared. Samples were incubated in the dark for 5 minutes at room temperature. At the end of the incubation, prepared samples were gently shaken, and absorbance measurement was carried out at 595 nm with a microplate reader spectrophotometer. A graph of the concentration versus absorbance was generated. The procedure described above was applied to determine the protein concentration in the collected eluate samples, and the absorbance-based protein concentration was calculated using the standard curve equation (y=ax+b).

3.2.9 Enzyme Activity and Inhibition Studies

The absorbance measurements for all procedures detailed below were performed at 340 nm with a Biotek Epoch UV Plate Reader in a 96-well plate.

3.2.9.1 Enzyme Activity Assay

The activity of the target enzyme was determined by measuring the oxidation of the NADPH cofactor. The reaction mixture was prepared at a volume of 200 μL, as follows: firstly, 100 mM Tris-HCl (pH: 8.0), 10 mM $MgCl_2$, 0.5 mM NADPH, 2 μL (4.49 mg/mL) DXR were incubated at room temperature for 10 minutes by shaking at 300 rpm and the reaction was started with 0.5 mM DXP substrate. Then, short shaking was applied, and the absorbance was measured for 2 minutes. The reaction activity was calculated using equation 3.1.

$$\Delta A_{340}/min \tag{3.1}$$

The specific activity of the enzyme (3.2) was determined by taking into account the calculated enzyme activity value, the molar absorption coefficient of NADPH (ε_{NADPH}=6200 M^{-1} cm^{-1}) [118] , the total reaction volume (V_T), 96-well corning UV plates pathlength (0.56 cm) and the amount of enzyme (mg). The specific activity of the enzyme in the units of u/mg was established using equation 3.2.

$$u/mg = \frac{(\Delta A_{340}/min \times V_T) \,/\, (\varepsilon_{NADPH} \times Pathlength\, of\, the\, Light)}{The\, Amount\, of\, Enzyme\, Used\, in\, the\, Reaction} \tag{3.2}$$

3.2.9.2 Kinetic Parameters Determination

The reaction mixture for kinetic parameters determination was prepared at a volume of 200 μL containing 100 mM Tris-HCl, 10 mM $MgCl_2$, 0.15 mM NADPH, 2 μL (3.949 mg/mL) enzymes, and variable concentrations of DXP (0.5-0.25-0.125-0.0625-0.03125 mM). The prepared mixture was incubated at room temperature for 10 minutes by shaking at 300 rpm. The reaction was initiated with DXP, and measurement was carried out in triplicate for 5 minutes. The steady-state kinetic graph was generated in GraphPad Prism 6.0 (GraphPad Software Ltd., La Jalla, USA), and K_m and V_{max} values were calculated using the enzyme kinetics module of the software.

3.2.9.3 Half-Maximal Inhibitory Concentration Determination

For inhibition studies with fosmidomycin (FSM), the reaction mixture was prepared at a volume of 200 μL: 100 mM Tris-HCl (pH: 8.0), 10 mM $MgCl_2$, 0.5 mM NADPH, 2 μL (4.49 mg/mL) enzyme, and dilution series of FSM (125 nM, 156.25 nM, 187.5 nM, 250 nM). The prepared mixture was incubated for 10 minutes at room temperature by shaking at 300 rpm. Then, the reaction was initiated with DXP at a final concentration of 0.5 mM, and the absorbance measurement was performed for 2 minutes. The sample substituted with water instead of fosmidomycin was used as a negative control. The percentage of fosmidomycin inhibition was calculated using equation 3.3.

$$Inhibition\,(\%) = \frac{\Delta A_{340}c - \Delta A_{340}s}{\Delta A_{340}c} \times 100 \tag{3.3}$$

$A_{340}c$: absorbance of the control sample
$A_{340}s$: absorbance of the analyzed sample

The IC_{50} value of fosmidomycin was calculated by plotting the percentage inhibition values against the natural logarithmic values of four different concentrations of the inhibitor using GraphPad Prism 6.0 (GraphPad Software Ltd., La Jalla, USA).

4
RESULTS AND DISCUSSION

Within the scope of the thesis, studies on 1-deoxy-D-xylulose 5-phosphate reductoisomerase production were performed in two stages. The first stage comprises *Neisseria gonorrhoeae* 1-deoxy-D-xylulose 5-phosphate reductoisomerase (*Ng*DXR) production, while the second includes production of *Escherichia coli* 1-deoxy-D-xylulose 5-phosphate reductoisomerase (*Ec*DXR) and studies performed will be given, respectively.
The methods applied for the recombinant production of *Neisseria gonorrhoeae* 1-deoxy-D-xylulose 5-phosphate reductoisomerase (*Ng*DXR) during the thesis period, were summarized in Figure 4.1 to facilitate follow-up.

Expression strategies for *Ng*DXR production were categorized according to the gene used. Each study indicated in Figure 4.1 will be discussed below.

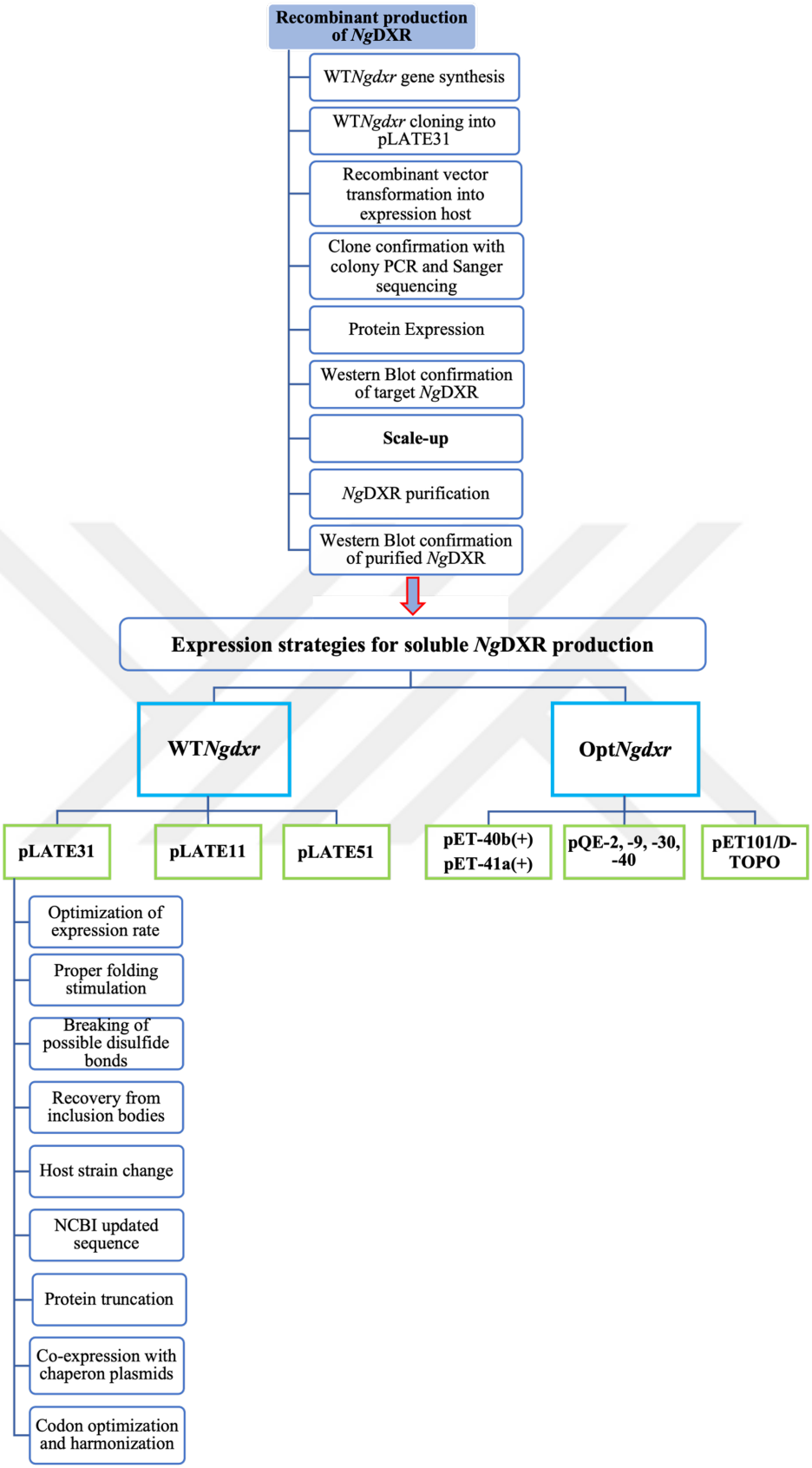

Figure 4.1 Studies applied for recombinant production of *Ng*DXR

4.1 Control of Commercially Synthesized WT*Ngdxr* by Agarose Gel Electrophoresis

The 1-deoxy-D-xylulose 5-phosphate reductoisomerase gene (*dxr*) sequence of *Neisseria gonorrhoeae* American Type Culture Collection (ATCC) 49226 strain (WT*Ngdxr*) was downloaded from NCBI (CP045728.1:1701541-1702725) and synthesized commercially. The WT*Ngdxr* gene sequence is given in Figure 4.2

```
ATGACACCACAAGTCCTGACCATATTAGGCAGTACCGGCAGCATAGGCGAAAGCACGC
TGGACGTTGTCTCCCGCCATCCCGAAAAATTCCGCGTATTCGCGCTGGCAGGGCATAAG
CAGGTCGAGAAACTGGCGGCTCAATGTCAAACGTTCCGCCCCGAATATGCCGTCGTTG
CCGATGCCGAACACGCCGCCCGGCTTGAAGCCCTGTTGAAACGCGACGGCACGGCGA
CTCAGATTTTACACGGCGCGCAGGCATTGGTTGACGTTGCGTCTGCCGACGAAGTCAG
CGGCGTCATGTGCGCCATCGTCGGGGCGGCGGGGCTGCCTTCCGCGCTCGCAGCGGCG
CAAAAAGGCAAAACCATTTATCTGGCAAACAAAGAAACGCTGGTGGTTTCCGGCGCG
TTGTTTATGGAAACCGCCCGCGCAAACGGCGCGGCAGTGTTGCCCGTCGACAGCGAAC
ACAACGCCATTTTCCAAGTTTTGCCGCGCGATTACACAGACCGTCTGAACGAACACGG
CATCGATTCGATTATCCTGACCGCTTCCGGCGGCCCGTTTTTAACAACCGATTTAAGCA
CGTTCGACAGCATTACGCCCGAGCAGGCGGTCAAACACCCCAATTGGCGTATGGGGCG
CAAAATCTCCGTCGATTCAGCCACTATGGCAAACAAGGGCTTGGAACTGATTGAAGCG
CATTGGCTGTTCAACTGTCCGCCCGACAAACTCGAAGTCGTCATCCATCCCCAATCCGT
GATACACAGTATGGTGCGCTACCGCGACGGCTCCGTGCTGGCGCAACTGGGCAATCCC
GATATGCGAACGCCCATCGCCTATTGTTTGGGCTTGCCCGAGCGCATCGATTCGGGTGT
CGGCAAACTCGATTTCGGCGCATTGTCCGCGCTGACCTTCCAAAAGCCCGACTTCGGC
CGCTTCCCCTGCCTGAAGTTCGCCTATGAAACCATAAACGCAGGCGCAGCCGCGCCCT
GCGTATTGAACGCCGCCAACGAAACCGCCGTCGCCGCCTTTTTGGACGGACAGATTAA
GTTTACCGACATTGCCAAAACCGTCGCCCACTGTCTTGCACAAGACTTTTCAAACGGC
ATGGGCGATATAGAAGGACTGTTGGCGCAAGATGCCCGGACACGCGCACAAGCGCGG
GCATTTATCGGCACACTGCGCTGA
```

Figure 4.2 *dxr* gene sequence of *Neisseria gonorrhoeae* ATCC 49226 strain

Lyophilized WT*Ngdxr* was dissolved in sterile dH_20 and diluted to a 1 ng/μL stock concentration. 1 ng of the WT*Ngdxr* was analyzed on a 1% agarose gel to check the availability of the gene at the correct size (Figure 4.3).

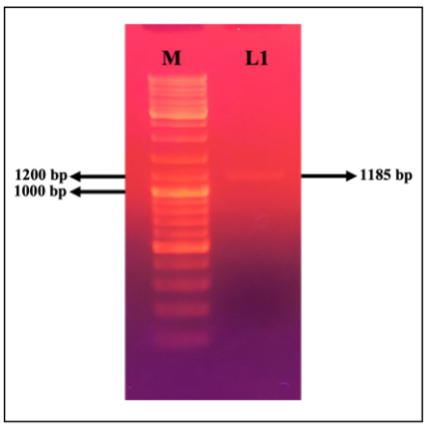

Figure 4.3 WT*Ngdxr* gene confirmation; M: GeneRuler DNA marker, L1: WT*Ngdxr* (1 ng)

The 1185 bp long WT*Ngdxr* gene was confirmed in agarose gel, and gene cloning studies were performed to accomplish the ultimate aim of the thesis study.

4.2 Studies for Recombinant Production of *Ng*DXR

4.2.1 Subcloning of WT*Ngdxr* Gene into the pLATE31 Expression Vector System

The WT*Ngdxr* gene was amplified with Phusion High-Fidelity DNA Polymerase using specifically designed forward (NgdxrF) and reverse (NgdxrR) primers before cloning into aLICator Ligation Independent Cloning and Expression Kit 3 (pLATE31).

The correct size of the 1185 base pairs long WT*Ngdxr* was confirmed by agarose gel electrophoresis (Figure 4.4).

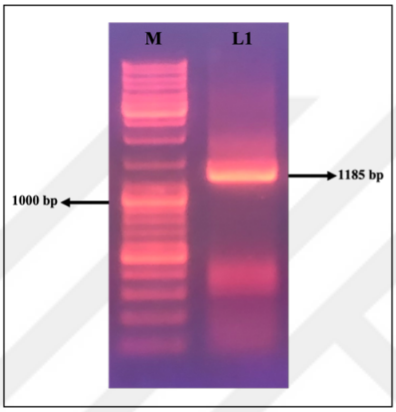

Figure 4.4 Agarose gel image of WT*Ngdxr* amplified with forward (NgdxrF) and reverse (NgdxrR) primers; M: GeneRuler DNA marker, L1: 1185 long amplified WT*Ngdxr*

WT*Ngdxr* was then cloned into the pLATE31 expression vector system, and the recombinant pLATE31 was transformed into the competent *E. coli* BL21(DE3) expression host strain. The availability of the target insert in the selected colonies was checked by colony PCR using *Taq* polymerase and specific (NgdxrF and NgdxrR) primers (Figure 4.5).

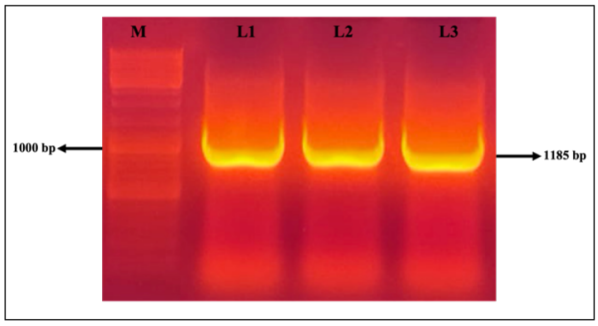

Figure 4.5 Colony PCR results of recombinant *E. coli*BL21(DE3) host cells; M: GeneRuler DNA marker, L1-L3: Colony PCR products of the selected recombinant colonies

Positive results were observed from the selected recombinant colonies.

In addition to colony PCR, the precise target gene availability was confirmed by bidirectional Sanger sequencing with T7 promoter (forward) and M13/pUC (reverse) universal primers.

The bidirectional Sanger sequencing results and WT*Ngdxr* were aligned using the Multiple Sequence Comparison by Log-Expectation (MUSCLE) [119] from European Molecular Biology Laboratory-European Bioinformatics Institute (EMBL-EBI) online tools. Jalview images of alignment results, chromatogram images of the Sanger sequencing with forward and reverse universal primers were given in Figures 4.6, 4.7, and 4.8, respectively.

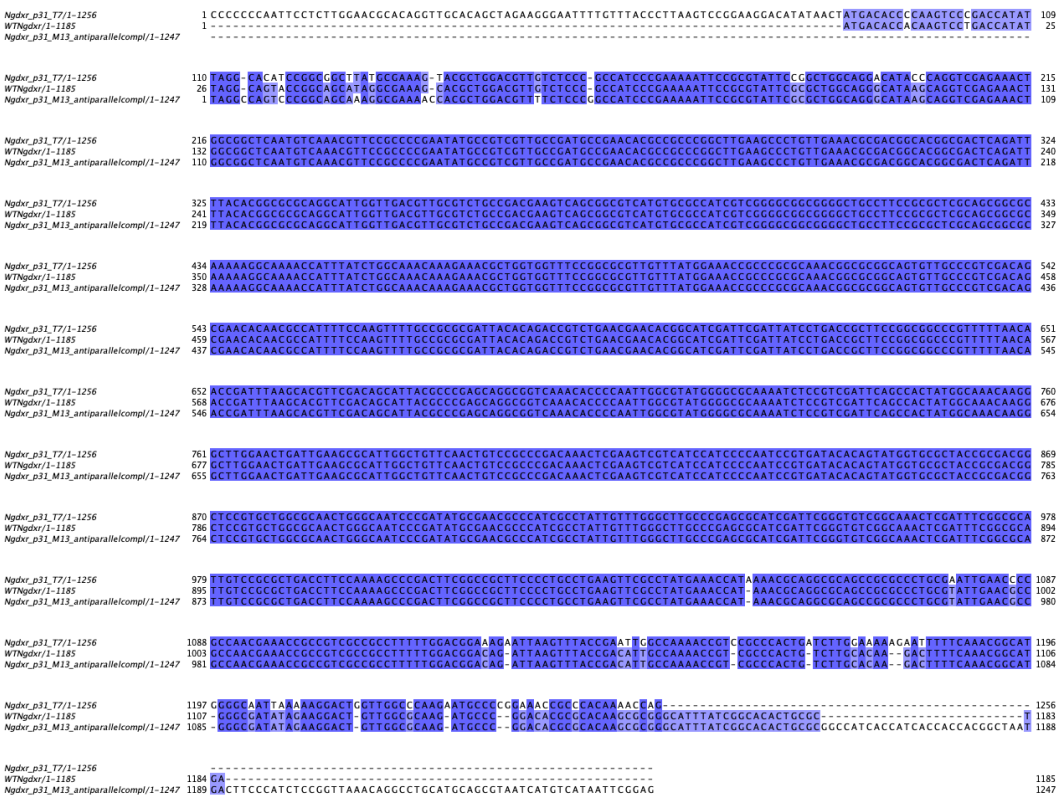

Figure 4.6 Alignment of bidirectional Sanger sequencing results of WT*Ngdxr* in pLATE31 with the WT*Ngdxr* sequence from the NCBI

Figure 4.7 Sanger sequencing chromatogram results (T7 promoter (forward)) of WT*Ngdxr* in pLATE31

Figure 4.8 Sanger sequencing chromatogram results (M13/pUC (Reverse)) of WT*Ngdxr* in pLATE31

The cloned sequence was confirmed to be the WT*Ngdxr* gene.

4.2.2 Expression Analysis of *Ng*DXR by SDS-PAGE

Recombinant expression of *Ng*DXR encoded by WT*Ngdxr* using pLATE31 in *E. coli* BL21(DE3) was induced with IPTG at a final concentration of 0.5 mM, and protein expression was evaluated for 3 and 5 hours at 37°C, 180 rpm. To evaluate the protein expression, the non-recombinant, uninduced *E. coli* BL21(DE3) (NI); non-recombinant 0.5 mM IPTG-induced *E. coli* BL21(DE3) (I); and recombinant uninduced *E. coli* BL21(DE3) (R NI) were cultured under the same conditions as mentioned for recombinant 0.5 mM IPTG-induced *E. coli* BL21(DE3) (R I). Recombinant cultures were supplemented with 100 μg/mL ampicillin based on the antibiotic resistance of pLATE31 [100].

Unless otherwise stated, in this study, the lysis of expression samples was done with lysis buffer A solution. Before the SDS-PAGE analysis of the expressed protein, the estimated molecular weight of *Ng*DXR was calculated using online tools [114, 115]. The molecular weight of *Ng*DXR was determined as 42.051 kDa, and the protein band of approximately 42 kDa corresponding to *Ng*DXR was expected to be observed.

Cell lysates were analyzed by SDS-PAGE, and the results are given in Figure 4.9.

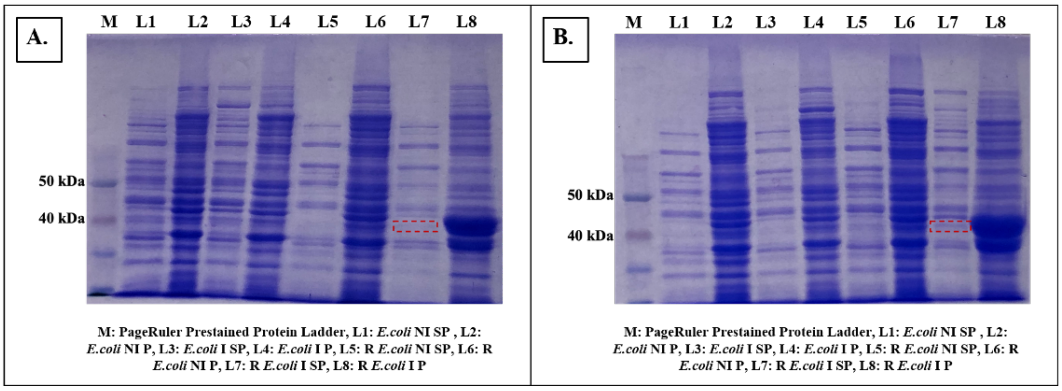

Figure 4.9 SDS-PAGE gel images of *E. coli* control and recombinant cell lysates; A. Expression/cultivation of *E. coli* control and recombinant cells for 3 hours, B. Expression/cultivation of *E. coli* control and recombinant cells for 5 hours

Lines 7 and 8 on the SDS-PAGE gel images in Figure 4.9 contain the supernatant and pellet fractions of recombinant IPTG-induced *E. coli* BL21(DE3) cell lysates, respectively. SDS-PAGE analysis revealed the presence of thin protein bands (highlighted with red dashes), possibly corresponding to *Ng*DXR, in the supernatant fractions (Figure 4.9 A., B. L7) compared to control samples expressed/cultured under the same conditions. Despite the thin soluble protein band in the supernatant

fractions, the overexpressed recombinant protein was mainly obtained as insoluble aggregates (inclusion bodies) in the pellet fractions (Figure 4.9 A., B. L8). Confirmation of the expressed recombinant protein was intended to be performed by Western Blot analysis.

4.2.3 Identification of Expressed *Ng*DXR with Western Blot Analysis

Based on the sensitivity of Western Blot (WB), WB analysis was performed to detect the possible expressed *Ng*DXR. WB analysis was conducted for the supernatant fraction of the cell lysate obtained from overnight expression of the WT*Ngdxr* clone (Figure 4.10).

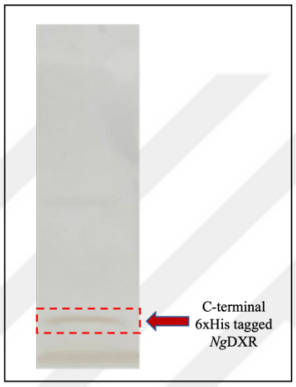

Figure 4.10 Western Blot analysis of C-terminal 6xHis-tagged *Ng*DXR

The C-terminal His-tagged recombinant protein detected with specific antibodies was highlighted with red dashes (Figure 4.10). Although the WB results confirmed the *Ng*DXR presence in the soluble form, it was predicted that the amount of protein produced could be too low for future biochemical studies. Therefore, a scale-up strategy was implemented to increase the efficiency of soluble protein expression.

4.2.4 Scale-up Optimization for *Ng*DXR Expression and Purification of 6xHis-tagged *Ng*DXR by HisTALON Gravity Column

A scale-up strategy from 50 mL to 400 mL was applied to increase the soluble protein yield. Recombinant protein production was induced with 0.5 mM IPTG and expressed overnight at 37°C, 180 rpm. The non-recombinant host cells were subjected to expression under the same conditions and used as a control.

Cultures were harvested by centrifugation, and the cell pellets were resuspended in lysis buffer A. Then, cells were subjected to sonication at 40% amplitude for 2 minutes (10 sec on, 10 sec off).

Expression samples were purified using the HisTALON gravity column. The His-tagged protein purification with Cobalt-loaded TALON columns is based on the principle of metal affinity chromatography [116]. Pure C-terminal 6xHis-tagged recombinant *Ng*DXR was aimed to be obtained as a result of the HisTALON gravity column purification. Purified samples were analyzed by WB.

4.2.5 Confirmation of Purified *Ng*DXR with Western Blot Analysis

WB analyses were performed to confirm pure recombinant protein, and the induced non-recombinant *E. coli* BL21(DE3) sample was used to validate that the produced protein is not of host cellular origin. WB results are given in Figure 4.11.

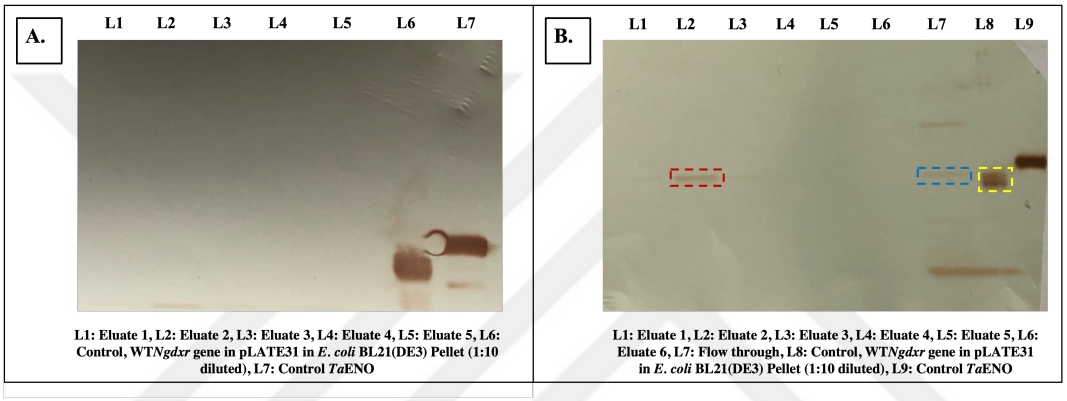

Figure 4.11 Western Blot analysis of C-terminal 6xHis-tagged *Ng*DXR A. HisTALON gravity column purified induced non-recombinant *E. coli* BL21(DE3). B. HisTALON gravity column purified recombinant *Ng*DXR

To verify the antibody/WB analysis functionality, *Theileria annulata* enolase (*Ta*ENO), with a molecular weight of 48 kDa (Figure 4.11 A. L7; Figure 4.11 B. L9) previously studied in the laboratory, was used as a control. The presence of 6xHis-tagged *Ng*DXR with purity over 95% was confirmed by WB (Figure 4.11 B. L2). No bands were observed in purified expression samples of non-recombinant *E. coli* BL21(DE3). A thin protein band aligned with pure 6xHis-tagged *Ng*DXR (L2) was observed in the flow through sample (Figure 4.11 B. L7, highlighted with blue dashes), which indicates that a certain amount of target protein passed through the column without being retained during purification.

The analyzed 1:10 diluted pellet sample appeared as two separate bands at almost equal quantities (Figure 4.11 B. L8, highlighted with yellow dashes), and the upper band was aligned with the soluble *Ng*DXR band in L2 (Figure 4.11 B). Since both bands in the pellet fraction were detected by Anti-6-His Polyclonal Rabbit Antibody in WB, it was hypothesized that the upper protein band in the pellet fraction may belong to the full-length *Ng*DXR and the lower band to the truncated form.

The concentration of purified protein was determined using Brand Assay and the amount of protein was observed to be insufficient for biochemical analysis.

The *Ng*DXR, produced through the expression of WT*Ngdxr* using the pLATE31 vector system in *E. coli* Bl21(DE3) host cells, has been observed and verified to be in a small amount at soluble form and predominantly in form of inclusion bodies in the pellet fraction. In addition to being obtained as inclusion bodies in the pellet, the possible N-terminal protein truncation was predicted based on the WB results. Since the produced soluble protein was insufficient for the intended biochemical studies, strategies were applied to improve soluble protein production.

Inclusion body formation due to the dysregulation of protein homeostasis in *E. coli* host cells is correlated with elevated heterologous protein expression levels, environmental conditions, and specific properties of the expressed target protein [120, 121]. Numerous strategies for soluble protein production have been developed and are widely used to overcome the inclusion body problem in recombinant technology [121, 122].

4.3 Expression Strategies for Soluble Recombinant *Ng*DXR Production Using the pLATE31 Expression Vector System

Based on extensive literature research and *in silico* studies, production rate optimization, correct folding promotion, breaking of possible disulfide bonds, expression with divalent cations, inclusion body solubilization, host cell change, *Ng*DXR expression as updated amino acid sequence, expression of *Ng*DXR in truncated form, co-expression with molecular chaperones, gene sequence optimization and harmonization of WT*Ngdxr* are strategies applied to improve *Ng*DXR production using the pLATE31 vector system.
The justifications and results of all implemented strategies are provided below.
Due to the comprehensive SDS-PAGE analyses performed throughout the thesis, one SDS-PAGE result will be given for each optimization performed, but all results will be reported and discussed in the text.

4.3.1 Optimizations of *Ng*DXR Expression Rate

The elevated translation rate triggered by the high expression temperature and high inducer concentration can cause the inability of the host cell to cope with the overexpressed recombinant protein and lead to the accumulation of expressed proteins within the cell as insoluble aggregates [123, 124]. Lowering the expression temperature and the IPTG concentration are among the critical strategies to reduce

the protein synthesis rate and thus prevent the formation of inclusion bodies [100, 125]. Furthermore, the impact of temperature reduction on the decrease of temperature-dependent hydrophobic interactions, which play an essential role in inclusion body formation, has also been reported [125, 126]. In light of the reported studies and the manufacturer's instruction of the vector system [100], low expression temperatures (20°C and 30°C) along with the IPTG concentration (0.1 and 0.5 mM) optimizations were performed to produce *Ng*DXR in soluble form.
SDS-PAGE analysis result of the sample induced by 0.5 mM IPTG and expressed at 30°C is given in Figure 4.12.

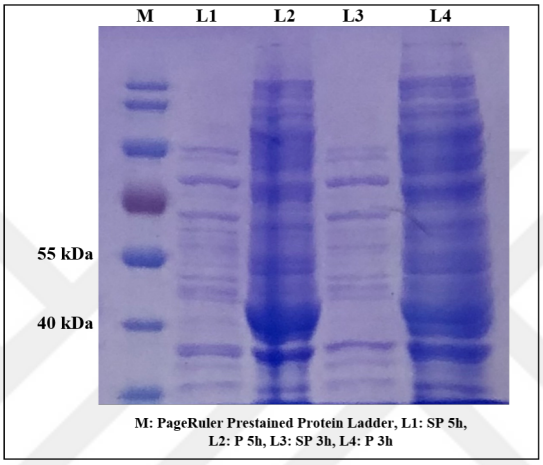

Figure 4.12 SDS-PAGE result of expression temperature impact on soluble *Ng*DXR expression

No significant change in expressed protein level was observed in samples induced with 0.5 mM IPTG and expressed for 5 hours at 30°C and 37°C. Temperature decrease up to 20°C did not contribute to soluble *Ng*DXR production, and even the expression level in the pellet decreased significantly. Nevertheless, protein solubility improvement by expression temperature and IPTG concentration reduction was observed in the study of Cayir et al., which was performed with the same expression system [127].
Due to unsuccessful attempts to express *Ng*DXR in soluble form by reducing the expression rate through IPTG and temperature optimizations, alternative approaches to reduce *Ng*DXR overexpression were evaluated.

The aeration level of the expression culture can variably affect the production of the target protein [128]. In the study of Boshtam et al., a better protein yield was achieved as a result of protein expression at a slower agitation speed [129]. To slow down the culture growth rate and thus possibly improve protein folding, the expression culture shaking speed of *Ng*DXR was reduced from 180 rpm to 50 rpm, but no effect on soluble protein expression was observed.

Despite the better effect of lower cell density on soluble recombinant protein production [130], soluble recombinant DXRs of *Francisella tularensis* [27] and *Yersinia pestis* [25] were obtained from recombinant cultures incubated till OD_{600nm} reached values of 1.1 and 1.8 before IPTG induction, respectively. The same OD_{600nm} (1.1 and 1.8) values were evaluated for *Ng*DXR, but higher pre-induction culture density did not affect the production of soluble *Ng*DXR.
No effect on the solubility of *Ng*DXR was observed with approaches applied to reduce the expression level and possibly prevent the formation of aggregates that may result from overexpression of *Ng*DXR.
Based on the knowledge that protein misfolding is a triggering factor for protein aggregation [131], approaches to ensure correct folding of *Ng*DXR were investigated.

4.3.2 Proper Folding Stimulation of *Ng*DXR by Glycerol, Ethanol and Divalent Metal Ions

The protein quality control system is maintained by chaperones that promote the correct folding of proteins and are categorized as molecular, chemical, and pharmacological [132–134]. The chemical chaperone group is composed of osmolytes and hydrophobic compounds [133].

A chemical chaperone, glycerol, has been reported to prevent aggregation formation by stabilizing the natural conformation of the proteins *in vivo* and *in vitro* [135]. The presence of glycerol in an aqueous solution enables the protein to adopt a compact form by improving the organization of the solvent molecules around the protein [136, 137]. Simultaneously with the *Ng*DXR expression induction by IPTG, glycerol was added to the expression culture medium at concentrations ranging from 2% to 10%, and the anti-aggregation impact of glycerol on *Ng*DXR was analyzed for samples expressed at 30°C and 37°C. SDS-PAGE analyses results of samples expressed in the LB supplemented with 7% and 10% glycerol are given in Figure 4.13.

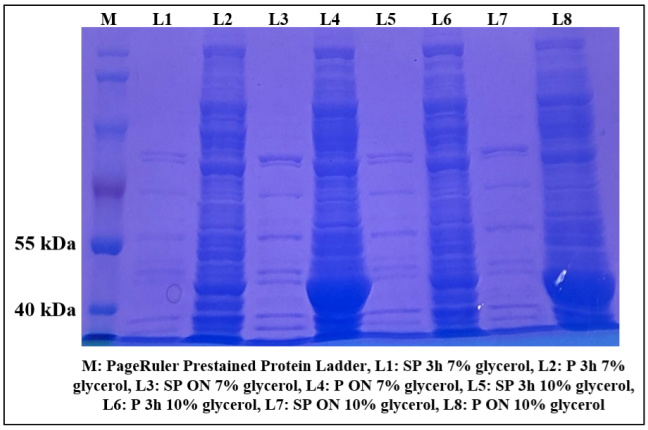

Figure 4.13 SDS-PAGE result of 7% and 10% glycerol effect on *Ng*DXR expression

As a result of evaluating the glycerol effect at two different temperatures and four glycerol concentrations (2%, 4%, 7%, and 10%), it was observed that the expressed protein was still trapped in the pellet fraction.

In another study, experiments were conducted to enhance the expression of molecular chaperones responsible for protein homeostasis within the cell [132] to promote the correct intracellular folding of *Ng*DXR.
Ethanol addition to the growth medium stimulates the heat shock effect in *E. coli*, which triggers the production of intracellular molecular chaperones such as DnaK and GroEL [132, 138]. Protein solubility improvement by ethanol addition to the culture medium has been reported in the literature [121, 138, 139]. To observe the effect of 3% ethanol on *Ng*DXR expression, based on the study of Chhetri et al., ethanol at a percentage of 3% was added to the expression medium simultaneously with primer culture inoculation [139], and the protein expression was carried out at 30°C, 180 rpm (Figure 4.14).

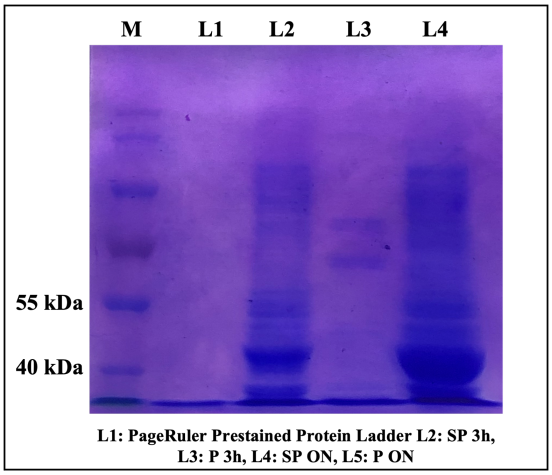

Figure 4.14 SDS-PAGE result of 3% ethanol effect on *Ng*DXR expression

However, insoluble protein in pellet fraction was obtained as a consequence of the applied ethanol addition strategy.

Chemical and molecular chaperone applications did not affect the protein solubility, and *Ng*DXR was still in the pellet fraction. Alternative studies were conducted to ensure possible correct folding.

Besides the function in the catalysis of the protein, the effect of divalent metal ions on protein folding has been reported in the literature [140]. The divalent metal ions (Co^{2+}, Mg^{2+} or Mn^{2+}), along with the NADPH cofactor, are essential components for the catalytical activity of DXR [141]. DXRs from different organisms exhibit variations in the preference for divalent metal ions [25]. The potential impact of the growing media supplementation with metal ions on protein solubility and stability [142, 143] was assessed for the *Ng*DXR. $MgCl_2$ and $MnCl_2$ at the concentration of 1 mM were added simultaneously with 0.5 mM IPTG induction to the independent cultures. No effect on protein solubility was observed as a result of the expression of *Ng*DXR with catalytically required DXR divalent metal ions.

Strategies aimed at ensuring proper protein folding did not affect the solubility of *Ng*DXR. The tendency of *Ng*DXR to form aggregation due to possible structural properties was considered.

4.3.3 Effect of Breaking Possible Intermolecular and Intramolecular Disulfide Bonds on *Ng*DXR

Improper disulfide bond formation can lead to failure in the native conformational establishment, protein aggregation, and dysfunction [144]. Based on the unknown *Ng*DXR structure and the reported tendency of DXRs to form octameric, hexameric and tetrameric structures [141, 145, 146], it was hypothesized that the possible existence of incorrect intermolecular and intramolecular disulfide bonds could lead to the production of *Ng*DXR in the form of inclusion bodies.

Among the reducing agents bearing free thiol groups, dithiothreitol (DTT) and 2-mercaptoethanol are frequently used in the reduction of disulfide bonds [147]. In addition to the disulfide bond reduction capability, the dithiothreitol and 2-mercaptoethanol maintain sulfhydryl groups in a reduced state, thus avoiding possible unnatural disulfide bond formation from air oxidation during cell disruption [148, 149].

The effect of 2 mM DTT and different concentrations of 2-mercaptoethanol (2 mM and 5 mM) were evaluated on *Ng*DXR soluble production. Harvested cells were

lysed in lysis buffer B (10 mM Tris-HCl, 100 mM NaCl, 2 mM 2-mercaptoethanol, pH: 8.0), lysis buffer 1 (30 mM Tris-HCl, 100 mM NaCl, 2 mM 2-mercaptoethanol, pH: 8.0), lysis buffer 2 (50 mM Tris-HCl, 250 mM NaCl, 5 mM 2-mercaptoethanol, pH: 8.0), lysis buffer 3 (100 mM Tris-HCl, 2.5 mM $MgCl_2$, 2 mM DTT, 0.1 mM phenyl-methylsulfonyl fluoride (PMSF), pH:7.5), lysis buffer 4 (100 mM Tris-HCl, 2.5 mM $MgCl_2$, 2 mM DTT, pH: 7.5), lysis buffer 5 (100 mM Tris-HCl, 300 mM NaCl, pH: 7.5) and cell lysate fractions were analyzed independently on SDS-PAGE (Figure 4. 15). Lysis buffer 3 was supplemented with PMSF, a serine protease inhibitor [150], to eliminate the potential effect of serine proteases on protein integrity. Additionally, $MgCl_2$ was added along with other agents to the lysis buffer 3 and 4 solutions to destabilize molecular hydrogen bonds [151].

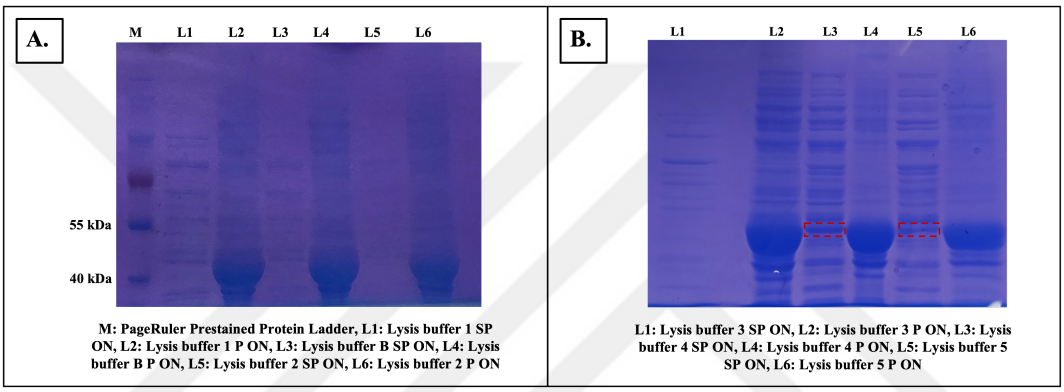

Figure 4.15 SDS-PAGE results of lysis buffer effect on *Ng*DXR solubility

Thin protein bands, possibly corresponding to *Ng*DXR, were observed in the supernatant fractions from lysis buffers 4 and 5 applications (highlighted with dashes), but most of the protein was still in the pellet fraction. However, the application of other buffers did not result in soluble protein, and the protein produced was in the pellet fraction.

4.3.4 Recovery of *Ng*DXR from Inclusion Body by Renaturation Strategy Using Urea

The active target protein recovery from the inclusion bodies can be achieved by purification of the inclusion bodies, denaturation of the aggregates, and, most importantly, refolding processes [152]. Extraction of the target protein from inclusion bodies can be accomplished using a combination of detergent (Triton X-100) and denaturing agents (urea or guanidine·HCl) [153].

A study for soluble *Ng*DXR retrieval from inclusion bodies was performed based on the research conducted by Xu et al. [154]. To evaluate the effect of urea-containing buffers on protein solubility, washing and solubilization processes were performed

on the expression sample induced with 0.5 mM IPTG and expressed with 4% glycerol. No soluble protein was observed in the supernatant fractions of *Ng*DXR treatment with urea, and all proteins were observed in the pellet fraction.

4.3.5 Host Strain Change Strategy to Overcome Possible Codon Bias and Ensure Correct Disulfide Bond Formation

Proper host strain selection is among the most critical factors influencing recombinant protein production, and the host choice depends on the features of the final product [130].

In the above-mentioned studies, *E. coli* BL21(DE3), deficient in Lon and OmpT proteases and encoding T7 polymerase [155], was used as the host cell for recombinant *Ng*DXR expression according to suggestions of the pLATE31 vector system manual [100]. Host strain change is a proposed strategy to improve recombinant soluble protein production, and a comprehensive list of modified host cells with specific features is available [130, 155].

In contrast to the abundance of rare codons in the recombinant gene, the low tRNA amount and codon preference of the host strain can give rise to the codon bias problem [155, 156]. This phenomenon can cause incorrect amino acid sequence formation and the production of the target protein in truncated form [156]. The *E. coli* BL21 Codon Plus strain, coding extra copies of tRNA [157], was used as the host strain to investigate the possible codon bias problem on *Ng*DXR expression.

As already explained in subsection 4.3.3, incorrect disulfide bond formation can lead to the production of proteins in the form of inclusion bodies. Since the structure of *Ng*DXR is unknown, studies were carried out to break possible incorrectly formed disulfide bonds, and the protein produced was predominantly obtained in the pellet. Ensuring the correct establishment of possible disulfide bonds was another strategy applied for soluble *Ng*DXR production. The streptomycin-resistant *E. coli* SHuffle T7 strain, which lacks thioredoxin reductase (*trxB*) and glutathione reductase (*gor*) but encodes cytoplasmic DsbC for isomerization of disulfide bonds [125, 155, 158], was used for proper establishment of possible disulfide bonds of expressed *Ng*DXR.

Based on the abovementioned information, the recombinant pLATE31 vector (WT*Ngdxr* in pLATE31) was transformed into competent *E. coli* BL21 Codon Plus and *E. coli* SHuffle T7 cells. Expression culture of *E. coli* BL21 Codon Plus was supplemented with 100 μg/mL ampicillin, and of *E. coli* SHuffle T7 with 100 μg/mL ampicillin and 25 μg/mL streptomycin. SDS-PAGE analysis results of

*Ng*DXR expressed in *E. coli* BL21 Codon Plus, and *E. coli* T7 SHuffle host cells at 30°C, with 0.5 mM IPTG, are given in Figure 4.16.

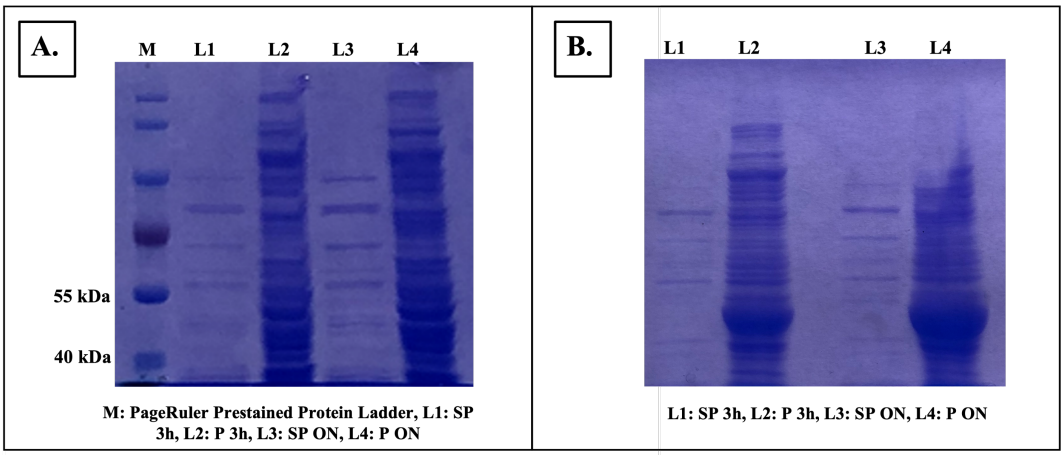

Figure 4.16 SDS-PAGE results of host strain change strategy; A. *Ng*DXR expression in *E. coli* BL21 Codon Plus host strain, B. *Ng*DXR expression in *E. coli* T7 SHuffle host strain.

In the expression of *Ng*DXR in *E. coli* BL21 Codon Plus, it was observed that the expression level, even in the pellet, was reduced compared to the *Ng*DXR expression in *E. coli* BL21(DE3). However, the *Ng*DXR expressed in *E. coli* T7 SHuffle was still observed in the pellet fraction. The host strain change strategy had no impact on the solubility of *Ng*DXR.

4.3.6 Expression of *Ng*DXR in the Length of 411 Amino Acid

At the beginning of the thesis study, the *Ng*DXR protein sequence in the length of 394 amino acids was confirmed in the NCBI database, and the studies were conducted with the coding target gene (WT*Ngdxr*). However, in March 2022, the amino acid sequence of *Ng*DXR in the NCBI database was updated to 411 amino acids [159]. The role of the additional amino acids in *Ng*DXR has yet to be reported in the literature. *In silico* modelling of 411 amino acids long *Ng*DXR using *Ec*DXR (PDB: 2EGH) structure as a reference in Modeller [160] (Figure 4.17) revealed that the additional 17 amino acids at the N-terminus are not part of the DXR catalytic domain. Then, cloning and expression studies were carried out to investigate the impact of the additional amino acids on protein solubility.

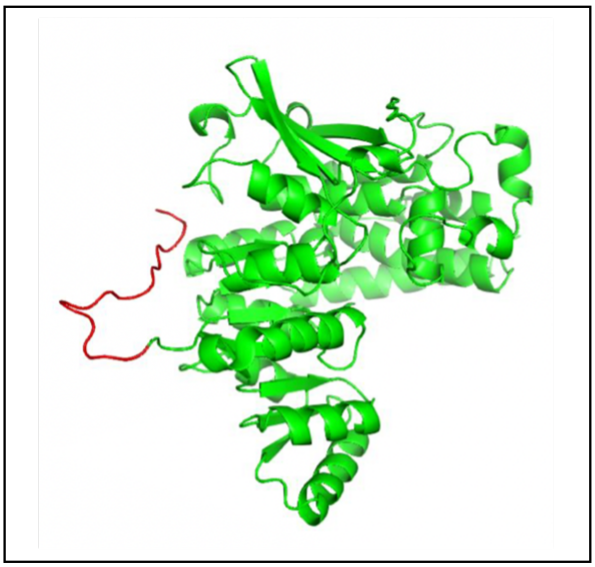

Figure 4.17 Model represents the addition of 17 amino acids in the N-terminal end of the *Ng*DXR; Added amino acids were indicated by red colour

WT*Ngdxr*, to be cloned into the pLATE31 vector system, was amplified by PCR using forward (17aaNgDxrF) and reverse (NgdxrR) primers designed to add 51 nucleotides. The confirmed 1236 bp gene was subcloned into the pLATE31, and then the recombinant vector was transformed into *E. coli* BL21(DE3) host strain. SDS-PAGE analysis results of the sample induced with 0.5 mM IPTG and expressed overnight at 37°C are given in Figure 4.18.

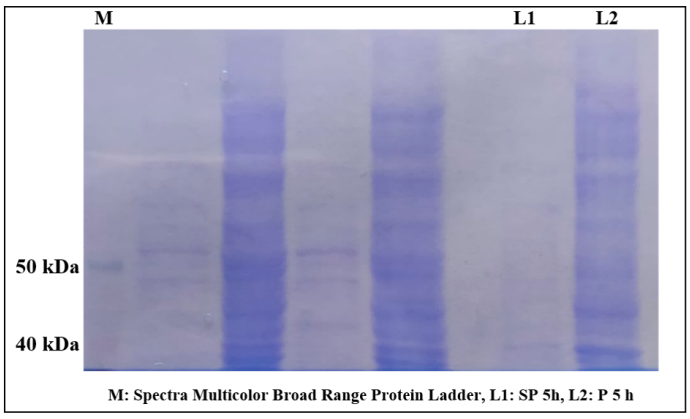

Figure 4.18 SDS-PAGE result of *Ng*DXR expression in the length of 411 amino acid

Previously, *Ng*DXR, in the length of 394 amino acids, was expressed as an inclusion body in the pellet under the conditions applied for 411 amino acid-length *Ng*DXR expression. However, in the experiment of *Ng*DXR production in the length of 411 amino acids under the same conditions, no production was observed, even in the pellet fraction.

4.3.7 Removal of Catalytically Non-essential First 2 Amino Acids from N-terminal End of *Ng*DXR

The recombinantly produced C-terminal His-tagged *Ng*DXR in the pellet fraction appeared as two separate bands by WB analysis described in subsection 4.2.5, and the possible protein truncation was emphasized. *In silico* modelling of *Ng*DXR using *Ec*DXR (PDB: 2EGH) structure as a reference in Modeller (Figure 4.19) showed that threonine and proline amino acids at the N-terminal end of *Ng*DXR are not located in the active site (Figure 4.19) and do not participate in the catalytic activity of the enzyme.

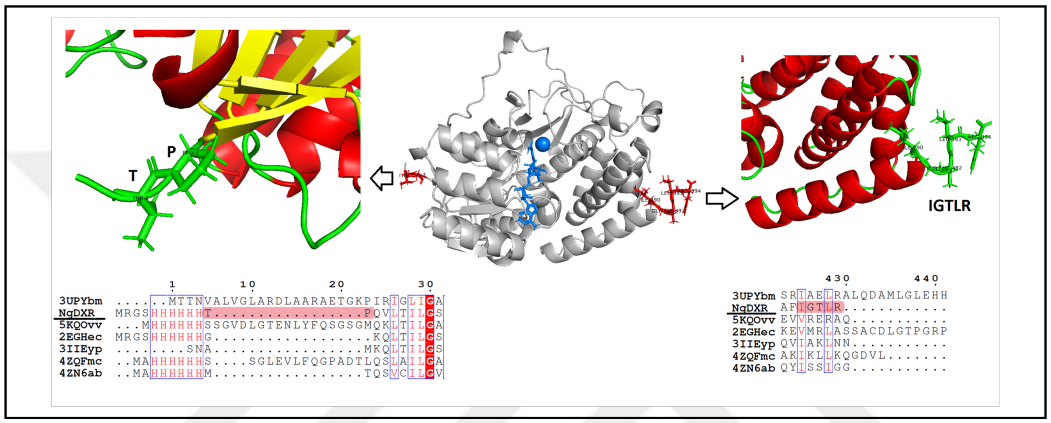

Figure 4.19 Model image of 2 amino acids removal from the N-terminus of the *Ng*DXR sequence

To evaluate the effect of these amino acids on the production of *Ng*DXR in soluble form, WT*Ngdxr* was truncated from the 5' end. Removal of 6 nucleotides from the 1185 bp long WT*Ngdxr* was achieved with the designed forward (TPNgdxrF) and reverse (NgdxrR) primers, and the 1179 base pair long gene was cloned into the pLATE31 vector system. SDS-PAGE analysis results of the sample induced with 0.5 mM IPTG and expressed at 37°C are given in Figure 4.20.

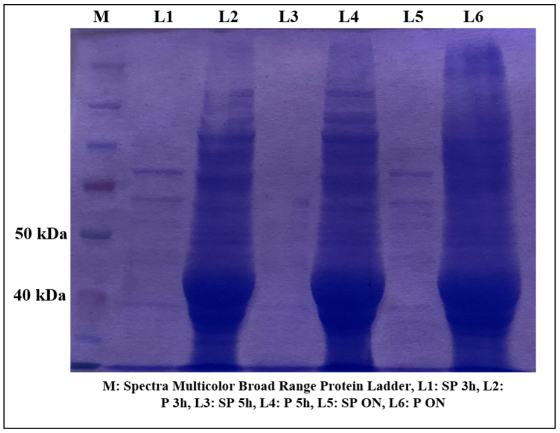

Figure 4.20 SDS-PAGE result of expressed *Ng*DXR in the truncated form

The removal of N-terminal threonine and proline amino acids did not affect the solubility of *Ng*DXR, and the protein still appeared in the pellet as inclusion bodies. Even though some studies report protein solubility increases as an effect of N-terminal protein truncation [161, 162], no impact of N-terminal 6 nucleotide truncation was observed on *Ng*DXR solubility.

4.3.8 Co-expression of *Ng*DXR with pG-Tf2, pGro7 and pG-KJE8 Chaperon Plasmids

Molecular chaperones participating in protein folding and prevention of aggregation are widely used to improve recombinant protein expression in *E. coli* [163–165]. An ATP-independent trigger factor and the ATP-dependent DnaK/DnaJ/GrpE and GroEL/ES prokaryotic chaperone systems are involved in the folding process of different cellular proteins [166]. Since molecular chaperones are found in small quantities in *E. coli* and can be insufficient for folding the overexpressed protein [130], a co-expression experiment with TAKARA chaperone plasmids was performed to investigate the effect of supplemented chaperones on soluble *Ng*DXR expression. Co-expression of *Ng*DXR with chaperone plasmids was carried out following the method described in subsection 3.2.3.1 and SDS-PAGE gel images were given in Figure 4.21.

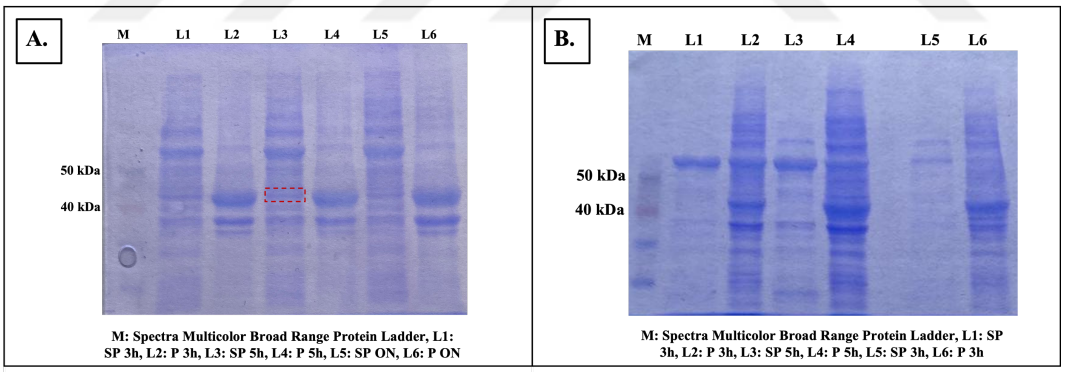

Figure 4.21 SDS-PAGE result of *Ng*DXR co-expression with chaperone plasmids; A. *Ng*DXR co-expression with pG-Tf2 chaperone plasmid, B. *Ng*DXR co-expression with pGro7 (L1-L4) and pG-KJE8 (L5-L6) chaperone plasmids

Voulgaridou et al. demonstrated that the simultaneous expression of the target gene with the combination GroES/GroEL and DnaK/DnaJ/GrpE systems enhanced the solubility of the produced 6xHis-tagged protein [167]. However, the production of *Ng*DXR with pG-KJE8-encoded GroES/GroEL and DnaK/DnaJ/GrpE chaperones did not yield any soluble protein (Figure 4.21 B, L5-6).

Although no expression was observed when the GroEL/GroES (pGro7) complex was used alone (Figure 4.21 B, L1-4), a possible soluble band of *Ng*DXR was

obtained when GroEL/GroES system was used together with the triggering factor (tig) (pG-Tf2) (Figure 4.21 A). The literature has also reported favourable results of GroEL/GroES and tig combinations in co-expression studies [164].

The confirmation of possible soluble band obtained from co-expression with pG-Tf2 chaperone plasmid was carried out with WB analysis, and the C-terminal 6xHis-tagged *Ng*DXR was detected (Figure 4.22).

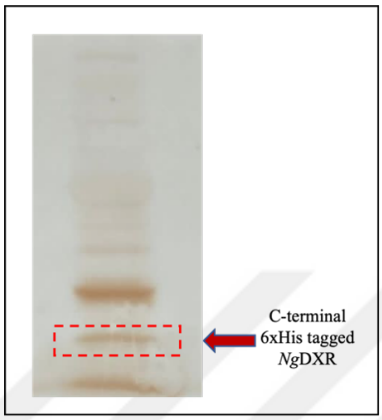

Figure 4.22 Western Blot result of 6xHis-tagged *Ng*DXR co-expressed with pG-Tf2 chaperone plasmid

Since the protein produced was still obtained as a thin protein band by the performed analyses, different strategies were applied to improve protein expression.

4.3.9 Codon Optimization and Harmonization of WT*Ngdxr* to Overcome Codon Bias

Regulation at the transcriptional level is one of the strategies applied for soluble recombinant protein production in *E. coli* hosts. For this purpose, codon optimization and harmonization approaches based on replacing target gene codons with synonymous ones without modifications in the amino acid sequence of the encoded protein are used [155, 168, 169]. Codon optimization is the substitution of rare codons in the target gene with the most often used synonymous codons. Nevertheless, in codon harmonization, the codons of the original protein are substituted by synonymous codons that have a corresponding frequency of usage in the expression host [170, 171].

Firstly, the codon-optimized version of WT*Ngdxr* sequence encoding *Ng*DXR suitable for the *E. coli* BL21(DE3) was obtained with the EMBOSS Backtranseq tool [172]. The codon-optimized gene sequence was then harmonized in the AGCT Codon Harmonizer online tool [173] for the target *E. coli* BL21(DE3). Comparative alignment analysis of the codon-optimized/harmonized WT*Ngdxr* gene (Opt*Ngdxr*)

sequence with the *dxr* gene sequence of *N. gonorrhoeae* strain ATCC 49226 (WT*Ngdxr*) is given in Figure 4.23.

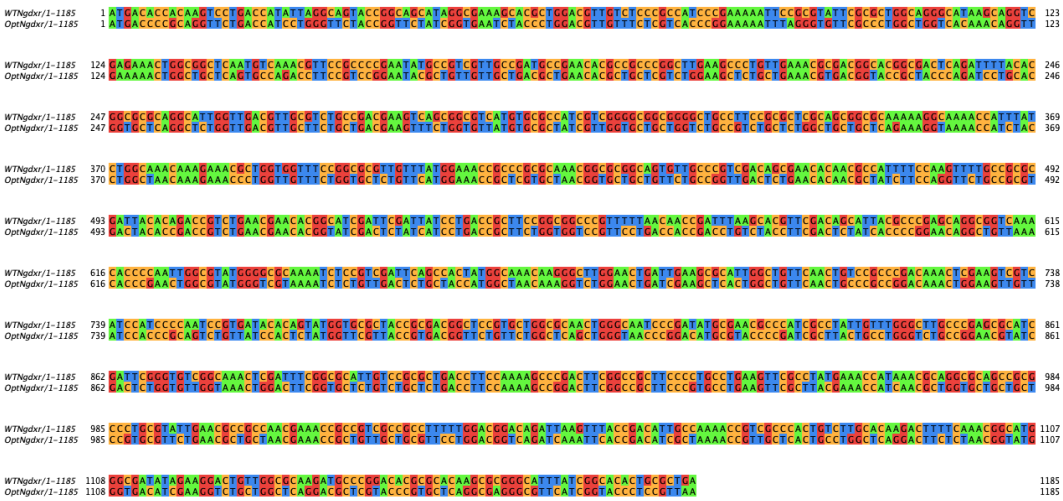

Figure 4.23 Comparative analysis of the WT*Ngdxr* with Opt*Ngdxr*

The Opt*Ngdxr* gene was amplified with forward (NgDxrF(H)) and reverse (NgDxrR(H)) primers and then cloned into the pLATE31 expression vector system. Recombinant gene expression was induced with IPTG at a final concentration of 0.5 mM for 5 hours at 37°C, 180 rpm. To evaluate *Ng*DXR expression, non-recombinant uninduced *E. coli* BL21(DE3) (NI), non-recombinant induced *E. coli* BL21(DE3) (I), and recombinant uninduced *E. coli* BL21(DE3) (R NI) were cultured under the same conditions as mentioned for recombinant *E. coli* BL21(DE3) (R I). The supernatant and pellet fractions from the expression of recombinant *Ng*DXR encoded by Opt*Ngdxr* were analyzed in Lines 7 and 8, respectively (Figure 4.24).

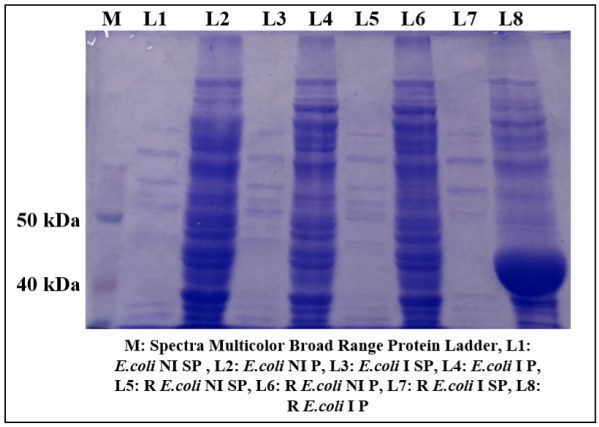

Figure 4.24 SDS-PAGE gel image of *E. coli* control and recombinant cell lysates

Even a low level of soluble *Ng*DXR was observed as a result of WT*Ngdxr* expression; despite the same expression conditions applied, *Ng*DXR produced by

Opt*Ngdxr* was entirely in the pellet fraction.

4.4 Production of *Ng*DXR in the Form of N-terminal 6xHis Tag and Without Tag

Small peptides or protein sequences linked to the N or C terminus of the target protein, known as fusion tags, are widely used in recombinant DNA technology to improve target protein production, enhance solubility, and facilitate purification [174]. Despite intensive efforts to produce C-terminal 6xHis-tagged *Ng*DXR, insufficient protein was obtained.

Busso et al. reported higher solubility of N-terminal 6xHis-tagged proteins compared to the C-terminal 6xHis-tagged [175]. However, a negative impact of N- and C-terminal 6xHis tags on recombinant protein solubility was observed on the protein studied by Woestenenk et al. [176].

To evaluate the position and unavailability of the 6xHis tag on *Ng*DXR production, WT*Ngdxr* was cloned into aLICator pLATE51 and pLATE11 expression vector systems. Production of N-terminal 6xHis-tagged *Ng*DXR was performed using pLATE51, while the production of *Ng*DXR without tag was carried out using pLATE11. The WT*Ngdxr* gene was cloned into expression vectors following amplification using forward (51FNgdxr) and reverse (51RNgdxr) primers for pLATE51 and using forward (11FNgdxr) and reverse (11RNgdxr) primers for pLATE11. The *Ng*DXR expression experiments using pLATE51 and pLATE11 expression vectors were performed at 30°C, with different IPTG concentrations (0.1, 0.5, 0.8, 1 mM) in *E. coli* BL21(DE3) and *E. coli* BL 21 Codon Plus host strains. SDS-PAGE analysis results of *Ng*DXR expression using pLATE51 and pLATE11 expression vector systems are given in Figure 4.25.

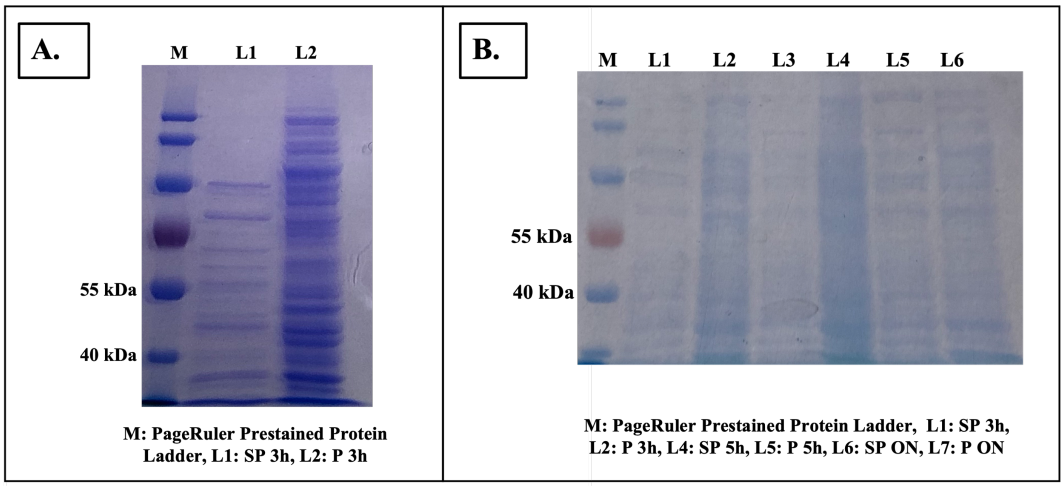

Figure 4.25 SDS-PAGE results of *Ng*DXR expression in N-terminal 6xHis-tagged and untagged forms; A. N-terminal 6xHis-tagged *Ng*DXR expression induced with 0.5 mM IPTG at 30°C; B. Untagged *Ng*DXR expression induced with 0.1 mM IPTG at 30°C

No protein expression was observed as a result of the studies performed.

Some expression studies using the WT*Ngdxr* and Opt*Ngdxr* genes were conducted simultaneously to achieve the final goal, and the results were given in the relevant sections.

4.5 Periplasmic Translocation and GST-tagged *Ng*DXR Production using pET Expression Vector Systems

Although the purposes of using pET expression vector systems for *Ng*DXR production differ, the usage purpose and observed results were given under the same subsection since the same methods and parameters were applied for *Ng*DXR production.

The reductive nature of the cytoplasm poses restrictions for intracellular expression of disulfide-bonded exogenous proteins in *E. coli*. The oxidative environment and lower protease content of the *E. coli* periplasm make the recombinant protein periplasmic translocation strategy attractive to overcome inclusion body formation in the cytoplasm [121, 163]. To establish proper protein folding and evaluate the influence of the periplasmic environment on *Ng*DXR solubility, *Ng*DXR was produced using a DsbC-encoded pET-40b(+) expression vector system. The DsbC tag, which acts as a signal sequence at the N-terminal end of the target protein, ensures the potential localization of the protein to the periplasm and is responsible for the bond isomerization of disulfide-bonded proteins in the oxidative

environment of the periplasm [101, 177].

Protein expression with a fusion tag is an alternative approach to producing soluble recombinant proteins. The positive effect of Thioredoxin (Trx), small ubiquitin-like modifier (SUMO), glutathione S-transferase (GST), green fluorescent protein (GFP), HaloTag, and maltose binding protein (MBP) fusion tags on protein expression and solubility have been reported [178, 179]. The pET-41a(+) expression vector system, encoding a GST tag at the N-terminal end, was used to assess the effectiveness of the GST tag in improving the solubility of the *Ng*DXR and protecting it from potential proteolytic degradation [180].

Opt*Ngdxr* to be subcloned into the pET expression vector was amplified with forward (pQENgdxrF) and reverse (pQE2NgdxrR) primers containing *Hind*III restriction sites. Recombinant vectors were transformed into *E. coli* BL21(DE3) host strain and availability of the target gene in recombinant colonies was checked by colony PCR using T7 forward control and gene-specific reverse (pQE2NgdxrR) primers. *Ng*DXR expression in the *E. coli* BL21(DE3) host strain was induced with 0.5 mM IPTG and performed at 30°C, 180 rpm. Expression culture was supplemented with 30 μg/mL kanamycin. SDS-PAGE analysis result of *Ng*DXR expressed using pET-41a(+) expression vector system is given in Figure 4.26.

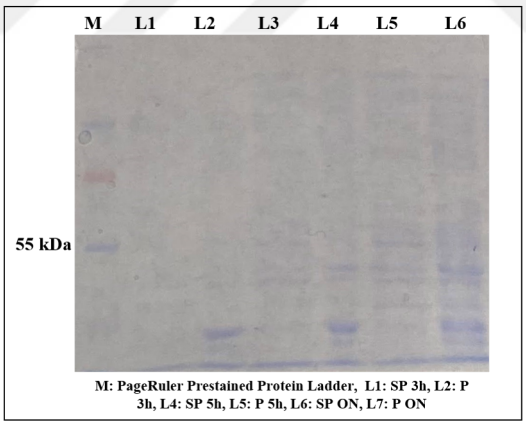

Figure 4.26 SDS-PAGE result of GST tagged *Ng*DXR

Periplasmic translocation and GST tag did not affect soluble *Ng*DXR expression, and protein was not observed even in the pellet fraction.

4.6 T5 Promoter Effect Evaluation on Soluble *Ng*DXR Production Using pQE Expression Vector Systems

The gene expression for *Ng*DXR production with the vector systems used in the studies reported above was controlled by the T7 RNA polymerase recognized T7

promoter.

It has been observed in the literature that pQE-9, pQE-30 and pQE-31 expression vector systems harbouring T5 promoter were used for DXR production from *Pseudomonas aeruginosa* [181], *E. coli* [21, 141, 182] and *P. falciparum* [28]. T5 promoter has double repressor binding lac operator (*lacO*) sequences to ensure tight regulation and high-level expression of recombinant proteins [104]. Plasmid instability, resulting from leaky expression under non-induced conditions, can also be suppressed by the T5 promoter-based systems [169].

To assess the effect of the *E. coli* RNA polymerase recognized T5 promoter [183] of pQE vector systems on *Ng*DXR production, Opt*Ngdxr* expression using TAGZyme pQE-2; pQE-9, pQE-31, and pQE-40 vectors was conducted. Opt*Ngdxr* prior subcloning into the TAGZyme pQE2 was amplified with forward (pQE2NgdxrF) and reverse (pQE2NgdxrR) primers. The forward and reverse primers contained *Nde*I and *Hind*III recognition sites, respectively. *Hind*III restriction endonuclease was chosen for cloning Opt*Ngdxr* into pQE-9, -30, and -40 expression vector systems and the gene was amplified by forward (pQENgdxrF) and reverse (pQE2NgdxrR) primers.

Several parameters on *Ng*DXR production using the TAGZyme pQE-2 expression vector system were tested separately or combined, including host strain change (*E. coli* XL1-Blue, *E. coli* JM105), IPTG concentration (0.2, 0.4, 0.5, 1, 1.5 mM), expression temperature (27°C, 37°C), expression media (TB), culture media supplement (carbenicillin) and pH value of lysis buffer (lysis buffer B pH: 7, 7.5, 8.5) optimizations.

The vector handbook states that any strain of *E. coli* can be used as an expression host if it possesses either the suppressor pREP4 plasmid or the lacI^q mutation. However, it has been reported that strains containing the pREP4 plasmid, notably M15[pREP4] host cells, show higher expression efficiency than those with the *lacI*^{q} mutation [104]. In this study, the lacI^q mutated *E. coli* XL1-Blue (1 μg/mL tetracycline) and *E. coli* JM105 (1 μg/mL tetracycline) cell lines were used as host strains for recombinant *Ng*DXR expression. Positive colony confirmation was performed by colony PCR; furthermore, in the case of pQE-9, -30, and -40, the cloned target gene was confirmed by cross-amplification with control and gene-specific primers.

For *Ng*DXR expression using pQE-2, the expression conditions utilized in previous studies were tried, but since protein production was not observed, optimizations were performed to improve *Ng*DXR expression.

In expression studies of DXR from *P. aeruginosa*, *E. coli*, and *P. falciparum* using pQE vector systems, lysis buffers containing 2-mercaptoethanol were used to lysate expression samples. In this thesis, the effect of buffer containing 2-mercaptoethanol reported in the literature [21, 28, 181] and different pH values (pH: 7, 7.5, 8.5) on *Ng*DXR was evaluated. Unless otherwise stated, the lysis of recombinant *E. coli* host cells harbouring pQE recombinant vector was done with lysis buffer B solution.

Medium change

The culture medium change strategy from LB to TB was applied to evaluate the effect of high protein level, buffering capacity, and additional carbon source in TB medium [184] on *Ng*DXR production.

Effect of carbenicillin

Recombinant plasmid instability during expression caused by ampicillin instability has been reported as a reason for the low expression level. Ampicillin replacement with a more stable antibiotic, carbenicillin (50 μg/mL) [100], was applied to enhance the stability of the recombinant plasmid within the cell and, thus, potentially increase the expression level of *Ng*DXR.

Extensive optimizations for *Ng*DXR production were performed using the TAGZyme pQ-2 expression vector system, as there was no significant difference in the properties of the pQE vector systems and to minimize the use of consumables, expression using the other pQE-9, 30, and 40 vector systems was performed in a single expression trial (*E. coli* XL1-Blue, induction with 1 mM IPTG, at 37°C).

As a result of the optimizations performed, the SDS-PAGE gel image (Figure 4.27) was presented only for *Ng*DXR expression using TAGZyme pQE-2 expression vector system in *E. coli* XL1-Blue host strain induced with 1 mM IPTG in TB and LB medium.

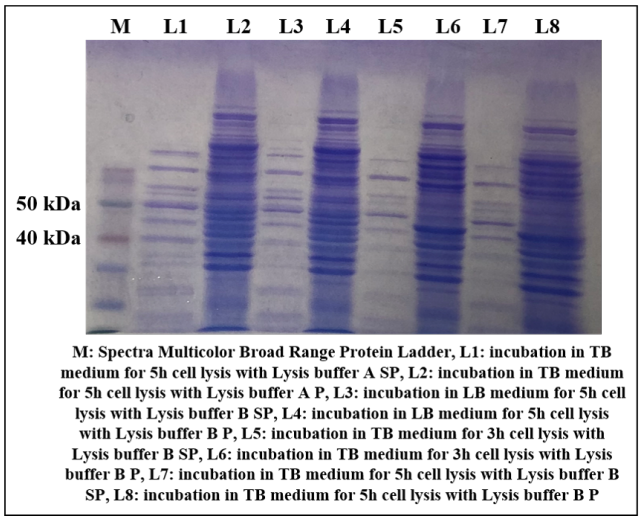

Figure 4.27 SDS-PAGE result of TAGZyme pQE-2 expression vector effect on *Ng*DXR production

Although literature exists on the production of DXR from different organisms with pQE expression vector systems, recombinant expression of *Ng*DXR using pQE vectors has not been achieved despite numerous optimizations.

4.7 *Ng*DXR Expression using pET101/D-TOPO Expression Vector System

An active soluble C-terminal His tagged DXR from *Francisella tularensis* has been produced with a pET101/D-TOPO expression vector system [27]. Based on the *Francisella tularensis* study, for the production of *Ng*DXR in active and soluble form, Opt*Ngdxr* was expressed using the pET101/D-TOPO expression vector system.

Opt*Ngdxr* to be cloned into the pET101/D-TOPO vector system was amplified using forward (101TOPONgdxr(H)F) and reverse (101TOPONgdxr(H)R) primers. Gene cloning and recombinant vector transformation procedures were done according to the manufacturer's instructions, and colonies obtained as a result of recombinant vector transformation into BL21 Star(DE3) One Shot Chemically Competent *E. coli* host strain were validated by colony PCR.

Two different IPTG concentrations (0.5 mM, 1 mM) were examined for the production of *Ng*DXR using the pET101/D-TOPO vector system, and the expression was carried out at 37°C, 180 rpm. Expression culture was supplemented with 100 μg/mL ampicillin, and the SDS-PAGE analysis result of expression sample induced with 0.5 mM IPTG is given in Figure 4.28.

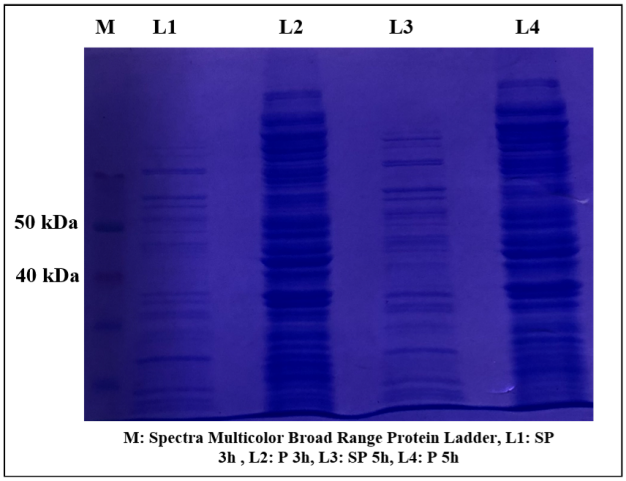

Figure 4.28 SDS-PAGE results of *Ng*DXR expression using pET101/D-TOPO

No protein expression was observed, even in the pellet fraction, so the pET101/D-TOPO expression vector system did not affect *Ng*DXR production.

This thesis is a part of the 121N818-numbered TÜBİTAK project for developing inhibitors against *Neisseria gonorrhoeae*, and recombinant production and biochemical analysis of the *Ng*DXR for high-throughput screening studies are within the scope of the study. Despite all efforts, no sufficient soluble *Ng*DXR was obtained, and an alternative method was used to achieve the final goal of the project and the studies performed are mentioned below.

4.8 Recombinant *Ec*DXR Production and Biochemical Characterization

Since the substrate/inhibitor binding site of *Ng*DXR is targeted for developing new inhibitors against *N. gonorrhoeae*, the preservation of active site functional residues of DXRs in *Ng*DXR was aimed to be evaluated. The active site functional residues of DXRs from different organisms were analyzed as a result of an extensive literature review, and the evaluation of functional residues was decided to be performed on the *Ec*DXR with the most well-defined structure.

Analysis of *Ec*DXR in a ternary complex with fosmidomycin and manganese revealed the interaction of divalent metal ions with Asp150, Glu152 and Glu231 residues, and the metal dication was coordinated by the hydroxamic acid moiety of fosmidomycin. Hydrogen bonding of the fosmidomycin phosphonate moiety with Ser186, Ser222, Asn227 and Lys228 residues of *Ec*DXR was identified within the same complex [85, 87]. Moreover, a direct interaction between the hydroxamic acid moiety of inhibitor with Glu152 and Glu231 was observed in the characterization

of *Ec*DXR in a low metal affinity environment [86]. The interaction of substrate (DXP) and *Ec*DXR was determined for the first time in a ternary complex with NADPH. The substrate phosphate moiety was identified to be hydrogen-bounded with Ser186, His209, Asn227 and Lys228 residues, and the substrate backbone with Trp 212, Lys125, Ser151, Glu152, Asn227, Lys228 and Glu231 residues of *Ec*DXR, as a result of the study [86].

To compare the *Ng*DXR amino acid sequence with bacterial DXR sequences that have been recombinantly produced and have had their crystallographic structure determined, sequences were downloaded from NCBI and ATCC and subjected to multiple alignment analyses (Figure 4.29).

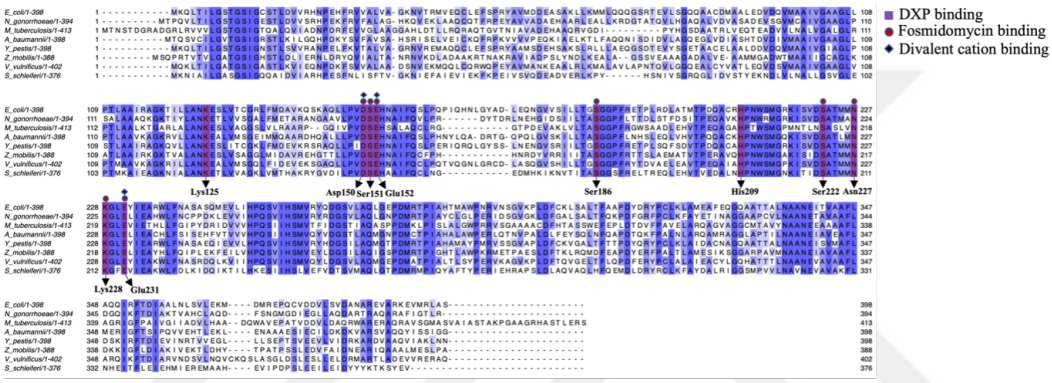

Figure 4.29 Multiple DXR amino acid sequence alignment

The active site functional residues of *Ec*DXR were found to be 100% conserved in the *Ng*DXR sequence. Based on the observed 100% identity of active site functional residues, recombinant *Ec*DXR was intended to be used in *in vitro* high-throughput screening studies. The cloning, expression and biochemical analysis results of *Ec*DXR to be used in the high-throughput screening studies are given below.

4.8.1 Expression, Purification and Biochemical Characterization of *Ec*DXR

The *Ecdxr* to be cloned into the pLATE31 vector system was PCR amplified with forward (pLATE31Ec(25922)dxrF) and reverse (pLATE31Ec(25922)dxrR) primers using genomic DNA of *E. coli* (ATCC 25922) as the template. The 1197 bp *Ecdxr* was confirmed by agarose gel electrophoresis (Figure 4.30), and the method mentioned in subsection 3.2.2.5 was applied for gene subcloning into the pLATE31.

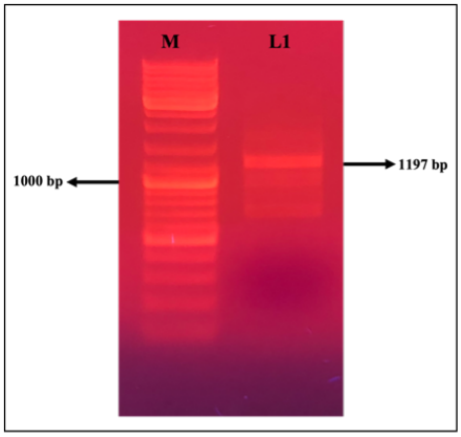

Figure 4.30 Agarose gel image of *Ecdxr* amplified with forward (pLATE31Ec(25922)dxrF) and reverse (pLATE31Ec(25922)dxrR) primers; M: GeneRuler DNA marker, L1: 1197 long amplified *Ecdxr*

Recombinant vectors were transformed into competent *E. coli* Bl21(DE3) expression hosts, and then clones containing recombinant vectors were analyzed by colony PCR. The expression of *Ec*DXR was induced with 0.5 mM IPTG and was performed under 37°C, 180 rpm conditions (Figure 4.31).

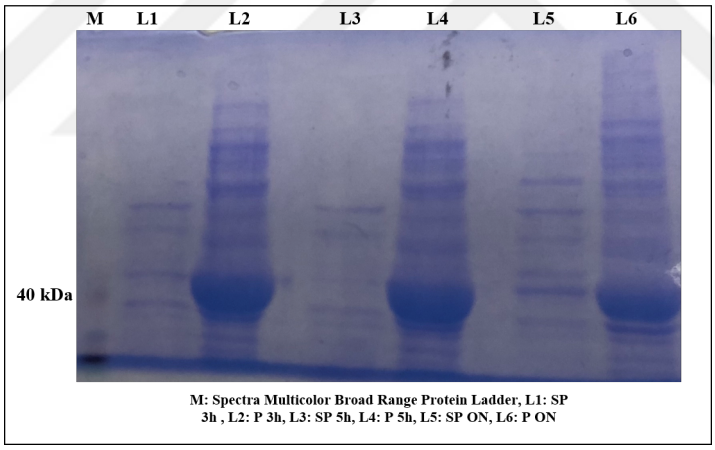

Figure 4.31 SDS-PAGE results of *Ec*DXR expression at 37°C

The molecular weight of the DXR encoded by the *E. coli* ATCC 25922 (*Ec*DXR) strain was determined as 43.4 kDa using online tools [114, 115], and the protein band at the specified size was expected to be observed by SDS-PAGE.

*Ec*DXR produced under the abovementioned conditions was obtained entirely in the pellet fraction. Temperature optimization was performed to ensure the possible soluble expression of *Ec*DXR, and the expression temperature was reduced from 37°C to 30°C. *Ec*DXR expression results induced with 0.5 mM IPTG at 30°C, 180 rpm are given in Figure 4.32.

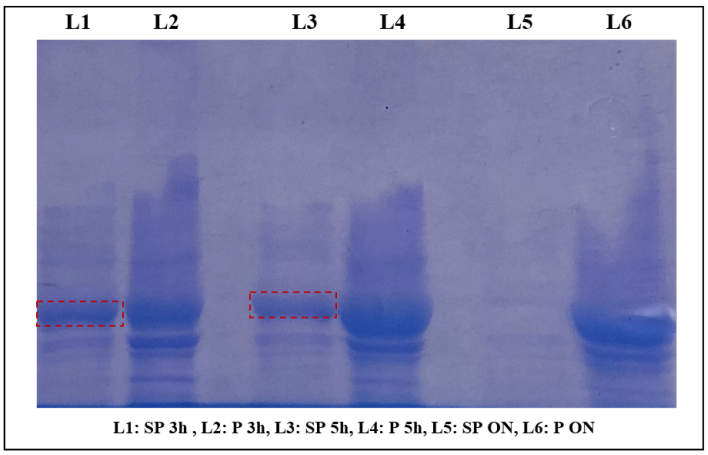

Figure 4.32 SDS-PAGE results of *Ec*DXR expression at 30°C

As shown in Figure 4.32, a band of the target protein was observed in the supernatant fractions of the expression samples collected at the 3rd and 5th hours (L1 and L3, respectively). However, no soluble protein was obtained from overnight expression under the same conditions. Although *Ec*DXR was produced in the soluble form, high protein levels still appeared in the pellet fraction. Experiments were conducted to enhance the soluble *Ec*DXR level by optimizing the IPTG concentration (0.2 mM) and the expression temperature (25°C), but no soluble protein was observed in SDS-PAGE.

To verify that the expressed protein is not from the host cell origin, recombinant *E. coli* BL21(DE3) and non-recombinant *E. coli* BL21(DE3) were induced with 0.5 mM IPTG, and cells were cultured for 3 hours at 30°C, 180 rpm (Figure 4.33).

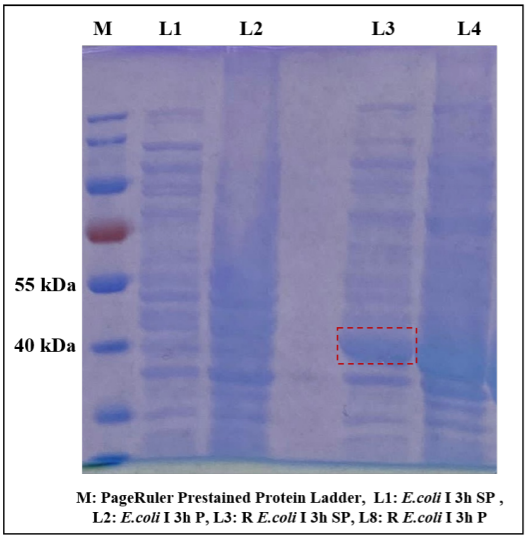

Figure 4.33 SDS-PAGE gel image of *E. coli* control and recombinant cell lysates

The protein band corresponding to recombinant *Ec*DXR, with a molecular weight of approximately 43 kDa, was highlighted with red dashes (Figure 4.33,

L3). No protein expression was detected at the same molecular weight in the non-recombinant *E. coli* BL21(DE3) expression sample.

Following expression confirmation of *Ec*DXR, a scale-up strategy was applied to overcome the possible protein insufficiency for biochemical analysis. *Ec*DXR production induced with 0.5 mM IPTG was carried out in 530 mL LB broth at 30°C, 180 rpm for 3 hours. The expression culture was then sonicated at 50% amplitude for 3 min (10 sec on, 10 sec off) and purified using the HisTALON gravity column. Cell lysate samples (supernatant, pellet) and combined eluates were analyzed using SDS-PAGE, and results are given in Figure 4.34.

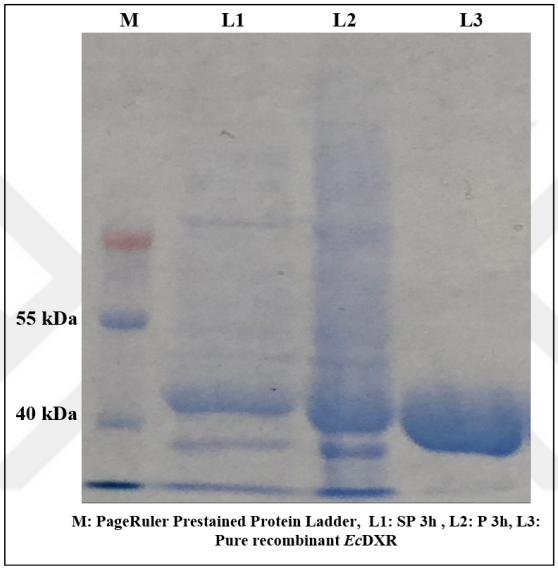

Figure 4.34 SDS-PAGE result of recombinant *E. coli* cell lysate and HisTALON gravity column purified *Ec*DXR

The obtained *Ec*DXR with purity over 95% was confirmed by SDS-PAGE analysis.

4.9 Biochemical Analysis of *Ec*DXR

The targeted biochemical analyses of *Ec*DXR include the identification of the kinetic parameters (V_{max}, K_m) and determination of IC_{50} value according to the inhibition potential of fosmidomycin.

4.9.1 Determination of *Ec*DXR Concentration Using Bradford Assay

Biochemical analyses of *Ec*DXR were conducted in two independent experimental setups, and protein concentration was determined for each one.

*Ec*DXR stock at the concentration of 4.49 mg/mL (530 mL expression culture) was

used to determine the IC_{50} value. The concentration of *Ec*DXR stock was calculated by the standard equation in Figure 4.35 using a 1:5 diluted form of the stock.

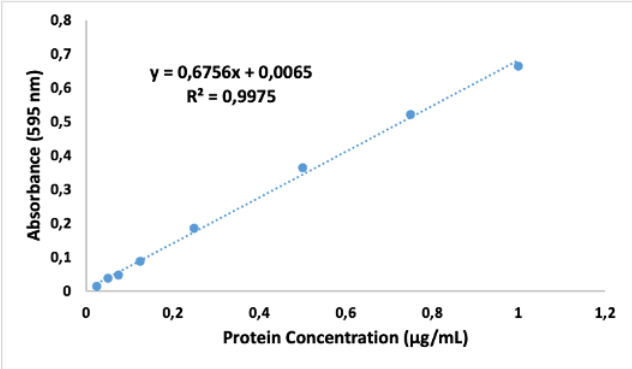

Figure 4.35 Protein concentration standard curve

*Ec*DXR stock at the concentration of 3.949 mg/mL (200 mL expression culture) was used in the identification of kinetic parameters. The concentration of the stock sample was determined using the standard equation given in Figure 4.36.

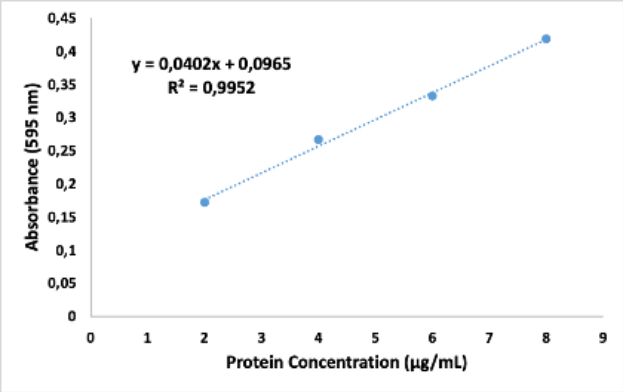

Figure 4.36 Protein concentration standard curve

4.9.2 Kinetic Analysis of Purified *Ec*DXR

The specific activity values obtained from measurements conducted with a range of substrate concentrations using 2 μL (3.949 mg/mL stock) of *Ec*DXR are given in Table 4.1.

Table 4.1 Specific activity values of *Ec*DXR

Substrate Concentration (mM)	Specific Activity (μmol/min^{-1}.mg^{-1})			Mean Specific Activity (μmol/min^{-1}.mg^{-1})
0.5	0.46	0.45	0.46	0.46
0.25	0.48	0.46	0.47	0.47
0.125	0.36	0.35	0.36	0.36
0.0625	0.20	0.20	0.20	0.20
0.03125	0.11	0.12	0.11	0.11

The steady-state kinetic graph of the enzyme was generated (Figure 4.37), the K_m and V_{max} values of *Ec*DXR were determined as 103.4±17.05 μM, 0.5985±0.03497 μmol/min.mg, respectively.

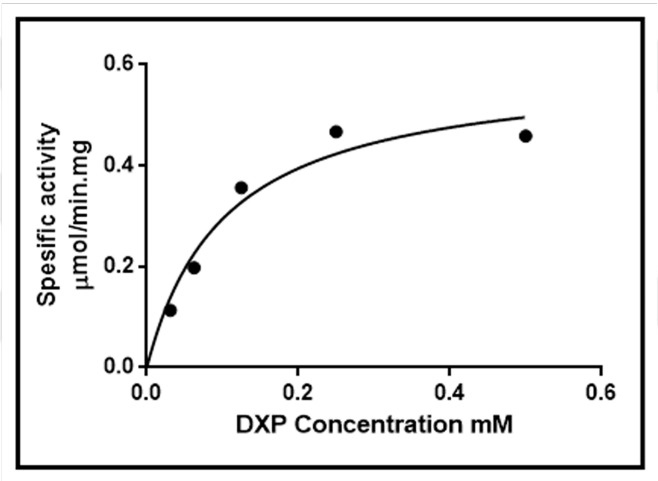

Figure 4.37 Steady-state kinetic graph of *Ec*DXR

The calculated K_m value was observed to be compatible with the 99 μM [82], 115 μM [99]and 150 μM [19] K_m values reported for *Ec*DXR.

4.9.3 The Half-maximal Inhibitory Concentration Determination of Fosmidomycin

The IC_{50} value refers to the concentration of inhibitor required to achieve 50% inhibition of an enzymatic reaction at a particular substrate concentration [185]. The inhibition (%) values were calculated as a result of absorbance measurements with variable inhibitor concentrations using 2 μL (4.49 mg/mL stock) *Ec*DXR and 0.5 mM DXP. Logarithm values of inhibitor concentrations and determined inhibition (%) values are given in Table 4.2.

Table 4.2 Inhibition (%) values of *Ec*DXR

Concentration of FSM (nM)	Inhibition (%) value	log concentration of FSM (μM)
125	5.555556	-0.903089987
156.25	45.06173	-0.806179974
187.5	81.85185	-0.726998728
250	91.97531	-0.602059991

The plot of inhibition (%) values versus the log concentration of the FSM was created (Figure 4.38) and the IC_{50} value of FSM against *Ec*DXR was determined as 160 nM. The observed value was between 34 nM [24], 42 nM [186], and 221.3 nM [187] fosmidomycin IC_{50} values of the *Ec*DXR reported in the literature.

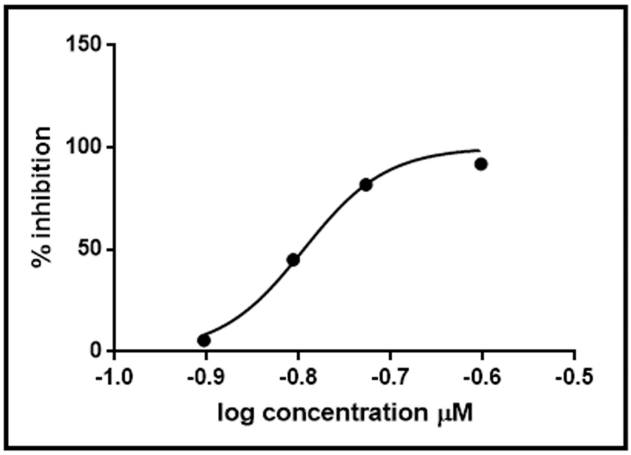

Figure 4.38 The plot of inhibition (%) versus the log concentration of the FSM

Although *Ng*DXR was produced in insufficient quantities, as mentioned in subsection 4.2.5, activity analysis of *Ng*DXR was intended to be performed using the activity assay optimized for *Ec*DXR. For this purpose, a scale-up strategy for *Ng*DXR expression in *E. coli* BL21(DE3) using the pLATE31 expression vector system was applied, and activity analysis of purified *Ng*DXR was carried out. However, the activity of *Ng*DXR produced in low amounts could not be detected.

5
CONCLUSION

5.1 Conclusion

Gonorrhea, caused by the multi-drug resistant *Neisseria gonorrhoeae*, is categorized as a priority infection in the global effort to eliminate sexually transmitted infections [45]. Potential targetable pathways that are vital for the bacterium but not present in the host were evaluated to combat the infection caused by *N. gonorrhoeae*. Studies targeting the biosynthetic MEP pathway of *N. gonorrhoeae* were not found in the literature. This study aimed recombinant production and biochemical analysis of the *Ng*DXR, which catalyzes the reductive isomerization of DXP to MEP in the bacterial vital MEP pathway. For this purpose, 1-deoxy-D-xylulose 5-phosphate reductoisomerase gene sequence of *N. gonorrhoeae* American Type Culture Collection (ATCC) 49226 strain was first cloned into the C-terminal 6xHis tagged aLICator pLATE31 vector system, and the protein was expressed in *E. coli* BL21(DE3) host strain. The expressed protein was analyzed by SDS-PAGE, and a thin protein band at approximately 42 kDa was observed, possibly corresponding to soluble *Ng*DXR; however, the expressed protein was mainly obtained in the pellet fraction in the form of inclusion bodies. The possible thin *Ng*DXR band was confirmed by Western Blot analysis, and the scale-up strategy was applied for soluble protein yield improvement. Expressed protein at the volume of 400 mL was purified using a HisTALON gravity column and pure 6xHis-tagged *Ng*DXR was detected in the second elution by Western Blot. In addition, a 1:10 diluted pellet fraction of the expression sample was also analyzed by Western Blot and detected as two separate bands. The upper band was thought to correspond to the full-length protein as it aligned with elution 2, but the lower band was hypothesized to be an N-terminal truncated formed of *Ng*DXR.

The expressed *Ng*DXR by the applied method was observed to be insufficient for biochemical analysis. Then, a range of methods and optimizations were applied to improve soluble protein yield. Among the studies carried out within the scope of the thesis for soluble *Ng*DXR production, a possible thin band corresponding to soluble

*Ng*DXR was observed as a result of SDS-PAGE analysis of samples subjected to lysis buffer applications containing DTT, NaCl. In addition, a thin protein band at supernatant fraction was observed by SDS-PAGE analysis of samples from *Ng*DXR co-expression study with pGT-f2 chaperone plasmid and the 6xHis-tagged *Ng*DXR was confirmed by Western Blot analysis. However, as a result of applied other numerous optimizations and methods for soluble *Ng*DXR production, the expressed protein was either obtained in the form of inclusion bodies in the pellet fraction or not produced at all. Obtained *Ng*DXR was still insufficient for biochemical analysis.

As a result of the extensive literature review and multiple sequence alignment analyses, *Ec*DXR, an alternative to *Ng*DXR was selected to be used in high-throughput screening studies. Consequently, recombinant production and biochemical characterization of *Ec*DXR were aimed to be performed in the scope of the thesis study. *Ec*DXR was cloned into the pLATE31 vector system and recombinant *Ec*DXR was then expressed in *E. coli* BL21(DE3) host cell. According to the optimizations for *Ec*DXR production, the best condition was determined as 0.5 mM of IPTG, and expression at 30°C for 3 hours. The biochemical analyses of *Ec*DXR, produced in high quantity and obtained with purity over 95% by HisTALON gravity column purification, were successfully performed. The activity assay of *Ec*DXR, was optimized for biochemical analysis and the kinetic parameters K_m and V_{max} of *Ec*DXR were determined as 103.4±17.05 μM, 0.5985±0.03497 μmol/min.mg, respectively.

Based on the successful expression of *Ec*DXR using the pLATE31 vector system at the soluble form and high concentration, it was concluded that there was no problem with the expression vector system, and *Ng*DXR could not be produced due to the structural features.

Overall, performed studies indicated that the *Ec*DXR produced in an active form can be used in the high-throughput screening of starting compounds for *Ng*DXR inhibition.

5.2 Future Perspectives

The results obtained within the scope of the thesis may serve as a basis for the studies mentioned below:

• Protein amino acid sequencing can be performed to identify the sequences of C-terminal His tagged proteins detected by Western Blot in the pellet fraction of the *Ng*DXR expression sample

• Further optimization studies can be carried out to increase the yield of soluble *Ng*DXR by co-expression with chaperone plasmids

• *Ng*DXR recovery in soluble and active form from the pellet fraction can be achieved through improved refolding studies

• The effect of *E. coli* M15[pREP4] strain on *Ng*DXR expression using the pQE vector system may be evaluated

• Physicochemical analysis of *Ec*DXR obtained in high-purity can be performed.

REFERENCES

[1] Y. A. Adebisi, "Balancing the risks and benefits of antibiotic use in a globalized world: The ethics of antimicrobial resistance," *Globalization and Health*, vol. 19, no. 1, p. 27, 2023.

[2] J. O'Neill, *Tackling drug-resistant infections globally: Final report and recommendations*, 2016.

[3] F. Prestinaci, P. Pezzotti, A. Pantosti, "Antimicrobial resistance: A global multifaceted phenomenon," *Pathogens and global health*, vol. 109, no. 7, pp. 309–318, 2015.

[4] *Who publishes list of bacteria for which new antibiotics are urgently needed.* [Online]. Available: `https://www.who.int/news/item/27-02-2017-who-publishes-list-of-bacteria-for-which-new-antibiotics-are-urgently-needed` (visited on 12/26/2023).

[5] W. H. Organization *et al.*, "Global progress report on hiv, viral hepatitis and sexually transmitted infections, 2021: Accountability for the global health sector strategies 2016–2021: Actions for impact," 2021.

[6] A. Qasim, S. Jaan, T. U. Wara, M. Shehroz, U. Nishan, S. Shams, M. Shah, S. C. Ojha, "Computer-aided genomic data analysis of drug-resistant neisseria gonorrhoeae for the identification of alternative therapeutic targets," *Frontiers in Cellular and Infection Microbiology*, vol. 13, p. 1 017 315, 2023.

[7] U. N. M. Omeershffudin, S. Kumar, "Emerging threat of antimicrobial resistance in neisseria gonorrhoeae: Pathogenesis, treatment challenges, and potential for vaccine development," *Archives of microbiology*, vol. 205, no. 10, p. 330, 2023.

[8] E. Rotman, H. S. Seifert, "The genetics of neisseria species," *Annual review of genetics*, vol. 48, pp. 405–431, 2014.

[9] M. Unemo, H. S. Seifert, E. W. Hook III, S. Hawkes, F. Ndowa, J.-A. R. Dillon, "Gonorrhoea," *Nature Reviews Disease Primers*, vol. 5, no. 1, p. 79, 2019.

[10] K. Y. Lim, C. A. Mullally, E. C. Haese, E. A. Kibble, N. R. McCluskey, E. C. Mikucki, V. C. Thai, K. A. Stubbs, M. Sarkar-Tyson, C. M. Kahler, "Anti-virulence therapeutic approaches for neisseria gonorrhoeae," *Antibiotics*, vol. 10, no. 2, p. 103, 2021.

[11] D. H. Rubin, J. D. Ross, Y. H. Grad, "The frontiers of addressing antibiotic resistance in neisseria gonorrhoeae," *Translational Research*, vol. 220, pp. 122–137, 2020.

[12] L. K. Whittles, P. J. White, J. Paul, X. Didelot, "Epidemiological trends of antibiotic resistant gonorrhoea in the united kingdom," *Antibiotics*, vol. 7, no. 3, p. 60, 2018.

[13] L. R. Vincent, A. E. Jerse, "Biological feasibility and importance of a gonorrhea vaccine for global public health," *Vaccine*, vol. 37, no. 50, pp. 7419–7426, 2019.

[14] S. Kesharwani, S. Sundriyal, "Non-hydroxamate inhibitors of 1-deoxy-d-xylulose 5-phosphate reductoisomerase (dxr): A critical review and future perspective," *European Journal of Medicinal Chemistry*, vol. 213, p. 113 055, 2021.

[15] S. Wang, M. Li, X. Luo, L. Yu, Z. Nie, Q. Liu, X. An, Y. Ao, Q. Liu, J. Chen, *et al.*, "Inhibitory effects of fosmidomycin against babesia microti in vitro," *Frontiers in Cell and Developmental Biology*, vol. 8, p. 247, 2020.

[16] H. Tian, B. Zada, B. H. Singh, C. Wang, S.-W. Kim, "Synthetic biology approaches for the production of isoprenoids in escherichia coli," in *Current Developments in Biotechnology and Bioengineering*, Elsevier, 2019, pp. 311–329.

[17] B. M. Lange, T. Rujan, W. Martin, R. Croteau, "Isoprenoid biosynthesis: The evolution of two ancient and distinct pathways across genomes," *Proceedings of the National Academy of Sciences*, vol. 97, no. 24, pp. 13 172–13 177, 2000.

[18] G. Daletos, G. Stephanopoulos, "Protein engineering strategies for microbial production of isoprenoids," *Metabolic engineering communications*, vol. 11, e00129, 2020.

[19] C. M. Armstrong, D. J. Meyers, L. S. Imlay, C. Freel Meyers, A. R. Odom, "Resistance to the antimicrobial agent fosmidomycin and an fr900098 prodrug through mutations in the deoxyxylulose phosphate reductoisomerase gene (dxr)," *Antimicrobial agents and chemotherapy*, vol. 59, no. 9, pp. 5511–5519, 2015.

[20] X. Wang, C. S. Dowd, "The methylerythritol phosphate pathway: Promising drug targets in the fight against tuberculosis," *ACS infectious diseases*, vol. 4, no. 3, pp. 278–290, 2018.

[21] K. Reuter, S. Sanderbrand, H. Jomaa, J. Wiesner, I. Steinbrecher, E. Beck, M. Hintz, G. Klebe, M. T. Stubbs, "Crystal structure of 1-deoxy-d-xylulose-5-phosphate reductoisomerase, a crucial enzyme in the non-mevalonate pathway of isoprenoid biosynthesis," *Journal of Biological Chemistry*, vol. 277, no. 7, pp. 5378–5384, 2002.

[22] S. Yajima, K. Hara, D. Iino, Y. Sasaki, T. Kuzuyama, K. Ohsawa, H. Seto, "Structure of 1-deoxy-d-xylulose 5-phosphate reductoisomerase in a quaternary complex with a magnesium ion, nadph and the antimalarial drug fosmidomycin," *Acta Crystallographica Section F: Structural Biology and Crystallization Communications*, vol. 63, no. 6, pp. 466–470, 2007.

[23] G. L. Patrick, "Drug targets in the apicoplast," in *Antimalarial Agents*, Elsevier, 2020, pp. 319–374.

[24] V. Devreux, J. Wiesner, H. Jomaa, J. Van der Eycken, S. Van Calenbergh, "Synthesis and evaluation of α, β-unsaturated α-aryl-substituted fosmidomycin analogues as dxr inhibitors," *Bioorganic & Medicinal Chemistry Letters*, vol. 17, no. 17, pp. 4920–4923, 2007.

[25] A. Haymond, C. Johny, T. Dowdy, B. Schweibenz, K. Villarroel, R. Young, C. J. Mantooth, T. Patel, J. Bases, G. S. Jose, *et al.*, "Kinetic characterization and allosteric inhibition of the yersinia pestis 1-deoxy-d-xylulose 5-phosphate reductoisomerase (mep synthase)," *PLoS One*, vol. 9, no. 8, e106243, 2014.

[26] R. K. Dhiman, M. L. Schaeffer, A. M. Bailey, C. A. Testa, H. Scherman, D. C. Crick, "1-deoxy-d-xylulose 5-phosphate reductoisomerase (ispc) from mycobacterium tuberculosis: Towards understanding mycobacterial resistance to fosmidomycin," *Journal of bacteriology*, vol. 187, no. 24, pp. 8395–8402, 2005.

[27] S. Jawaid, H. Seidle, W. Zhou, H. Abdirahman, M. Abadeer, J. H. Hix, M. L. van Hoek, R. D. Couch, "Kinetic characterization and phosphoregulation of the francisella tularensis 1-deoxy-d-xylulose 5-phosphate reductoisomerase (mep synthase)," *PLoS One*, vol. 4, no. 12, e8288, 2009.

[28] H. Jomaa, J. Wiesner, S. Sanderbrand, B. Altincicek, C. Weidemeyer, M. Hintz, I. Turbachova, M. Eberl, J. Zeidler, H. K. Lichtenthaler, *et al.*, "Inhibitors of the nonmevalonate pathway of isoprenoid biosynthesis as antimalarial drugs," *Science*, vol. 285, no. 5433, pp. 1573–1576, 1999.

[29] P. Di Martino, "Antimicrobial agents and microbial ecology," *AIMS microbiology*, vol. 8, no. 1, p. 1, 2022.

[30] F. Ramos-Martín, N. D'Amelio, "Drug resistance: An incessant fight against evolutionary strategies of survival," *Microbiology Research*, vol. 14, no. 2, pp. 507–542, 2023.

[31] P. Dadgostar, "Antimicrobial resistance: Implications and costs," *Infection and drug resistance*, pp. 3903–3910, 2019.

[32] M. A. Abushaheen, A. J. Fatani, M. Alosaimi, W. Mansy, M. George, S. Acharya, S. Rathod, D. D. Divakar, C. Jhugroo, S. Vellappally, *et al.*, "Antimicrobial resistance, mechanisms and its clinical significance," *Disease-a-Month*, vol. 66, no. 6, p. 100 971, 2020.

[33] E. J. Septimus, "Antimicrobial resistance: An antimicrobial/diagnostic stewardship and infection prevention approach," *Medical Clinics*, vol. 102, no. 5, pp. 819–829, 2018.

[34] *Awareness week: Preventing antimicrobial resistance together. world health organization*. [Online]. Available: `https://www.who.int/news/item/17-11-2023-world-amr-awareness-week--preventing-antimicrobial-resistance-together` (visited on 01/04/2024).

[35] C. J. Murray, K. S. Ikuta, F. Sharara, L. Swetschinski, G. R. Aguilar, A. Gray, C. Han, C. Bisignano, P. Rao, E. Wool, *et al.*, "Global burden of bacterial antimicrobial resistance in 2019: A systematic analysis," *The Lancet*, vol. 399, no. 10325, pp. 629–655, 2022.

[36] F. M. Wagenlehner, N. H. Brockmeyer, T. Discher, K. Friese, T. A. Wichelhaus, "The presentation, diagnosis, and treatment of sexually transmitted infections," *Deutsches Ärzteblatt International*, vol. 113, no. 1-2, p. 11, 2016.

[37] E. W. Anbesu, S. B. Aychiluhm, M. Alemayehu, "Preventive practices toward sexually transmitted infections and their determinants among young people in ethiopia: A protocol for systematic review and meta-analysis," *Plos one*, vol. 17, no. 2, e0262982, 2022.

[38] J. U. Igietseme, Y. Omosun, C. M. Black, "Bacterial sexually transmitted infections (stis): A clinical overview," *Molecular Medical Microbiology*, pp. 1403–1420, 2015.

[39] L. Fu, Y. Sun, M. Han, B. Wang, F. Xiao, Y. Zhou, Y. Gao, T. Fitzpatrick, T. Yuan, P. Li, *et al.*, "Incidence trends of five common sexually transmitted infections excluding hiv from 1990 to 2019 at the global, regional, and national levels: Results from the global burden of disease study 2019," *Frontiers in Medicine*, vol. 9, p. 851 635, 2022.

[40] L. Santacroce, M. Colella, I. A. Charitos, *The persistence and increase in sexually transmitted diseases (stds) to pandemic levels*, 2021.

[41] R. Rodrigues, P. Vieira-Baptista, C. Catalão, M. J. Borrego, C. Sousa, N. Vale, "Chlamydial and gonococcal genital infections: A narrative review," *Journal of Personalized Medicine*, vol. 13, no. 7, p. 1170, 2023.

[42] O. T. Van Gerwen, C. A. Muzny, J. M. Marrazzo, "Sexually transmitted infections and female reproductive health," *Nature Microbiology*, vol. 7, no. 8, pp. 1116–1126, 2022.

[43] J. Bennett, H. Bratcher, C. Brehony, O. Harrison, M. Maiden, "The genus neisseria," 2014.

[44] *Gonorrhoea (neisseria gonorrhoeae infection)*. [Online]. Available: `https://www.who.int/news-room/fact-sheets/detail/gonorrhoea-(neisseria-gonorrhoeae-infection)` (visited on 01/04/2024).

[45] W. H. Organization *et al.*, "Global health sector strategy on sexually transmitted infections 2016-2021: Toward ending stis," World Health Organization, Tech. Rep., 2016.

[46] S. J. Quillin, H. S. Seifert, "Neisseria gonorrhoeae host adaptation and pathogenesis," *Nature Reviews Microbiology*, vol. 16, no. 4, pp. 226–240, 2018.

[47] M. Unemo, J. Ross, A. Serwin, M. Gomberg, M. Cusini, J. Jensen, "2020 european guideline for the diagnosis and treatment of gonorrhoea in adults," *International journal of STD & AIDS*, p. 0 956 462 420 949 126, 2020.

[48] J. Sherrard, "Gonorrhoea," *Medicine*, vol. 42, no. 6, pp. 323–326, 2014.

[49] U. V. Johannes Elias Matthias Frosch, "Chapter 36 neisseria," in *Manual of Clinical Microbiology, 13th Edition*, ASM Press, Washington, DC, 2018, pp. 640–655, isbn: 9781683670438. doi: `doi : 10 . 1128 / 9781683670438.MCM.ch36`.

[50] G. G. McSheffrey, S. D. Gray-Owen, "Neisseria gonorrhoeae," in *Molecular medical microbiology*, Elsevier, 2015, pp. 1471–1485.

[51] C. K. Fairley, V. J. Cornelisse, J. S. Hocking, E. P. Chow, "Models of gonorrhoea transmission from the mouth and saliva," *The Lancet Infectious Diseases*, vol. 19, no. 10, e360–e366, 2019.

[52] M. K. Morgan, C. F. Decker, "Gonorrhea," *Disease-a-Month*, vol. 62, no. 8, pp. 260–268, 2016.

[53] V. Gaspari, A. Marangoni, A. D'Antuono, G. Roncarati, M. Salvo, C. Foschi, M. C. Re, "Pharyngeal chlamydia and gonorrhea: A hidden problem," *International journal of STD & AIDS*, vol. 30, no. 8, pp. 732–738, 2019.

[54] M. V. Humbert, M. Christodoulides, "Atypical, yet not infrequent, infections with neisseria species," *Pathogens*, vol. 9, no. 1, p. 10, 2019.

[55] S. Buder, H. Schöfer, T. Meyer, V. Bremer, P. K. Kohl, A. Skaletz-Rorowski, N. Brockmeyer, "Bacterial sexually transmitted infections," *JDDG: Journal der Deutschen Dermatologischen Gesellschaft*, vol. 17, no. 3, pp. 287–315, 2019.

[56] G. L. Aitolo, O. S. Adeyemi, B. L. Afolabi, A. O. Owolabi, "Neisseria gonorrhoeae antimicrobial resistance: Past to present to future," *Current Microbiology*, vol. 78, pp. 867–878, 2021.

[57] M. Unemo, J. S. Jensen, "Antimicrobial-resistant sexually transmitted infections: Gonorrhoea and mycoplasma genitalium," *Nature Reviews Urology*, vol. 14, no. 3, pp. 139–152, 2017.

[58] D. A. Lewis, "The gonococcus fights back: Is this time a knock out?" *Sexually transmitted infections*, 2010.

[59] M. Unemo, D. Golparian, D. W. Eyre, "Antimicrobial resistance in neisseria gonorrhoeae and treatment of gonorrhea," *Neisseria gonorrhoeae: methods and protocols*, pp. 37–58, 2019.

[60] B. Suay-García, M. T. Pérez-Gracia, "Future prospects for neisseria gonorrhoeae treatment," *Antibiotics*, vol. 7, no. 2, p. 49, 2018.

[61] W. H. Organization *et al.*, *WHO guidelines for the treatment of Neisseria gonorrhoeae*. World Health Organization, 2016.

[62] M. Unemo, "Current and future antimicrobial treatment of gonorrhoea–the rapidly evolving neisseria gonorrhoeae continues to challenge," *BMC infectious diseases*, vol. 15, no. 1, p. 364, 2015.

[63] J. M. Zenilman, "Control and prevention," *Sexually Transmitted Diseases: Vaccines, Prevention, and Control*, p. 369, 2000.

[64] J. W. Little, "Gonorrhea: Update," *Oral Surgery, Oral Medicine, Oral Pathology, Oral Radiology, and Endodontology*, vol. 101, no. 2, pp. 137–143, 2006, issn: 1079-2104. doi: https://doi.org/10.1016/j.tripleo.2005.05.077. [Online]. Available: https://www.sciencedirect.com/science/article/pii/S1079210405005974.

[65] J. M. Zenilman, C. D. Deal, "Chapter 16 - gonorrhea: Epidemiology, control, and prevention," in *Sexually Transmitted Diseases (Second Edition)*, L. R. Stanberry, S. L. Rosenthal, Eds., Second Edition, Academic Press, 2013, pp. 411–426, isbn: 978-0-12-391059-2. doi: https://doi.org/10.1016/B978-0-12-391059-2.00016-4.

[66] A. Kollipara, T. Darville, *et al.*, "Sexually transmitted infections and the urgent need for vaccines: A review of four major bacterial sti pathogens," *Mucosal Vaccines*, pp. 625–647, 2020.

[67] M. Wilson, P. Wilson, *Close Encounters of the Microbial Kind*. Springer, 2021.

[68] B. Młynarczyk-Bonikowska, A. Majewska, M. Malejczyk, G. Młynarczyk, S. Majewski, "Multiresistant neisseria gonorrhoeae: A new threat in second decade of the xxi century," *Medical microbiology and immunology*, vol. 209, pp. 95–108, 2020.

[69] M. Unemo, W. M. Shafer, "Antimicrobial resistance in neisseria gonorrhoeae in the 21st century: Past, evolution, and future," *Clinical microbiology reviews*, vol. 27, no. 3, pp. 587–613, 2014.

[70] B. Mlynarczyk-Bonikowska, C. Kowalewski, A. Krolak-Ulinska, W. Marusza, "Molecular mechanisms of drug resistance and epidemiology of multidrug-resistant variants of neisseria gonorrhoeae," *International Journal of Molecular Sciences*, vol. 23, no. 18, p. 10 499, 2022.

[71] E. Carsanba, M. Pintado, C. Oliveira, "Fermentation strategies for production of pharmaceutical terpenoids in engineered yeast," *Pharmaceuticals*, vol. 14, no. 4, p. 295, 2021.

[72] Y. Hoshino, E. A. Gaucher, "On the origin of isoprenoid biosynthesis," *Molecular biology and evolution*, vol. 35, no. 9, pp. 2185–2197, 2018.

[73] T. Kuzuyama, H. Seto, "Two distinct pathways for essential metabolic precursors for isoprenoid biosynthesis," *Proceedings of the Japan Academy, Series B*, vol. 88, no. 3, pp. 41–52, 2012.

[74] S. Heuston, M. Begley, C. G. Gahan, C. Hill, "Isoprenoid biosynthesis in bacterial pathogens," *Microbiology*, vol. 158, no. 6, pp. 1389–1401, 2012.

[75] D. N. Carruthers, T. S. Lee, "Diversifying isoprenoid platforms via atypical carbon substrates and non-model microorganisms," *Frontiers in Microbiology*, vol. 12, p. 791 089, 2021.

[76] K. Springob, T. M. Kutchan, "Introduction to the different classes of natural products," *Plant-derived natural products: Synthesis, function, and application*, pp. 3–50, 2009.

[77] E. Vranová, D. Coman, W. Gruissem, "Network analysis of the mva and mep pathways for isoprenoid synthesis," *Annual review of plant biology*, vol. 64, pp. 665–700, 2013.

[78] N. Singh, G. Chevé, M. A. Avery, C. R. McCurdy, "Targeting the methyl erythritol phosphate (mep) pathway for novel antimalarial, antibacterial and herbicidal drug discovery: Inhibition of 1-deoxy-d-xylulose-5-phosphate reductoisomerase (dxr) enzyme," *Current pharmaceutical design*, vol. 13, no. 11, pp. 1161–1177, 2007.

[79] M. Rohmer, M. Knani, P. Simonin, B. Sutter, H. Sahm, "Isoprenoid biosynthesis in bacteria: A novel pathway for the early steps leading to isopentenyl diphosphate," *Biochemical Journal*, vol. 295, no. 2, pp. 517–524, 1993.

[80] A. R. Odom, "Five questions about non-mevalonate isoprenoid biosynthesis," *PLoS pathogens*, vol. 7, no. 12, e1002323, 2011.

[81] E. R Jackson, C. S Dowd, "Inhibition of 1-deoxy-d-xylulose-5-phosphate reductoisomerase (dxr): A review of the synthesis and biological evaluation of recent inhibitors," *Current topics in medicinal chemistry*, vol. 12, no. 7, pp. 706–728, 2012.

[82] T. Kuzuyama, S. Takahashi, M. Takagi, H. Seto, "Characterization of 1-deoxy-d-xylulose 5-phosphate reductoisomerase, an enzyme involved in isopentenyl diphosphate biosynthesis, and identification of its catalytic amino acid residues," *Journal of Biological Chemistry*, vol. 275, no. 26, pp. 19 928–19 932, 2000.

[83] S. T. Withers, J. D. Keasling, "Biosynthesis and engineering of isoprenoid small molecules," *Applied microbiology and biotechnology*, vol. 73, pp. 980–990, 2007.

[84] D. Zhu, S. Johannsen, T. Masini, C. Simonin, J. Haupenthal, B. Illarionov, A. Andreas, M. Awale, R. M. Gierse, T. van der Laan, *et al.*, "Discovery of novel drug-like antitubercular hits targeting the mep pathway enzyme dxps by strategic application of ligand-based virtual screening," *Chemical science*, vol. 13, no. 36, pp. 10 686–10 698, 2022.

[85] S. Steinbacher, J. Kaiser, W. Eisenreich, R. Huber, A. Bacher, F. Rohdich, "Structural basis of fosmidomycin action revealed by the complex with 2-c-methyl-d-erythritol 4-phosphate synthase (ispc): Implications for the catalytic mechanism and anti-malaria drug development," *Journal of Biological Chemistry*, vol. 278, no. 20, pp. 18 401–18 407, 2003.

[86] A. Mac Sweeney, R. Lange, R. P. Fernandes, H. Schulz, G. E. Dale, A. Douangamath, P. J. Proteau, C. Oefner, "The crystal structure of e. coli 1-deoxy-d-xylulose-5-phosphate reductoisomerase in a ternary complex with the antimalarial compound fosmidomycin and nadph reveals a tight-binding closed enzyme conformation," *Journal of molecular biology*, vol. 345, no. 1, pp. 115–127, 2005.

[87] F. S. Krebs, J. Esque, R. H. Stote, "A computational study of the molecular basis of antibiotic resistance in a dxr mutant," *Journal of Computer-Aided Molecular Design*, vol. 33, pp. 927–940, 2019.

[88] L. M. Henriksson, C. Björkelid, S. L. Mowbray, T. Unge, "The 1.9 Å resolution structure of mycobacterium tuberculosis 1-deoxy-d-xylulose 5-phosphate reductoisomerase, a potential drug target," *Acta Crystallographica Section D: Biological Crystallography*, vol. 62, no. 7, pp. 807–813, 2006.

[89] C. Zinglé, L. Kuntz, D. Tritsch, C. Grosdemange-Billiard, M. Rohmer, "Modifications around the hydroxamic acid chelating group of fosmidomycin, an inhibitor of the metalloenzyme 1-deoxyxylulose 5-phosphate reductoisomerase (dxr)," *Bioorganic & medicinal chemistry letters*, vol. 22, no. 21, pp. 6563–6567, 2012.

[90] J. A. Slade, M. Brockett, R. Singh, G. W. Liechti, A. T. Maurelli, "Fosmidomycin, an inhibitor of isoprenoid synthesis, induces persistence in chlamydia by inhibiting peptidoglycan assembly," *PLoS pathogens*, vol. 15, no. 10, e1008078, 2019.

[91] T. Kuzuyama, H. Seto, "Diversity of the biosynthesis of the isoprene units," *Natural product reports*, vol. 20, no. 2, pp. 171–183, 2003.

[92] A. Frank, M. Groll, "The methylerythritol phosphate pathway to isoprenoids," *Chemical Reviews*, vol. 117, no. 8, pp. 5675–5703, 2017.

[93] T. Knak, M. A. Abdullaziz, S. Höfmann, L. A. Alves Avelar, S. Klein, M. Martin, M. Fischer, N. Tanaka, T. Kurz, "Over 40 years of fosmidomycin drug research: A comprehensive review and future opportunities," *Pharmaceuticals*, vol. 15, no. 12, p. 1553, 2022.

[94] T. Radykewicz, F. Rohdich, J. Wungsintaweekul, S. Herz, K. Kis, W. Eisenreich, A. Bacher, M. H. Zenk, D. Arigoni, "Biosynthesis of terpenoids: 1-deoxy-d-xylulose-5-phosphate reductoisomerase from escherichia coli is a class b dehydrogenase," *FEBS letters*, vol. 465, no. 2-3, pp. 157–160, 2000.

[95] J. Wiesner, S. Borrmann, H. Jomaa, "Fosmidomycin for the treatment of malaria," *Parasitology research*, vol. 90, S71–S76, 2003.

[96] T. Kuzuyama, T. Shimizu, S. Takahashi, H. Seto, "Fosmidomycin, a specific inhibitor of 1-deoxy-d-xylulose 5-phosphate reductoisomerase in the nonmevalonate pathway for terpenoid biosynthesis," *Tetrahedron letters*, vol. 39, no. 43, pp. 7913–7916, 1998.

[97] J. Zeidler, J. Schwender, C. Müller, J. Wiesner, C. Weidemeyer, E. Beck, H. Jomaa, H. K. Lichtenthaler, "Inhibition of the non-mevalonate 1-deoxy--xylulose-5-phosphate pathway of plant isoprenoid biosynthesis by fosmidomycin," *Zeitschrift für Naturforschung C*, vol. 53, no. 11-12, pp. 980–986, 1998.

[98] Y.-H. Woo, R. P. Fernandes, P. J. Proteau, "Evaluation of fosmidomycin analogs as inhibitors of the synechocystis sp. pcc6803 1-deoxy-d-xylulose 5-phosphate reductoisomerase," *Bioorganic & medicinal chemistry*, vol. 14, no. 7, pp. 2375–2385, 2006.

[99] A. T. Koppisch, D. T. Fox, B. S. Blagg, C. Poulter, "E. coli mep synthase: Steady-state kinetic analysis and substrate binding," *Biochemistry*, vol. 41, no. 1, pp. 236–243, 2002.

[100] *Alicator ligation independent cloning and expression system, product information*, Thermo Fisher Scientific Inc., 2013.

[101] *Pet system manual*, TB055, 11th Edition, 01/06, Novagen.

[102] *Pet-40b(+) expression vector system*. [Online]. Available: https://noys4.weizmann.ac.il/plasmidb/queryplasmid?vector_or_plasmid_name=pET40b (visited on 01/04/2024).

[103] *Pet-41a(+) expression vector system*. [Online]. Available: https://noys4.weizmann.ac.il/plasmidb/queryplasmid?vector_or_plasmid_name=pET41a (visited on 01/04/2024).

[104] A. QIAexpressionist, "A handbook for high-level expression and purification of 6xhis-tagged proteins," *Qiagen. p1-125*, 2002.

[105] *Tagzyme handbook for exoproteolytic cleavage of n-terminal his tags*, 12/2021, HB-2042-002, © 2021, QIAGEN.

[106] *Invitrogen champion pet directional topo manual*, part no. 25-0400, MAN0000214.

[107] Takara Bio Inc., *Takara chaperone plasmid system manual*, Catalog Number: 3340, Version: v201701Da, Takara Bio Inc., 2017.

[108] D. W. Russell, J. Sambrook, *Molecular cloning: a laboratory manual*. Cold Spring Harbor Laboratory Cold Spring Harbor, NY, 2001, vol. 1.

[109] *The national center for biotechnology information (ncbi), nucleotide sequence*. [Online]. Available: http://www.ncbi.nlm.nih.gov/ (visited on 01/04/2024).

[110] *American type culture collection*. [Online]. Available: https://www.atcc.org (visited on 01/04/2024).

[111] *Promega, wizard® sv gel and pcr clean-up system technical bulletin*. [Online]. Available: http://www.promega.co.uk (visited on 11/11/2023).

[112] *Protocols and applications guide, third edition (1996)*, Part 9PIM180. Printed in USA. Revised 4/18, Promega Corporation.

[113] *Promega, wizard® plus sv minipreps dna purification system technical bulletin*. [Online]. Available: https://www.promega.com (visited on 11/11/2023).

[114] *Expasy protparam tool*. [Online]. Available: https://web.expasy.org/protparam/ (visited on 01/04/2024).

[115] *Aat bioquest peptide and the protein molecular weight calculator*. [Online]. Available: https://www.aatbio.com/tools/calculate-peptide-and-protein-molecular-weight-mw (visited on 01/04/2024).

[116] *Clontech laboratories, inc. histalon gravity column purification kit user manual*, Cat. Nos. 635651, 635654 & 635655 PT4435-1 (032216), Clontech Laboratories, Inc.

[117] U. K. Laemmli, "Cleavage of structural proteins during the assembly of the head of bacteriophage t4," *nature*, vol. 227, no. 5259, pp. 680–685, 1970.

[118] K. Ma, M. W. Adams, "[4] ferredoxin: Nadp oxidoreductase from pyrococcus furiosus," in *Methods in enzymology*, vol. 334, Elsevier, 2001, pp. 40–45.

[119] *Multiple sequence comparison by log-expectation*. [Online]. Available: https://www.ebi.ac.uk/Tools/msa/muscle/ (visited on 01/04/2024).

[120] S. M. Singh, A. Sharma, A. K. Upadhyay, A. Singh, L. C. Garg, A. K. Panda, "Solubilization of inclusion body proteins using n-propanol and its refolding into bioactive form," *Protein expression and purification*, vol. 81, no. 1, pp. 75–82, 2012.

[121] A. Bhatwa, W. Wang, Y. I. Hassan, N. Abraham, X.-Z. Li, T. Zhou, "Challenges associated with the formation of recombinant protein inclusion bodies in escherichia coli and strategies to address them for industrial applications," *Frontiers in Bioengineering and Biotechnology*, vol. 9, p. 630 551, 2021.

[122] S. Mital, G. Christie, D. Dikicioglu, "Recombinant expression of insoluble enzymes in escherichia coli: A systematic review of experimental design and its manufacturing implications," *Microbial cell factories*, vol. 20, pp. 1–20, 2021.

[123] A. Singh, V. Upadhyay, A. K. Upadhyay, S. M. Singh, A. K. Panda, "Protein recovery from inclusion bodies of escherichia coli using mild solubilization process," *Microbial cell factories*, vol. 14, no. 1, pp. 1–10, 2015.

[124] A. Fazaeli, A. Golestani, M. Lakzaei, S. S. Rasi Varaei, M. Aminian, "Expression optimization of recombinant cholesterol oxidase in escherichia coli and its purification and characterization," *AMB Express*, vol. 8, pp. 1–9, 2018.

[125] S. M. Hayat, N. Farahani, B. Golichenari, A. Sahebkar, "Recombinant protein expression in escherichia coli (e. coli): What we need to know," *Current pharmaceutical design*, vol. 24, no. 6, pp. 718–725, 2018.

[126] T. Kiefhaber, R. Rudolph, H.-H. Kohler, J. Buchner, "Protein aggregation in vitro and in vivo: A quantitative model of the kinetic competition between folding and aggregation," *Bio/technology*, vol. 9, no. 9, pp. 825–829, 1991.

[127] E. Cayir, A. Erdemir, E. Ozkan, M. Topuzogullari, Z. B. Bolat, A. Akat, D. Turgut-Balik, "Cloning of intron-removed enolase gene and expression, purification, kinetic characterization of the enzyme from theileria annulata," *Molecular biotechnology*, vol. 56, pp. 689–696, 2014.

[128] M. Fathi-Roudsari, A. Akhavian-Tehrani, N. Maghsoudi, "Comparison of three escherichia coli strains in recombinant production of reteplase," *Avicenna journal of medical biotechnology*, vol. 8, no. 1, p. 16, 2016.

[129] M. Boshtam, H. Khanahmad Shahreza, S. Feizollahzadeh, I. Rahimmanesh, S. Asgary, "Expression and purification of biologically active recombinant rabbit monocyte chemoattractant protein1 in escherichia coli," *FEMS microbiology letters*, vol. 365, no. 9, fny070, 2018.

[130] S. Falak, M. Sajed, N. Rashid, "Strategies to enhance soluble production of heterologous proteins in escherichia coli," *Biologia*, vol. 77, no. 3, pp. 893–905, 2022.

[131] M. R. Ajmal, “Protein misfolding and aggregation in proteinopathies: Causes, mechanism and cellular response,” *Diseases*, vol. 11, no. 1, p. 30, 2023.

[132] A. Beygmoradi, A. Homaei, R. Hemmati, P. Fernandes, “Recombinant protein expression: Challenges in production and folding related matters,” *International Journal of Biological Macromolecules*, p. 123 407, 2023.

[133] H. Adsi, S. A. Levkovich, E. Haimov, T. Kreiser, M. Meli, H. Engel, L. Simhaev, S. Karidi-Heller, G. Colombo, E. Gazit, *et al.*, “Chemical chaperones modulate the formation of metabolite assemblies,” *International Journal of Molecular Sciences*, vol. 22, no. 17, p. 9172, 2021.

[134] G. Litwack, “Proteins,” in Jan. 2018, pp. 63–94, isbn: 9780123838643. doi: 10.1016/B978-0-12-383864-3.00004-1.

[135] R. Mishra, R. Bhat, R. Seckler, “Chemical chaperone-mediated protein folding: Stabilization of p22 tailspike folding intermediates by glycerol,” 2007.

[136] V. Vagenende, M. G. Yap, B. L. Trout, “Mechanisms of protein stabilization and prevention of protein aggregation by glycerol,” *Biochemistry*, vol. 48, no. 46, pp. 11 084–11 096, 2009.

[137] H. Yamaguchi, M. Miyazaki, “Refolding techniques for recovering biologically active recombinant proteins from inclusion bodies,” *Biomolecules*, vol. 4, no. 1, pp. 235–251, 2014.

[138] J. G. Thomas, F. Baneyx, “Protein misfolding and inclusion body formation in recombinant escherichia coli cells overexpressing heat-shock proteins (),” *Journal of Biological Chemistry*, vol. 271, no. 19, pp. 11 141–11 147, 1996.

[139] G. Chhetri, P. Kalita, T. Tripathi, “An efficient protocol to enhance recombinant protein expression using ethanol in escherichia coli,” *MethodsX*, vol. 2, pp. 385–391, 2015.

[140] E. Tannous, K. Yokoyama, D.-J. You, Y. Koga, S. Kanaya, “A dual role of divalent metal ions in catalysis and folding of rnase h1 from extreme halophilic archaeon halobacterium sp. nrc-1,” *FEBS Open Bio*, vol. 2, pp. 345–352, 2012.

[141] T. Kuzuyama, S. Takahashi, H. Watanabe, H. Seto, “Direct formation of 2-c-methyl-d-erythritol 4-phosphate from 1-deoxy-d-xylulose 5-phosphate by 1-deoxy-d-xylulose 5-phosphate reductoisomerase, a new enzyme in the non-mevalonate pathway to isopentenyl diphosphate,” *Tetrahedron Letters*, vol. 39, no. 25, pp. 4509–4512, 1998.

[142] K. A. Coskun, N. Yurekli, E. C. Abay, M. Tutar, M. Al, Y. Tutar, “Structure-and design-based difficulties in recombinant protein purification in bacterial expression,” *Protein Detection*, p. 3, 2022.

[143] A. Singh, V. Upadhyay, A. K. Panda, “Solubilization and refolding of inclusion body proteins,” *Insoluble proteins: methods and protocols*, pp. 283–291, 2015.

[144] L. Zhang, C. P. Chou, M. Moo-Young, "Disulfide bond formation and its impact on the biological activity and stability of recombinant therapeutic proteins produced by escherichia coli expression system," *Biotechnology advances*, vol. 29, no. 6, pp. 923–929, 2011.

[145] S. Grolle, S. Bringer-Meyer, H. Sahm, "Isolation of the dxr gene of zymomonas mobilis and characterization of the 1-deoxy-d-xylulose 5-phosphate reductoisomerase," *FEMS microbiology letters*, vol. 191, no. 1, pp. 131–137, 2000.

[146] S. Takahashi, T. Kuzuyama, H. Watanabe, H. Seto, "A 1-deoxy-d-xylulose 5-phosphate reductoisomerase catalyzing the formation of 2-c-methyl-d-erythritol 4-phosphate in an alternative nonmevalonate pathway for terpenoid biosynthesis," *Proceedings of the National Academy of Sciences*, vol. 95, no. 17, pp. 9879–9884, 1998.

[147] Y. Y. Siew, W. Zhang, "Downstream processing of recombinant human insulin and its analogues production from e. coli inclusion bodies," *Bioresources and Bioprocessing*, vol. 8, no. 1, pp. 1–27, 2021.

[148] B. Ban, M. Sharma, J. Shetty, "Optimization of methods for the production and refolding of biologically active disulfide bond-rich antibody fragments in microbial hosts," *Antibodies*, vol. 9, no. 3, p. 39, 2020.

[149] L. F. Vallejo, U. Rinas, "Strategies for the recovery of active proteins through refolding of bacterial inclusion body proteins," *Microbial cell factories*, vol. 3, pp. 1–12, 2004.

[150] J. W. Nichols, A. D. Hoffman, J. A. Swintek, S. T. Droge, P. N. Fitzsimmons, "Addition of phenylmethylsulfonyl fluoride increases the working lifetime of the trout liver s9 substrate depletion assay, resulting in improved detection of low intrinsic clearance rates," *Environmental toxicology and chemistry*, vol. 40, no. 1, pp. 148–161, 2021.

[151] N. B. Pham, W. S. Meng, "Protein aggregation and immunogenicity of biotherapeutics," *International journal of pharmaceutics*, vol. 585, p. 119 523, 2020.

[152] A. Villaverde, M. Mar Carrió, "Protein aggregation in recombinant bacteria: Biological role of inclusion bodies," *Biotechnology letters*, vol. 25, pp. 1385–1395, 2003.

[153] P. T. Wingfield, "Overview of the purification of recombinant proteins," *Current protocols in protein science*, vol. 80, no. 1, pp. 6–1, 2015.

[154] C. Xu, H. Wei, A. Movahedi, W. Sun, X. Ma, D. Li, T. Yin, Q. Zhuge, "Evaluation, characterization, expression profiling, and functional analysis of dxs and dxr genes of populus trichocarpa," *Plant Physiology and Biochemistry*, vol. 142, pp. 94–105, 2019.

[155] G. J. Gopal, A. Kumar, "Strategies for the production of recombinant protein in escherichia coli," *The protein journal*, vol. 32, pp. 419–425, 2013.

[156] G. L. Rosano, E. A. Ceccarelli, "Rare codon content affects the solubility of recombinant proteins in a codon bias-adjusted escherichia coli strain," *Microbial cell factories*, vol. 8, no. 1, pp. 1–9, 2009.

[157] *Bl21-codon plus competent cells*, I. Manual.

[158] J. Lobstein, C. A. Emrich, C. Jeans, M. Faulkner, P. Riggs, M. Berkmen, "Shuffle, a novel escherichia coli protein expression strain capable of correctly folding disulfide bonded proteins in its cytoplasm," *Microbial cell factories*, vol. 11, pp. 1–16, 2012.

[159] *1-deoxy-d-xylulose-5-phosphate reductoisomerase neisseria gonorrhoeae 411*. [Online]. Available: `https://www.ncbi.nlm.nih.gov/protein/WP_180374256.1/` (visited on 01/04/2024).

[160] N. Eswar, D. Eramian, B. Webb, M.-Y. Shen, A. Sali, "Protein structure modeling with modeller," *Structural proteomics: high-throughput methods*, pp. 145–159, 2008.

[161] M. De Kerpel, I. Van Molle, L. Brys, L. Wyns, H. De Greve, J. Bouckaert, "N-terminal truncation enables crystallization of the receptor-binding domain of the fedf bacterial adhesin," *Acta Crystallographica Section F: Structural Biology and Crystallization Communications*, vol. 62, no. 12, pp. 1278–1282, 2006.

[162] C. Aygün, S. Kocer, Ö. Danış, S. Cubuk, O. Mutlu, "Heterologous expression, purification, and partial characterisation of the apicoplast protein 3-oxoacyl-[acyl-carrier-protein] reductase from toxoplasma gondii," *Protein Expression and Purification*, vol. 202, p. 106 187, 2023.

[163] J. Kaur, A. Kumar, J. Kaur, "Strategies for optimization of heterologous protein expression in e. coli: Roadblocks and reinforcements," *International Journal of Biological Macromolecules*, vol. 106, pp. 803–822, 2018.

[164] K. Fatima, F. Naqvi, H. Younas, "A review: Molecular chaperone-mediated folding, unfolding and disaggregation of expressed recombinant proteins," *Cell Biochemistry and Biophysics*, vol. 79, pp. 153–174, 2021.

[165] H. P. Sørensen, K. K. Mortensen, "Advanced genetic strategies for recombinant protein expression in escherichia coli," *Journal of biotechnology*, vol. 115, no. 2, pp. 113–128, 2005.

[166] M. Alibolandi, H. Mirzahoseini, F. M. Nehi, G. Tabatabaian, H. Amini, S. Sardari, "Improving recombinant protein solubility in escherichia coli: Identification of best chaperone combination which assists folding of human basic fibroblast growth factor," *African Journal of Biotechnology*, vol. 9, no. 47, pp. 8100–8109, 2010.

[167] G.-P. Voulgaridou, T. Mantso, K. Chlichlia, M. I. Panayiotidis, A. Pappa, "Efficient e. coli expression strategies for production of soluble human crystallin aldh3a1," *PloS one*, vol. 8, no. 2, e56582, 2013.

[168] H. Arsın, A. Jasilionis, H. Dahle, R.-A. Sandaa, R. Stokke, E. Nordberg Karlsson, I. H. Steen, "Exploring codon adjustment strategies towards escherichia coli-based production of viral proteins encoded by hth1, a novel prophage of the marine bacterium hypnocyclicus thermotrophus," *Viruses*, vol. 13, no. 7, p. 1215, 2021.

[169] G. L. Rosano, E. A. Ceccarelli, "Recombinant protein expression in escherichia coli: Advances and challenges," *Frontiers in microbiology*, vol. 5, p. 172, 2014.

[170] J. Athey, A. Alexaki, E. Osipova, A. Rostovtsev, L. V. Santana-Quintero, U. Katneni, V. Simonyan, C. Kimchi-Sarfaty, "A new and updated resource for codon usage tables," *BMC bioinformatics*, vol. 18, pp. 1–10, 2017.

[171] E. Angov, C. J. Hillier, R. L. Kincaid, J. A. Lyon, "Heterologous protein expression is enhanced by harmonizing the codon usage frequencies of the target gene with those of the expression host," *PloS one*, vol. 3, no. 5, e2189, 2008.

[172] *Emboss backtranseq tool*. [Online]. Available: `https://www.ebi.ac.uk/Tools/st/emboss_backtranseq/` (visited on 01/04/2024).

[173] *Agct codon harmonizer online tool*. [Online]. Available: `http://biocatalysis.uni-graz.at/sites/codonharmonizer.html` (visited on 01/04/2024).

[174] A. Malhotra, "Tagging for protein expression," *Methods in enzymology*, vol. 463, pp. 239–258, 2009.

[175] D. Busso, R. Kim, S.-H. Kim, "Using an escherichia coli cell-free extract to screen for soluble expression of recombinant proteins," *Journal of Structural and Functional Genomics*, vol. 5, pp. 69–74, 2004.

[176] E. A. Woestenenk, M. Hammarström, S. van den Berg, T. Härd, H. Berglund, "His tag effect on solubility of human proteins produced in escherichia coli: A comparison between four expression vectors," *Journal of structural and functional genomics*, vol. 5, pp. 217–229, 2004.

[177] S. A. Cantrell, "Vectors for the expression of recombinant proteins in e. coli," *E. coli Plasmid Vectors: Methods and Applications*, pp. 257–275, 2003.

[178] B. Jia, C. O. Jeon, "High-throughput recombinant protein expression in escherichia coli: Current status and future perspectives," *Open biology*, vol. 6, no. 8, p. 160 196, 2016.

[179] T. W. Overton, "Recombinant protein production in bacterial hosts," *Drug discovery today*, vol. 19, no. 5, pp. 590–601, 2014.

[180] S. Costa, A. Almeida, A. Castro, L. Domingues, "Fusion tags for protein solubility, purification and immunogenicity in escherichia coli: The novel fh8 system," *Frontiers in microbiology*, vol. 5, p. 63, 2014.

[181] B. Altincicek, M. Hintz, S. Sanderbrand, J. Wiesner, E. Beck, H. Jomaa, "Tools for discovery of inhibitors of the 1-deoxy-d-xylulose 5-phosphate (dxp) synthase and dxp reductoisomerase: An approach with enzymes from the pathogenic bacterium pseudomonas aeruginosa," *FEMS microbiology letters*, vol. 190, no. 2, pp. 329–333, 2000.

[182] S. Hecht, J. Wungsintaweekul, F. Rohdich, K. Kis, T. Radykewicz, C. A. Schuhr, W. Eisenreich, G. Richter, A. Bacher, "Biosynthesis of terpenoids: Efficient multistep biotransformation procedures affording isotope-labeled 2 c-methyl-d-erythritol 4-phosphate using recombinant 2 c-methyl-d-erythritol 4-phosphate synthase," *The Journal of organic chemistry*, vol. 66, no. 23, pp. 7770–7775, 2001.

[183] J. Samuelson, “Bacterial systems,” *Production of membrane proteins: strategies for expression and isolation*, pp. 11–35, 2011.

[184] K. E. Kram, S. E. Finkel, “Rich medium composition affects escherichia coli survival, glycation, and mutation frequency during long-term batch culture,” *Applied and environmental microbiology*, vol. 81, no. 13, pp. 4442–4450, 2015.

[185] C. Yung-Chi, W. H. Prusoff, “Relationship between the inhibition constant (ki) and the concentration of inhibitor which causes 50 per cent inhibition (i50) of an enzymatic reaction,” *Biochemical pharmacology*, vol. 22, no. 23, pp. 3099–3108, 1973.

[186] A. Dreneau, F. S. Krebs, M. Munier, C. Ngov, D. Tritsch, D. Lièvremont, M. Rohmer, C. Grosdemange-Billiard, “α, α-difluorophosphonohydroxamic acid derivatives among the best antibacterial fosmidomycin analogues,” *Molecules*, vol. 26, no. 16, p. 5111, 2021.

[187] C. T. Behrendt, A. Kunfermann, V. Illarionova, A. Matheeussen, T. Gräwert, M. Groll, F. Rohdich, A. Bacher, W. Eisenreich, M. Fischer, *et al.*, “Synthesis and antiplasmodial activity of highly active reverse analogues of the antimalarial drug candidate fosmidomycin,” *ChemMedChem*, vol. 5, no. 10, pp. 1673–1676, 2010.

PUBLICATIONS FROM THE THESIS

Conference Papers

1. M. Orlenco, E. Ugurel, T.G. Inci, O.M. Ugurel, M.N. Hasimoglu, S. Akar, R. Lawung, W. Deeknamkul, B. Windshügel, D. Turgut Balik "Approaches for recombinant production of *Neisseria gonorrhoeae* 1-deoxy-D-xylulose 5-phosphate reductoisomerase" 47th FEBS Congress, 8-12 July 2023, Tours/France.

2. M. Orlenco, E. Ugurel, M. N. Hasimoglu, O. M. Ugurel, S. Akar, T. G. Inci, R. Lawung, W. Deeknamkul, B. Windshügel, D. Turgut Balik, "Recombinant production of 1-deoxy-D-xylulose 5-phosphate reductoisomerase for drug development studies" BIO Turkiye International Biotechnology Congress, 28-30 September 2023, Istanbul/Türkiye.